Technology of Semiactive Devices and Applications in Vibration Mitigation

Fabio Casciati
University of Pavia, Italy

Georges Magonette
European Laboratory for Structural Assessment, Italy

Francesco Marazzi
Consultant on Dynamics, Italy

John Wiley & Sons, Ltd

Technology of Semiactive Devices and Applications in Vibration Mitigation

Technology of Semiactive Devices and Applications in Vibration Mitigation

Fabio Casciati
University of Pavia, Italy

Georges Magonette
European Laboratory for Structural Assessment, Italy

Francesco Marazzi
Consultant on Dynamics, Italy

John Wiley & Sons, Ltd

Telephone (+44) 1243 779777

Email (for orders and customer service enquiries): cs-books@wiley.co.uk
Visit our Home Page on www.wiley.com

Other Wiley Editorial Offices

John Wiley & Sons Inc., 111 River Street, Hoboken, NJ 07030, USA

Jossey-Bass, 989 Market Street, San Francisco, CA 94103-1741, USA

Wiley-VCH Verlag GmbH, Boschstr. 12, D-69469 Weinheim, Germany

John Wiley & Sons Australia Ltd, 42 McDougall Street, Milton, Queensland 4064, Australia

John Wiley & Sons (Asia) Pte Ltd, 2 Clementi Loop #02-01, Jin Xing Distripark, Singapore 129809

John Wiley & Sons Canada Ltd, 22 Worcester Road, Etobicoke, Ontario, Canada M9W 1L1

Wiley also publishes its books in a variety of electronic formats. Some content that appears in print may not be available in electronic books.

Library of Congress Cataloging in Publication Data

Casciati, Fabio.
Technology of semiactive devices and applications in vibration mitigation / Fabio Casciati, Georges Magonette, Francesco Marazzi.
p. cm.
Includes bibliographical references and index.
ISBN 0-470-02289-2 (alk. paper)
1. Vibration. 2. Damping (Mechanics) 3. Structural control (Engineering) I. Magonette, Georges. II. Marazzi, Francesco. III. Title.

TA355.C345 2006
624.1'76—dc22 2005057713

British Library Cataloguing in Publication Data

A catalogue record for this book is available from the British Library

ISBN-13 978-0-470-02289-4 (HB)
ISBN-10 0-470-02289-2 (HB)

Typeset in 12/14pt Palatino by Integra Software Services Pvt. Ltd, Pondicherry, India
Printed and bound in Great Britain by TJ International, Padstow, Cornwall
This book is printed on acid-free paper responsibly manufactured from sustainable forestry in which at least two trees are planted for each one used for paper production.

To our wives

Contents

Figures

Tables

Algorithms

Symbols

ξ	damping ratio
$\mathbf{x}$	system state vector
$\mathbf{y}$	system observed vector
$\mathbf{z}$	system response vector
$\mathbf{u}$	controllable and forcing vector
$\boldsymbol{\mathcal{A}}$	status matrix
$\boldsymbol{\mathcal{B}}$	topological control matrix
$\boldsymbol{\mathcal{C}}$	output matrix
$\boldsymbol{\mathcal{D}}$	disturbance matrix
$\mathbf{M}$	mass matrix
$\mathbf{C}$	damping matrix
$\mathbf{K}$	stiffness matrix
$\mathbf{G}(s)$	transfer function matrix
m	element of the mass matrix
c	element of the damping matrix
k	element of the stiffness matrix
β	ratio between input (Ω) and natural (ω) frequencies
$V(.)$	Lyapunov function

Introduction

OBJECTIVES

Civil engineering structures do not show the innovation rate which characterizes mechanical and aerospace engineering. There are three ingredients able to generate innovation: the design rationale, the construction materials and the quality process. The first ingredient has not seen much revolution in the last century, while the second suggested fascinating innovative solutions, but they are still under durability examination to satisfy the long expected lifetimes which characterize civil infrastructure components. Therefore, certification and quality control have driven the innovation of the last half century within the usual framework of increasing the strength of a structure. This can be mainly obtained by making larger and larger sections, so that stiffer and more massive buildings result. One concentrates here on the carrying capacity, and, hence, the framework can be referred to as capacity design.

This design approach is unable to satisfy some needs which have a risen in the last few years:

- Higher safety-level demand: there is an increasing demand for safer buildings, of both ordinary and special

Technology of Semiactive Devices and Applications in Vibration Mitigation Fabio Casciati, Georges Magonette and Francesco Marazzi

nature. However, with the capacity design the inertial masses just become greater and greater.

- Stricter performance requests: once safety has been guaranteed, the structures are constrained to deform appropriately, either within the elastic range or up to a limited amount of damage.
- Slender structures trend: there is a tendency to build structures that are slender increasingly and so more prone to vibrate under dynamic loading.

The last decade of the last millennium introduced two potential innovations (Soong 1989):

- structural control can offer a solution from the point of view of both safety and comfort;
- to avoid long delays in adopting innovative devices, they should be conceived as periodically replaceable.

The objection to the unavailability of power during events which seriously affect the structure has placed attention on passive devices (Soong and Dargush 1997). Consequently, a further class of semiactive control devices was introduced. Their definition is given in Chapter 1. However, it is reasonable to list here the reasons which soon made them very promising. They are not very far from passive devices with:

- low energy consumption: the power needed for operation is very low, orders of magnitude lower than any active system requirement, because it is used only for modifying some properties of the device (the opening of a valve, for example);
- no need for external power: since the energy consumption is very low, there is no need for an external power

supply (like a pumping system, for example), but a set of batteries can be enough;

- robustness: even in the worst case (some failure in a sensor, for example) the device has intrinsically dissipative properties, never putting energy into the controlled system.

And they have the advantages of active systems:

- adaptability: the device is built with the possibility of adapting itself to different operating conditions, to different loading paths, to different levels of excitation;
- optimality: the control system is designed to have optimal response characteristics over a wide spectrum of frequencies;
- flexibility in tuning: if the controlled structure changes its characteristics over time, as, for example, ageing effects do on tall buildings, the control device can be reprogrammed without any replacement;
- monitoring: the controlled structure will be instrumented with sensors. The data flow can be observed and stored for continuous monitoring of the health status of the structure.

The development of a control strategy can be divided into several steps (Figure 1): first of all there is an idea on how (and why) to design a new control strategy, then a theory must be developed and a solid mathematical background must be established. This can be done from scratch or a useful basis can be borrowed from another scientific field. In this latter case there are surely some adaptations to be considered, some conditions to be checked, some limitations to be posed, but usually the cross-fertilization among different scientific sectors produces very useful results.

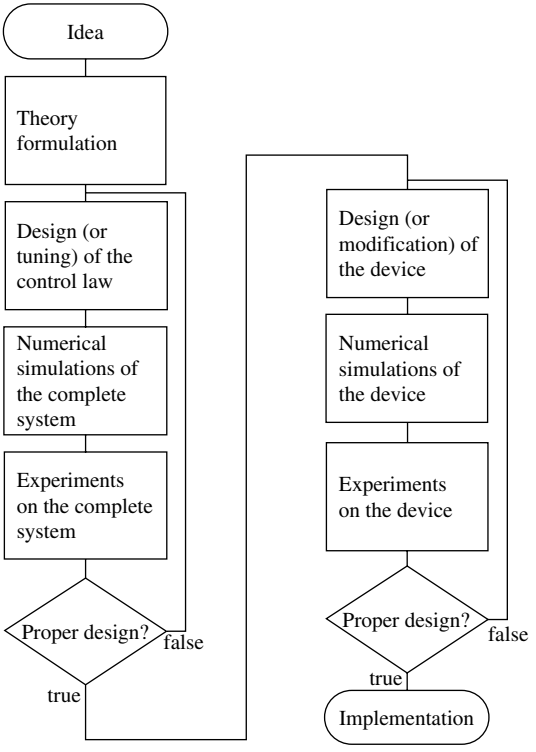

Figure 1 Flowchart of the development of a control system procedure

Before entering into the details of the control law design, the semiactive device must be constructed. This means that it must be designed, its behaviour must be simulated and an experimental campaign must be conducted in order to characterize it. This procedure is usually iterative: if some unexpected behaviour appears, the device must be modified accordingly. Once the device has been manufactured, it is possible to design the control law. Numerical simulations must be conducted on the whole system (both the structure to be controlled and the semiactive device) to get an idea of the final behaviour. This is a fundamental step,

before the whole process is tested in a real application, with all the mechanical, electrical and structural limitations or problems that can arise in practice. The final step will be the implementation of the control strategy in a real structure, with all the arrangements that are necessary.

The global process towards a new control system must constantly consider the typical problems that usually arise in practical implantations. For this reason a deep comparison between collocated and non-collocated systems has been conducted: it is important to know, in different operating conditions and a real environment, which is the best choice from the practical point of view. Moreover, a real control program, to be implemented on a commercial semiactive device, incorporates many security checks of saturation points, of transient conditions in switching the device on and off, and converts a simple control program of a few lines into a list of hundreds of statements. On the other hand, it may be that some critical behaviour seen in the theory and the simulations is never reached in the specific real application: in this case a simplified design method can be derived in order to speed up the implementation process and the installation and calibration.

ORGANIZATION OF THE BOOK

The chapters in the book can be categorized into two parts. The first part covers the more theoretical contributions, with general considerations of the different types of control schemes and strategies. The second part is devoted to experimental evaluations of the previously explained concepts and to the related implementational aspects.

In more detail, within the former part, Chapter 1 provides the necessary definitions of passive, active, semiactive and hybrid control. Proper motivations for this study

are given and the common state-space representation of dynamic systems is introduced to facilitate comprehension of the following chapters. In Chapter 2 a comparison between collocated and non-collocated systems is presented. A proper definition is given and the advantages and disadvantages of these two control schemes are presented. This chapter is different to the other ones because it is not related to a particular control type (active, semiactive, passive or hybrid), but deals with the general philosophy that underlies the selection of the control type and the control law.

The next four chapters form the second part of contributions. Chapter 3 deals with the history of semiactive control and provides a bibliographical review of the most common semiactive control strategies. Chapter 4 proposes the implementation schemes to be adopted to follow the control law described above. The main steps are presented, even if in a schematic way, to allow coding of the described control laws in C or Fortran. Chapter 5 is devoted to a description of the implementation of the semiactive control strategies. The appropriate flowcharts are developed in detail: the main background on the architecture adopted, the hardware and software needed, and the connections to be prepared are described following the guidelines given by the work conducted in recent years at the ELSA Laboratory and at the University of Pavia. Once the general control frame has been described, the developed semiactive control software is presented in detail. The next chapter, Chapter 6, describes the testing procedures developed at ELSA to verify the structural control devices experimentally by using the on-line testing method with substructuring.

Finally, in Chapter 7, the theoretical aspects of stability are revisited before the conclusions and further future developments are presented. An appendix concludes the

book: it contains some critical considerations about the concept and the evaluation of the original damping of a structure. This is a critical aspect when dealing with semiactive control systems which are usually designed to increase the structural damping.

In writing this book, the authors had mainly in mind its potential end users, namely:

1. Civil engineers active in the areas of bridges, high-rise buildings, railways, aseismic structures.
2. Automotive engineers.
3. Mechanical engineers working on vibration problems.
4. Consultants.
5. Post graduate students.

1
Reliability, Robustness and Structural Control

1.1 PRELIMINARY CONCEPTS

The third author of this book began his PhD thesis (Marazzi 2003) with these words:

> Since ancient times the designers of civil engineering structures have been responsible for building collapse: in the Code of Hammurabi, King of Mesopotamia during the XVIII century B.C., builders were punished with the death penalty in case the building failed. Article 229 says: "The builder has built a house for a man and his work is not strong: if the house he has built falls in and kills a householder, that builder shall be slain." It was implicit in the law that collapse could happen for ordinary loads, let's say dead loads (caused for example by a large number of people in the same room) or common dynamic loads (for example, a strong but common wind). On the contrary, collapse caused by extraordinary loads, such as, for example, earthquakes and hurricanes, was not taken into consideration, because it was considered beyond the control of the designer and the builder and was retained as a manifestation of a "supernatural" event sent by the gods as a punishment or simply for playing a joke on human beings. Later on, as the

Technology of Semiactive Devices and Applications in Vibration Mitigation Fabio Casciati, Georges Magonette and Francesco Marazzi

> belief that these events were of supernatural origin progressively disappeared, the idea that the designer could not take into account the effects of such loads still persisted. On the one hand earthquakes and hurricanes were considered completely unpredictable, in both occurrence and intensity, while, on the other hand, there were no suitable techniques to reduce the risk of collapse.

The Code of Hammurabi is a collection of laws written in 51 columns on a stele discovered at the beginning of the twentieth century and now held at the Louvre Museum in Paris. It consists of a prologue and an epilogue celebrative of the king and of 282 articles regarding various aspects of the civil, penal and commercial law. It is one of the first examples of written laws. The question is: how far has human society moved after 37 centuries? A quick, nearly blasphemous, answer might be: we are slowly coming back to the starting point! Indeed, after one century of prescriptive rules (which in some countries were made laws), as well as after 30 years of attempts at unifying them across Europe (Eurocodes) and around the world, the so-called "performance-based design" is rediscovering the fascinating Hammurabi idea of performance. This prevailing framework is generally promoted by those designers who want to preserve their identity, role and responsibilities, rather than being replaced by sophisticated software able to navigate across prescriptions better than any human being.

But the reader must have noted that the border between predictable and unpredictable events in the previous scheme is rather fuzzy. Are we still there after 37 centuries? It must be said that a rational effort was made and today the results are summarized in the probabilistic model code prepared by the Joint Committee of Structural Safety and which has been available on the Internet for 10 years [http://www.jcss.ethz.ch/] as follows.

Structures and structural elements shall be designed, constructed and maintained in such a way that they are suited for their use during the design working life and in an economic way. In particular they shall, with appropriate levels of reliability, fulfil the following requirements:

- They shall remain fit for the use for which they are required (serviceability, limit state requirement)
- They shall withstand extreme and/or frequently repeated actions occurring during their construction and anticipated use (ultimate limit state requirement)
- They shall not be damaged by accidental events like fire, explosions, impact or consequences of human errors, to an extent disproportionate to the triggering event (robustness requirement)

There are three main innovations:

1. Success and failure are situations characterized by their probability of occurrence; it is the society which decides the target to be pursued for ultimate limit states.
2. Serviceability limit states are ruled by the desiderata of the contractor, as well as the relevant probability of failure.
3. In any case the designer cannot conceive structural architectures which result in weakness to accidental events. They can be introduced as likely events, without the chance of associating a probability of occurrence to them. In other words, they can be conceived, but not assessed on a statistical basis.

The usual carrying capacity design, originally developed for static loading conditions, evolved through the assignment of a proper level of ductility reserve to the structural

members. The structure remains elastic for the major part of its life (under ordinary loads), but it will enter the plastic state under exceptional lateral loads; in this way the input energy should be dissipated. Even if there might be permanent damage to the structural members, the building is designed in such a way that it should not collapse, so no loss of life should result. On the other hand, however, the structure should be retrofitted after each strong event in which damage occurs in the structure, and this can be very expensive and time consuming.

This capacity design approach also has another drawback: it is not able to mitigate vibrations that do not induce damage in the structure. This means that comfort aspects cannot be considered with this technique. So the problem of swaying of tall buildings caused by not very intense winds, for example, is not resolvable. It must be noted that, for very flexible structures such as long bridges or tall buildings, the comfort requirements can be more stringent than the ones related to the resistance.

For all these reasons the engineering community has moved towards the concept of "structural control". This means that the structure is regarded as a dynamic system in which some properties, typically the stiffness or the damping, can be adjusted in such a way that the dynamic effect of the load on the building decreases to an acceptable level. The natural frequency of the structure, its natural shape and the corresponding damping values are changed in such a way that the dynamic forces from the environmental loads are reduced. This can be done using a large variety of techniques that can be collected in four classes: passive, active, hybrid and semiactive. From an historical point of view, the first class of control techniques (passive) was extensively studied from both the theoretical and the experimental sides, and many practical realizations have already been implemented, especially in the USA, Japan,

China and Italy. A large number of researchers are still working in this field on a second generation of passive devices, while the first generation (for example, rubber bearings) needs only the approval of official designing and application rules for its certification.

Active control techniques have been studied extensively from a theoretical, numerical and, more recently, an experimental point of view. They are surely the most effective ones, but they also show some disadvantages (for example, the need for a lot of power to operate) that have lead to a low number of implementations. Hybrid techniques are a combination of the first two techniques, so their development directly follows that of the first two. Their application is still limited, even if some tuned mass dampers equipped with a little active mass driver were patented and installed in some buildings in Japan. Semiactive techniques are, at present, the most studied solution, from theoretical, numerical and experimental points of view, because of their excellent characteristics intermediate between those of active and passive techniques.

1.2 DEFINITIONS

Before entering into the core of the discussion, a clarification must be made about the terminology used in this book. The following definitions of some key terms are provided:

Definition 1 (Active Control) *An active control system is a system in which an external source powers one or many control actuators that apply forces to the structure in a prescribed manner. These forces can be used either to add or dissipate energy in the structure.*

In an active feedback control system, the signals sent to the control actuators are functions of the response of

the system measured by physical sensors. Active control makes use of a wide variety of actuators, including active mass dampers, hybrid mass dampers and active tendons, which may employ hydraulic, pneumatic, electromagnetic or motor-driven ball–screw actuation.

An essential feature of the active control system is that external power is used to effect the control action. This makes such systems vulnerable to power failure, which is always very likely during a strong environmental event.

Definition 2 (Passive Control) *A passive control system consists of an appended or embedded device that modifies the stiffness or the damping of the structure in an appropriate manner without requiring an external power source to operate and feeding energy to the system.*

Passive control devices impart forces that are generated by the mutual displacement of the two connection points of the device inside the protected structure. Passive control may depend on the initial design of the structure, on the addition of viscoelastic material to the structure, on the use of impact dampers, or on the use of tuned mass dampers. The initial design consists of tapered distributions of mass and stiffness, or uses techniques of base isolation, where the lowest floor is deliberately made very flexible, thereby reducing the transmission of forces into the upper storeys. The energy of a passively controlled structural system cannot be increased by the passive controller devices.

Though seldom as effective as active control, passive control has three main advantages:

1. It is usually relatively inexpensive.
2. It consumes no external energy.
3. It is inherently stable.

Definition 3 (Hybrid Control) *The common meaning of the term "hybrid control" implies the combined use of active and passive control systems.*

A hybrid control system may use active control to supplement and improve the performance of a passive control scheme. Alternatively, passive control may be added to an active control scheme to decrease its energy requirements. For example, as a structure equipped with distributed viscoelastic damping supplemented with an active mass damper on the top of the structure, or a base-isolated structure with actuators actively controlled to enhance performance.

It should be noted that the only essential difference between an active and a hybrid control scheme is, in many cases, the amount of external energy used to implement control. Hybrid control schemes alleviate some of the limitations that exist for either a passive or an active control acting alone, thus leading to an improved solution.

A side benefit of hybrid control is that, in the case of a power failure, the passive component of the control still offers some degree of protection, unlike an active control system.

Definition 4 (Semiactive Control) *Semiactive control systems are a class of systems for which energy is used to change the mechanical properties of the device.*

For this reason, usually the semiactive control system energy requirements are orders of magnitude smaller than typical active control systems. Typically, battery power is sufficient to make them operational. Semiactive control devices do not add mechanical energy to the structural system, therefore bounded-input bounded-output stability is guaranteed, in the sense that no instability can

occur, except for the considerations summarized in the last chapter of this book. Indeed, the system overall energy can be increased by adding a passive system! This depends on the external excitation. The passively controlled system may have resonances that coincide with the main excitation frequencies differently from those that happened before "appending" the passive device. In this case much more energy than in the unprotected case will go into the system. This means that bad performances can be obtained if passive or even semiactive systems are improperly tuned. Passive or semiactive devices can even be dangerous because they allow the external excitation to feed a system that would be (partially) isolated otherwise.

Semiactive control devices are often viewed as controllable passive devices. Preliminary studies indicate that appropriately implemented semiactive systems perform significantly better than passive devices and have the potential to achieve the performance of fully active systems, thus allowing for the possibility of effective response reduction during a wide array of dynamic loading conditions. Examples of such devices include variable-orifice fluid dampers, controllable friction devices, variable-stiffness devices, semiactive impact dampers, adjustable tuned liquid dampers, and controllable fluid dampers (with electrorheological and magnetorheological fluids) (Casciati 2004; Spencer and Sain 1997). Details are provided in Chapter 3.

1.3 SYSTEM REPRESENTATION

Dynamic system representation increases in complexity due mainly to the requirements of high accuracy and reliability to analyse complex functionalities and to represent device characteristics. Complex systems may have multiple

inputs and outputs, may be linear or non-linear and may be time invariant or time varying. A powerful technique for analysing such systems is the state-space approach, based on the concept of state. An essential benefit of this method is the combination of the concept of state and the capability of high-speed solution of differential equations by use of a digital processor. Furthermore the state-space approach is very general and can be applied to both linear and non-linear systems and to both time-invariant and time-variant systems.

Let us consider a linear time-invariant system formulated in the state space by the following equations:

$$\dot{\mathbf{x}}(t) = \boldsymbol{\mathcal{A}}\mathbf{x}(t) + \boldsymbol{\mathcal{B}}\mathbf{u}(t) \tag{1.1a}$$

$$\mathbf{y}(t) = \boldsymbol{\mathcal{C}}\mathbf{x}(t) + \boldsymbol{\mathcal{D}}\mathbf{u}(t) \tag{1.1b}$$

where

1. $\mathbf{x}$ is the $2n$-dimensional vector of the state variables,
2. $\mathbf{y}$ is the p-dimensional vector of the measurable variables,
3. $\mathbf{u}$ is the m-dimensional vector of the controllable and forcing variables,
4. $\boldsymbol{\mathcal{A}} \in \mathcal{R}^{2n\times 2n}$, $\boldsymbol{\mathcal{B}} \in \mathcal{R}^{2n\times m}$,
5. $\boldsymbol{\mathcal{C}} \in \mathcal{R}^{p\times 2n}$, $\boldsymbol{\mathcal{D}} \in \mathcal{R}^{p\times m}$.

This *state-space representation* is commonly used in structural control engineering.

The equation of motion of a generic system with n degrees of freedom can be considered:

$$\mathbf{M}\ddot{\mathbf{z}} + \mathbf{C}\dot{\mathbf{z}} + \mathbf{K}\mathbf{z} = \mathbf{F}(t) \tag{1.2}$$

where $\mathbf{M}$, $\mathbf{C}$ and $\mathbf{K}$ are square matrices of dimension n, $\mathbf{z}$ are the inter-mass displacements (in the case of a building

structure, the inter-storey displacements) and $\mathbf{F}(t)$ are the external forces. These forces can be generated by external excitations such as seismic disturbance or wind load. In controlled structures, these forces also include the actuators' load. Note that in the following, to retain agreement with the control engineering community, we will substitute the notation $\mathbf{F}(t)$ by $\mathbf{u}$.

By calling the displacement vector $\mathbf{x_1}$ and the velocity vector $\mathbf{x_2}$, the system represented by (1.2) can be rewritten in the following form:

$$\begin{cases} \dot{\mathbf{x}}_1 = \mathbf{x}_2 \\ \dot{\mathbf{x}}_2 = -\mathbf{M}^{-1}\mathbf{K}\mathbf{x}_1 - \mathbf{M}^{-1}\mathbf{C}\mathbf{x}_2 + \mathbf{M}^{-1}\mathbf{u} \end{cases} \tag{1.3}$$

or in state-space representation:

$$\begin{bmatrix} \dot{\mathbf{x}}_1 \\ \dot{\mathbf{x}}_2 \end{bmatrix} = \begin{bmatrix} \mathbf{0} & \mathbf{I} \\ -\mathbf{M}^{-1}\mathbf{K} & -\mathbf{M}^{-1}\mathbf{C} \end{bmatrix} \begin{bmatrix} \mathbf{x}_1 \\ \mathbf{x}_2 \end{bmatrix} + \begin{bmatrix} \mathbf{0} \\ \mathbf{M}^{-1} \end{bmatrix} \mathbf{u} \tag{1.4}$$

where the state matrix $\boldsymbol{\mathcal{A}}$ and the control matrix $\boldsymbol{\mathcal{B}}$ are given by:

$$\boldsymbol{\mathcal{A}} = \begin{bmatrix} \mathbf{0} & \mathbf{I} \\ -\mathbf{M}^{-1}\mathbf{K} & -\mathbf{M}^{-1}\mathbf{C} \end{bmatrix} \tag{1.5}$$

and

$$\boldsymbol{\mathcal{B}} = \begin{bmatrix} \mathbf{0} \\ \mathbf{M}^{-1} \end{bmatrix} \tag{1.6}$$

The output vector (1.1b) (or measurable variables) is a weighted sum of the state and control variables. Matrix $\boldsymbol{\mathcal{C}}$ is a weighting matrix that combines the states of the system (1.2), matrix $\boldsymbol{\mathcal{D}}$ is a weighting matrix that combines the control input, and the sum of these two quantities gives the output $\mathbf{y}(t)$. Because the direct action of control variable $\mathbf{u}$ on the output vector $\mathbf{y}(t)$ is often negligible, the matrix $\boldsymbol{\mathcal{D}}$ is null in most practical applications.

The transfer function $\mathbf{G}(s)$ related to system (1.1) can be very easily obtained with the following expression:

$$\mathbf{G}(s) = \boldsymbol{\mathcal{C}}(s\mathbf{I} - \boldsymbol{\mathcal{A}})^{-1}\boldsymbol{\mathcal{B}} + \boldsymbol{\mathcal{D}} \tag{1.7}$$

with s indicating the Laplace variable. It expresses the link between output and input Laplace transforms. It must be recalled that this representation is not applicable to non-linear systems.

Just for the sake of exemplification, a shear-type n-storey building is a good example of the use of the state-space representation in civil engineering. This type of building can be idealized as lumped masses at floors connected by springs and dashpots describing the columns' behaviour under horizontal loadings (Figure 1.1). These assumptions are true if the mass of the columns is one order of magnitude lower than the storey mass and if the floors are very rigid (and so are not subject to significant deformation). In practice the mass of the columns is incorporated in the mass of the floors. The stiffness and the damping are completely due to columns, walls, non-structural vertical elements.

In this case, the three matrices **M**, **C** and **K** can be obtained as follows. The forces acting on each storey are depicted in Figure 1.2. The inertial force due to the acceleration of the storey is proportional to the acceleration itself times the floor mass.

On both the lower and the upper side of the mass there are two forces: the viscous and the elastic forces. These forces are related to the inter-storey displacement and the inter-storey velocity.

Balancing all the forces acting on each storey, the generic equation for the i^{th} storey can be obtained:

$$\begin{aligned} m_i\ddot{z}_n + (c_{i+1} + c_i)\dot{z}_i + (k_{i+1} + k_i)z_i - c_{i+1}\dot{z}_{i+1} - c_i\dot{z}_{i-1} \\ -k_{i+1}z_{i+1} - k_i z_{i-1} = u_i \end{aligned} \tag{1.8}$$

where u_i is the generic control force acting on the i^{th} floor.

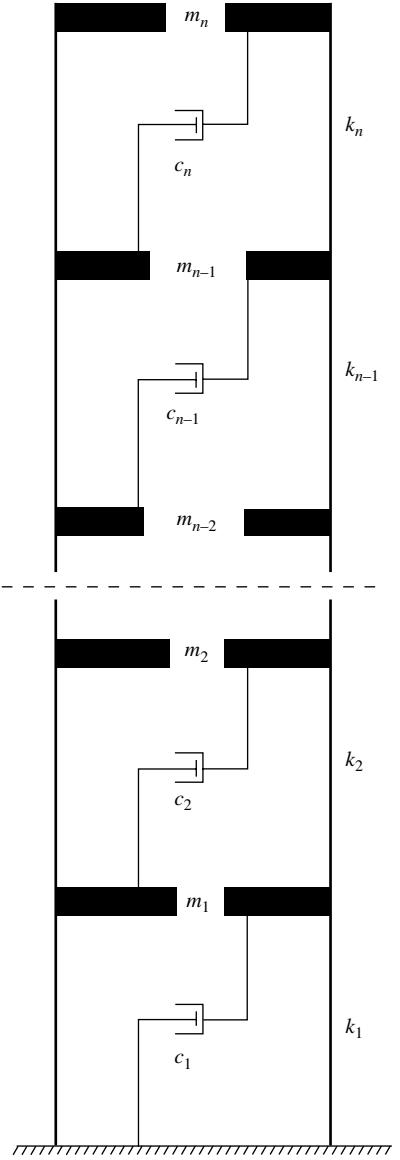

Figure 1.1 Simplified model of a multi-storey building

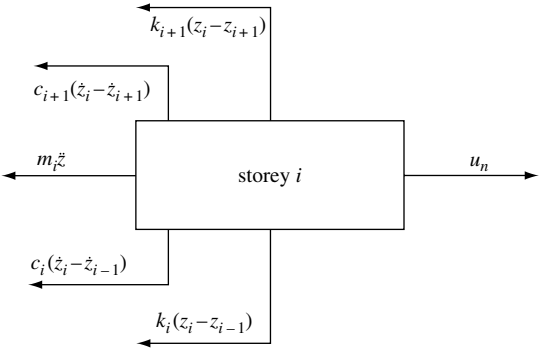

Figure 1.2 Forces acting on the i^{th} storey

After some calculations, **M**, **C** and **K** can be obtained from (1.8) as follows (the omitted terms are all zero):

$$\mathbf{M} = \begin{bmatrix} m_1 & & & & & \\ & m_2 & & & & \\ & & \ddots & & & \\ & & & m_i & & \\ & & & & \ddots & \\ & & & & & m_n \end{bmatrix}$$

$$\mathbf{C} = \begin{bmatrix} c_1 + c_2 & -c_2 & & & & & \\ -c_2 & c_2 + c_3 & -c_3 & & & & \\ & \ddots & \ddots & \ddots & & & \\ & & -c_i & c_i + c_{i+1} & -c_{i+i} & & \\ & & & \ddots & \ddots & \ddots & \\ & & & & -c_{n-1} & c_{n-1} + c_n & -c_n \\ & & & & & -c_n & c_n \end{bmatrix}$$

$$\mathbf{K} = \begin{bmatrix} k_1 + k_2 & -k_2 & & & & & & \\ -k_2 & k_2 + k_3 & -k_3 & & & & & \\ & \ddots & \ddots & \ddots & & & & \\ & & -k_i & k_i + k_{i+1} & -k_{i+i} & & & \\ & & & \ddots & \ddots & \ddots & & \\ & & & & -k_{n-1} & k_{n-1} + k_n & -k_n & \\ & & & & & -k_n & k_n & \end{bmatrix}$$

It can be observed that $\mathbf{M}$ is a diagonal matrix, while $\mathbf{C}$ and $\mathbf{K}$ are tri-diagonal. Matrix $\boldsymbol{\mathcal{A}}$ can be obtained from Equation (1.5). Matrix $\boldsymbol{\mathcal{B}}$ usually has more than one column: some of them are usually related to the forcing actions (such as the forces induced by the ground acceleration caused by an earthquake or given by the wind acting on the façade of the building) and can be obtained by Equation (1.6). The columns of $\boldsymbol{\mathcal{B}}$ related to the action of the control actuators must be evaluated following the idea that matrix $\boldsymbol{\mathcal{B}}$ will be a kind of topological operator indicating where the actuators are acting. For example, if this multi-storey building is equipped with only one actuator on the top floor, matrix $\boldsymbol{\mathcal{B}}$ is zero everywhere except for that degree of freedom. Matrix $\boldsymbol{\mathcal{D}}$, as already said, is usually set to zero.

As regards matrix $\boldsymbol{\mathcal{C}}$, it must be constructed according to the aims of the particular problem. One favourable choice is to use the identity matrix in order to have direct access to the states of the system: in this case each output is directly related with a state variable.

1.4 A COMPARISON OF PASSIVE, ACTIVE AND SEMIACTIVE CONTROL STRATEGIES

A brief comparison among passive, active and semiactive control strategies is given hereafter considering a single degree-of-freedom (SDOF) system. This system consists of

a rigid body representing a mass (that could be a machine) connected to a foundation by an isolator that consists of a spring and a damper. In this simple case the function of the vibration isolator is to reduce the amplitude of force transmitted from the vibratory mass to its foundation or to reduce the magnitude of motion transmitted from a vibratory foundation to the mass.

The transmissibility of this system is a measure of the reduction of transmitted force or motion provided by the isolator. If the source of vibration (excitation force) is attached to the mass, transmissibility is the ratio of the force amplitude transmitted to the foundation to the amplitude of the exciting force. If the source of vibration is a vibratory motion of the foundation (excitation motion), transmissibility is the ratio of the vibration amplitude of the mass to the vibration amplitude of the foundation.

Figure 1.3 shows the transmissibility of the system in terms of damping ratio ξ and frequency ratio β (where β is the ratio of the excitation frequency to the natural frequency). From this graphic representation it appears clearly that increased damping decreases the transmissibility for frequencies lower than the system's natural frequency multiplied by $\sqrt{2}$, but increases the transmissibility at higher frequencies. This means that the insertion of passive dissipation devices into a structure can sometimes lead to unwanted effects, especially during transient response (Pinkaew and Fujino 2001). Usually an augmented level of damping also induces a higher level of forces at some structural connection. With a semiactive device it is possible to adjust the damping in the most proper manner, for example using an on–off control law that switches the damping value from a high value to a low one. In the example of Figure 1.3 a switching frequency ratio β of 1.414 can be chosen. Using more sophisticated control laws (for example, skyhook control or clipping control, see

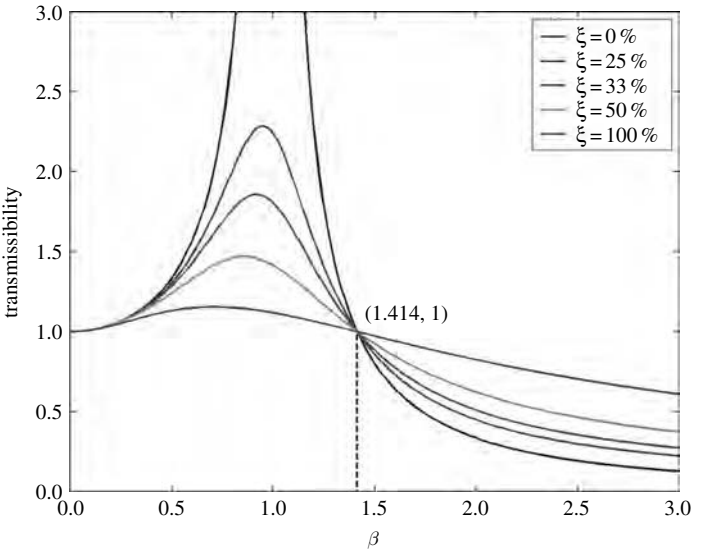

Figure 1.3 Transmissibility of a SDOF system for several values of supplemental damping

Chapter 4) performances comparable with active devices can be achieved.

Figure 1.4 summarizes this basic concept. The hatched region between the active and passive response curves is the theoretically possible working area of a semiactive system (for more details on the transfer function of semiactive systems see also (Pinkaew and Fujino 2001)). This figure has the advantage of showing in a very simple manner how the semiactive control is better than a passive one and how it can approach the performance of the active systems. However, in real applications, the damping is not the only critical parameter that can be modified. The forces that are present at the various storeys of the structure, the inter-storey drifts and the accelerations must also be attentively considered. It is usually necessary to obtain a balance among all these constrains.

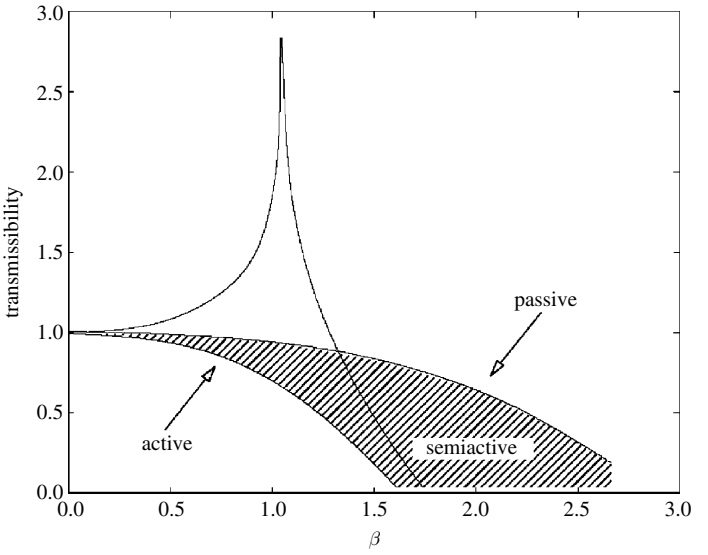

Figure 1.4 Transmissibility of a SDOF system with active, semiactive and passive control systems

To assume the role of structural designers again, one understands that safety against ultimate limit states can be matched by passive control ideas, provided quality control and maintenance plans are introduced in the management of the structure in use, due to the limited lifetime of such devices. To state a similar affirmation for active control systems would require the full availability of the corresponding devices. Nevertheless, such a high availability level is not required if the target is no longer safety against ultimate limit states, but serviceability or robustness. Such important features, however, do not justify the high costs of active control realizations. Semiactive solutions emerge from this discussion as the approach which could better fit a cost–benefit analysis in structural design.

2
Collocated and Non-collocated Systems

2.1 INTRODUCTION

This chapter mainly provides the definitions which allow the reader to frame the developments of the next chapters within the general theory.

2.2 DEFINITION OF COLLOCATED SYSTEM

A control system is collocated when the force generated by an actuator in a point of the structure is measured by a force sensor at the same location. This definition implicitly assumes that the transfer function that can be obtained is related to the same location of the structure. Under this hypothesis, and for an ideal situation in which the actuator and the sensor are connected exactly in the same location, the definition holds, but it is rather specific.

Following the way paved by (Curtain and Zwart 1995), but in a more mathematical language, Degryse and

Technology of Semiactive Devices and Applications in Vibration Mitigation Fabio Casciati, Georges Magonette and Francesco Marazzi

Mottelet (Degryse and Mottelet 2000) give a definition based on the relation between the control matrix $\boldsymbol{\mathcal{B}}$ and the output matrix $\boldsymbol{\mathcal{C}}$ (see Chapter 1 for the definition of the notation).

Definition 5 *When $\boldsymbol{\mathcal{C}} = \boldsymbol{\mathcal{B}}^T$ the sensors and the actuators are collocated.*

In this definition it must be considered that the operators $\boldsymbol{\mathcal{B}}$ and $\boldsymbol{\mathcal{C}}$ are defined up to some multiplicative constant. In fact the outputs of the measurement devices and the inputs of the actuators are voltages which are proportional to the physical quantities of interest. So normalization constants are inserted all along the formulation. Moreover, multiplying $\boldsymbol{\mathcal{B}}$ by some constant does not change the system.

Each time that the hypothesis in Definition 5 is satisfied, the feedback law $\mathbf{u} = -\mathbf{k}\mathbf{y}$, with $\mathbf{k} > \mathbf{0}$, provides the unconditional stability of the system (1.1).

The transfer function of the system (1.1) is

$$\mathbf{G}(s) = \sum_{k>0} \frac{\boldsymbol{\mathcal{C}}\phi_k \boldsymbol{\mathcal{B}}\phi_k^T}{s^2 + \lambda_k^2} s \tag{2.1}$$

where ϕ_k are the eigenvectors of $\boldsymbol{\mathcal{A}}$ and λ_k^2 are its eigenvalues ($k > 0$).

The transfer function is proved to be positive-real

$$G(s) > 0 \quad \text{for} \quad \mathcal{R}(s) > 0 \tag{2.2}$$

and positive-real systems can be stabilized by strictly positive-real gain matrices through negative feedback.

Besides this definition of collocation, a relaxation of the hypothesis is presented in (Degryse and Mottelet 2000). Unconditional stability is nevertheless preserved. In fact, it can be shown that if the following inequalities are verified

$$\boldsymbol{\mathcal{C}}\phi_k \boldsymbol{\mathcal{B}}\phi_k^T > 0 \quad k > 0 \tag{2.3}$$

then unconditional stability can be proved even if $\mathcal{C} \neq \mathcal{B}^T$. It can be shown that (2.3) implies that the transfer function (2.1) is positive-real, but the necessity of placing the sensors and the actuators at the same location still remains, at least when $\mathcal{B}$ and $\mathcal{C}$ are bounded, as shown in (Degryse and Mottelet 2000). This means that actuators and sensors must still have the same supports, even if it is possible to control an actuator using the input coming from a sensor placed in the location of another actuator.

A further point must be noted: if a time delay occurs, even if the collocation definition is respected, the transfer function is distorted. In practice, time delays that are much smaller than the system dynamics can be neglected (see Chapter 7). So, the hypothesis that no time delay occurs in the measurement and command chain should be present in civil engineering controlled structures.

2.3 CENTRALIZED AND NON-CENTRALIZED SYSTEMS

In the literature there is sometimes a little confusion between the pair collocated/non-collocated systems and the pair centralized/non-centralized systems (improperly called distributed and non-distributed systems by some authors). This confusion comes from the fact that a collocated system is likely to be also a non-centralized system and a non-collocated system a centralized system. But this is not always the case. The two concepts are different as briefly explained below.

Definition 6 *A system is considered centralized if the control system is managed by a unique computer that takes the inputs from all the sensors and gives the command outputs to all the actuators.*

The definition of non-centralized system follows consequently:

Definition 7 *A system is considered non-centralized if the control system is managed by several computers that take the input from some specific sensors and give the command outputs to some actuators.*

With these definitions in mind, it is evident that collocation has nothing to do with centralization: in some cases it may happen that a completely non-centralized system can also be a collocated system, but this is not compulsory. For example, one could conceive of a collocated system in which the control is performed by a central computer, or structures controlled by several sets of non-collocated control systems. This last situation can be used to avoid problems related to the failure of a portion of the whole control system.

2.4 LINEAR AND NON-LINEAR SYSTEMS

One distinguishes:

1. **Linear systems** in which the equations describing their dynamic behaviour are linear.
2. **Non-linear systems** in which the equations are no longer linear.

The first class is characterized by the linearity, which implies that the superposition principle can be applied and proportional causes give proportional effects.

The second class is rather a non-class, in the sense that every system not belonging to the first one naturally falls into this second one. In this case no general rules can be

assessed, even if some particular sub-classes may still be found.

In civil engineering applications, especially in earthquake engineering, non-linear behaviour is very common as a consequence of inelastic deformations and damage (Barroso 1999). This is especially true if no protection is added to the structure. If a control system is designed to help the structure to resist environment loads, it can be designed in order to maintain the structure in a linear range. In this case the real behaviour of the system can be linearized around an equilibrium point and the definition of a linear system still applies.

In the next sections of this chapter, the concept of transfer function is used, which is strictly related to the linearity of the system.

2.4.1 Properties of the Transfer Function

The following expression can be written (Preumont 1997):[1]

$$\mathbf{G}(\omega) \simeq \sum_{i=1}^{n} \frac{\phi_i \phi_i^T}{\mu_i(\omega_i^2 - \omega^2 + 2j\xi_i\omega_i\omega)} \tag{2.4}$$

where the sum extends to all modes, μ_i is the modal mass of mode i, ξ_i is the modal damping ratio, ω_i is the natural frequency of mode i and ϕ_i is the corresponding natural mode shape.

---

[1] The transfer function is defined by Equation (1.7). It shows its matrix nature there. The same transfer function can also be written in the Fourier domain ω instead of in the Laplace domain s. For this purpose, one writes $\mathbf{G}(\omega)$ instead of $\mathbf{G}(s)$. This transformation can be done very easily in this case, substituting s with $j\omega$ and s^2 with $-\omega^2$. The single entry $G_{lk}(\omega)$ expresses the complex amplitude of the structural response of degree of freedom l when the structure is exposed to a steady-state harmonic excitation $e^{j\omega t}$ at degree of freedom k.

For a limited frequency band, it is possible to select a sufficiently high index m with which to split (2.4) into two parts: the first one will respond dynamically and the part with high-frequency modes will respond statically:

$$\mathbf{G}(\omega) \simeq \sum_{i=1}^{m} \frac{\phi_i \phi_i^T}{\mu_i(\omega_i^2 - \omega^2 + 2j\xi_i\omega_i\omega)} + \sum_{i=m+1}^{n} \frac{\phi_i \phi_i^T}{-\mu_i\omega_i^2} \qquad (2.5)$$

or, in a different form,

$$\mathbf{G}(\omega) \simeq \sum_{i=1}^{m} \frac{\phi_i \phi_i^T}{\mu_i(\omega_i^2 - \omega^2 + 2j\xi_i\omega_i\omega)} + \mathbf{R} - \sum_{i=1}^{m} \frac{\phi_i \phi_i^T}{-\mu_i\omega_i^2} \qquad (2.6)$$

where $\mathbf{R}$ is the static contribution of all modes. It is independent of the frequency ω and introduces a feed-through component in the transfer matrix: part of the output is proportional to the input. Truncating the modal expansion of the transfer function without introducing a residual mode can lead to substantial errors in the calculation of the open-loop zeros and, as a result, of the performance of the control system.

With this in mind, consider the diagonal k^{th} term in Equation (2.6) for an undamped system:

$$G_{kk}(\omega) = \sum_{i=1}^{m} \frac{\phi_i^2(k)}{-\mu_i\omega_i^2} + \sum_{i=1}^{m} \frac{\phi_i^2(k)}{\mu_i(\omega_i^2 - \omega^2)} + R_{kk} \qquad (2.7)$$

Equation (2.7) is the transfer function between the input and the output of the corresponding degree of freedom, and, hence, allows one to study the behaviour of a collocated system.

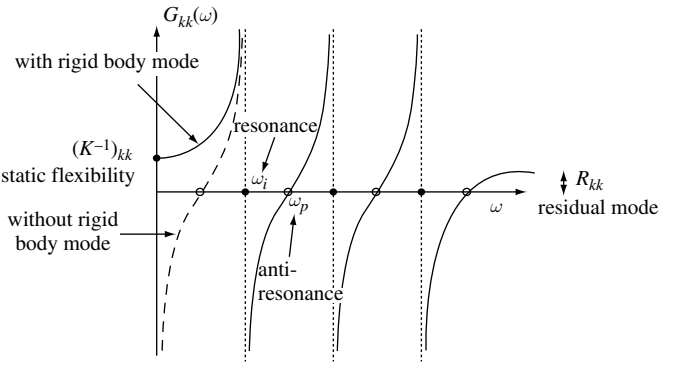

Figure 2.1 Transfer function of an undamped structure with collocated actuator and sensor

The behaviour of $G_{kk}(\omega)$ is represented in Figure 2.1 for a three degree-of-freedom system. The shape of this transfer function reflects the fact that the derivative of $G_{kk}(\omega)$ with respect to ω is always positive. This means that the function must always be increasing. It will go from $-\infty$ to $+\infty$ passing zero at the anti-resonance frequency. The amplitude of the transfer function goes to $\pm\infty$ at the resonance frequencies ω_i. A series of properties can be inferred:

- If there is no damping, control systems using collocated actuator and sensor pairs have alternate poles and zeros in the left-half complex plane, close to the imaginary axis. In the case of little damping (a very common case when unacceptable vibrations are observed), the poles and zeros still alternate near the imaginary axis of the left-half complex plane. This observation will be very useful for studying the stability.
- A harmonic excitation at an anti-resonance frequency produces no response at the degree of freedom where the excitation is applied: as can be seen from Figure 2.1, the

transfer function has a value of 0 at these points, so nothing is transmitted. This means that, at anti-resonance frequency, the structure behaves as if an additional restraint has been added to that point.

- In contrast to the resonance frequencies, the anti-resonance frequencies depend on the actuator location, so if another diagonal term $G_{kk}(\omega)$ is considered, the anti-resonance frequencies will, in general, change.

2.5 THE PROBLEM OF SPILLOVER

Generally speaking, any structure can be viewed as a distributed parameter system with an infinite number of degrees of freedom. A real physical system, in fact, always has infinite natural modal shapes and frequencies. Spillover is related to the discretization and the approximation of a continuous system to a finite degree-of-freedom system. From an engineering and practical point of view, it is common practice to operate two kinds of reduction to the number of degrees of freedom:

- a continuous system is discretized in a finite number of degrees of freedom (for example, using some finite element method (FEM) or by simplified considerations of mass and stiffness concentration in some structural members);
- the discretization of a system, especially if obtained with a FEM procedure, is often either too heavy to be treated by a control system or not economically feasible. Only the lowest and most meaningful frequencies are then taken into consideration.

These discretizations (the first approach is compulsory if numerical solutions are sought, while the second

simplification can be introduced or not, according to the complexity of the considered structure) lead to the consequence that the obtained model is able to describe only a part of the real system dynamics. The numerical model (often called the reduced model) will deal with the few dominant low-frequency modes.

In this scenario, when dealing with flexible structures, there is the danger that the state feedback based on the reduced model destabilizes the high-frequency remaining modes (also called "residual modes") which are not included in the model of the structure. This can lead to a destabilization of the reduced model. This phenomenon is called spillover.

2.5.1 Observation and Control Spillover

The sensor outputs are contaminated by the residual modes through the (so-called) observation spillover and the feedback control excites these modes through the control spillover (see Figure 2.2).

Pioneering work in the definition and study of spillover can be found in (Balas 1978), where the control and

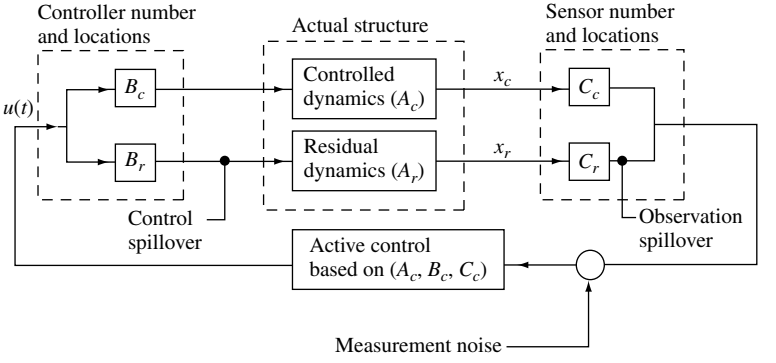

Figure 2.2 Control and observation spillover

observation spillovers due to residual (uncontrolled) modes are examined and the combined effect of control and observation spillover is shown to lead to potential instabilities in the closed-loop system. It is also proved that, if observation spillover is absent, control spillover itself cannot destabilize the system. In this case, control spillover causes unwanted excitation of the residual modes that can degrade the system response but cannot destabilize the system.

The same conclusions are achieved in (Meirovitch 1990). It is observed that, because the term given by control spillover has no effect on the eigenvalues of the close-loop system, it can be concluded that control spillover cannot destabilize the system, although it can cause some degradation in the system performance. So, only observation spillover is really dangerous.

Some solutions for reducing observation spillover are also proposed in the same book (Meirovitch 1990). As a rule of thumb, it can be greatly reduced by using a large number of sensors. The instability in the residual modes given by observation spillover can often be overcome by a small amount of inherent damping in the structure or can be eliminated if the sensor signals are prefiltered so as to screen out the contribution of the uncontrolled modes. However, this last solution is not as simple as it seems, because one must know in advance which are the uncontrolled modes. Direct output feedback control is proposed to avoid spillover, but in this proposal one does not consider that time delay can occur and can still generate instability.

A clear scheme of the two-stage model reduction procedure (the distributed parameter system to be controlled is first reduced to a many degree-of-freedom system discretized in space, then to a reduced order system with only

a small number of degree of freedom) is given in (Soong 1989). Since the control law design is based on this reduced order system, spillover is always possible.

For spillover reduction, it should be better to locate controllers and sensors at or very near the zeros of the affected modes, but this is usually quite impossible. Because the controller is designed taking into consideration only the lowest modes, a method that penalizes the highest and unmodelled modes should be preferred. Clearly this method can be effective only for spillover due to the second step of discretization, because the designer must know in advance which modes not to consider.

2.5.2 Mathematical Formulation

In order to see the effect of spillovers (both observable and control ones), let us consider a discretized system given by Equation (1.1), here rewritten for the reader's convenience:

$$\dot{\mathbf{x}}(t) = \boldsymbol{\mathcal{A}}\mathbf{x}(t) + \boldsymbol{\mathcal{B}}\mathbf{u}(t) \tag{2.8}$$

$$\mathbf{y}(t) = \boldsymbol{\mathcal{C}}\mathbf{x}(t) \tag{2.9}$$

where $\mathbf{x}(t)$ is the $2n$-dimensional state vector of the structural system with n degree of freedom, $\mathbf{u}(t)$ is the m-dimensional control vector and $\mathbf{y}(t)$ is the p-dimensional observation vector.

A reduced order model can be generated through aggregation or modal eigenfunction expansion techniques by retaining only the controlled modes of the system, giving

$$\dot{\mathbf{x}}_c(t) = \boldsymbol{\mathcal{A}}_c\mathbf{x}_c(t) + \boldsymbol{\mathcal{B}}_c\mathbf{u}(t) + \boldsymbol{\mathcal{E}}_c(t) \tag{2.10}$$

with the observation equation

$$\mathbf{y}(t) = \boldsymbol{\mathcal{C}}_c\mathbf{x}_c(t) + \boldsymbol{\mathcal{R}}_c(t) \tag{2.11}$$

In the above, $\mathbf{x}_c(t)$ is the controlled portion of the state vector $\mathbf{x}(t)$, whose dimension is in general much smaller. $\boldsymbol{\mathcal{E}}_c(t)$ and $\boldsymbol{\mathcal{R}}_c(t)$ are error terms introduced through the truncation process; they can be represented by

$$\boldsymbol{\mathcal{E}}_c(t) = \boldsymbol{\mathcal{A}}_{cr}\mathbf{x}_r(t) \tag{2.12}$$

and

$$\boldsymbol{\mathcal{R}}_c(t) = \boldsymbol{\mathcal{C}}_r\mathbf{x}_r(t) \tag{2.13}$$

where $\mathbf{x}_r(t)$ is the state vector associated with the residual (or uncontrolled) modes of the system (2.8). It is governed by

$$\dot{\mathbf{x}}_r(t) = \boldsymbol{\mathcal{A}}_r\mathbf{x}_r(t) + \boldsymbol{\mathcal{B}}_r\mathbf{u}(t) + \boldsymbol{\mathcal{E}}_r(t) \tag{2.14}$$

The error term $\boldsymbol{\mathcal{E}}_r(t)$ in the residual equation has the form

$$\boldsymbol{\mathcal{E}}_r(t) = \boldsymbol{\mathcal{A}}_{rc}\mathbf{x}_c(t) \tag{2.15}$$

The error term $\boldsymbol{\mathcal{E}}_c(t)$ in Equation (2.10) represents the modelling error due to the model reduction process. The term $\boldsymbol{\mathcal{B}}_r(t)\mathbf{u}(t)$ in Equation (2.14) shows the effect of control $\mathbf{u}(t)$ entering the residual subsystem, or control spillover, on the residual modes. The contamination of observation spillover in Equation (2.11) with residual information $\boldsymbol{\mathcal{R}}_c(t)$ produces observation spillover. Thus, the controller imparts energy to the residual modes through the interaction term $\boldsymbol{\mathcal{B}}_r(t)$ and the resulting residual mode excitation is detected by the sensors through the term $\boldsymbol{\mathcal{R}}_c(t)$ for the control design, resulting in an escalating degradation in performance.

These interactions are shown graphically in Figure 2.2. It can be shown that spillovers can reduce the stability margins of the actual structure and are at the heart of the control problem based on the reduced order models.

Clearly, the magnitude of the control and observation spillover is a function of the model reduction process. It is also a function of the controller and sensor locations and their effects on the residual modes. Spillover effect is important when the control design is carried out based on the reduce order model assuming that $\boldsymbol{\mathcal{E}}_c(t) = \mathbf{0}$ and $\boldsymbol{\mathcal{R}}_c(t) = \mathbf{0}$, but is applied to the full-order system given by Equations (2.8) and (2.9).

2.5.3 Physical Interpretation of Spillover

To give a more physical meaning to the above definition of spillover, a practical explanation of this effect is given hereafter with reference to Figure 2.3.

A force actuator is placed under a simple supported beam and is controlled via an active controller. The input signal to the control algorithm is given by a position sensor (in this case a laser transducer sensor) placed somewhere on the beam but not in the same position as the actuator. So the beam is controlled at a point measuring the displacement at a different point (this is the typical non-collocated architecture).

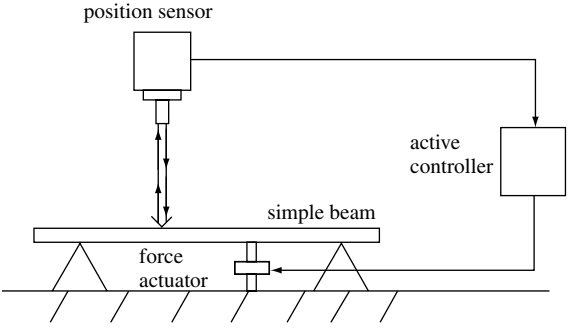

Figure 2.3 Control of a simply supported beam

In an ideal world, the actuator will exactly follow the command signal that the controller sends it and the sensor will exactly measure the current displacement without any delay. The controller will execute the algorithm instantaneously and communication times among the parts will be zero.

Even in this case, however, instability can occur because of the spillover phenomenon. The controlled beam, in fact, has its internal dynamics: this means that the waves generated by the actuator will propagates along the beam. A continuous beam has infinite natural modes but only a few of them can be taken into account when designing the control law. This means that there will surely be some modes that the control strategy has not been designed for. If the sensor is placed at a distance that is a multiple of the half wavelength of the displacement travelling wave of an uncontrolled beam mode, the resulting signal could be a displacement with an inverted sign with respect to the displacement at the location of the force actuator.

This mode has not been properly taken into account in the design process of the non-collocated control law, so it may happen that the algorithm commands the actuator to generate forces that excite the beam instead of stopping it.

This means that the dynamic behaviour of the beam must be considered in the controller design with the highest possible definition. Obviously, in the controller process design it is not realistic to consider more than a few modes, usually just the modes associated with the lower frequencies. This means that the controller can give improper command signals to the actuator due to the lack of the highest modes.

If there is no observation spillover, however, control spillover cannot destabilize the system, even if it can induce cyclic oscillations, as emphasized in Section 2.5.1.

2.6 ADVANTAGES AND DISADVANTAGES OF COLLOCATED AND NON-COLLOCATED SYSTEMS

In order to achieve an unbiased judgement about the opportunity of adopting a collocated or a non-collocated control system, the main characteristics of these two schemes will be discussed extensively below. It is important to note that no best solutions can be taken a priori, because the right choice depends on the particular needs and on the control systems for that particular case. Constraints are different from one situation to another and they must be evaluated by the control designer.

2.6.1 Robustness

As was explained in the previous sections, depending on the control law and the actuator dynamics, theoretically speaking a collocated control system is inherently stable. This is true only if the system is strictly collocated in the sense of Definition 5 and if there are no delays in the measurement chain, the actuator is ideal, no saturation effects occur, etc. In this case it was shown that the transfer function has poles and zeros alternating on the left side of the imaginary axis and the root locus gives a trajectory always included in the left part of the complex plane. This means that any chosen gain of the control system ensures stability, the remaining question being to choose the optimal gain value.

The robustness of some collocated strategies is also related to the fact that, for a particular choice of control law, they do not require a description of the mathematical model in order to run properly: this means that the control system can be designed and optimized with nominal values for the parameters involved and it will work even

in non-nominal conditions. In the latter case, the efficiency will probably decrease, but stability is related only to local considerations and is independent of the real behaviour of the structure, so only optimality is lost. In conclusion, collocated systems can be considered inherently robust.

A non-collocated control system is always subject to spillover problems, regarding either observation spillover or control spillover, as mentioned earlier. This problem is inherent in the non-collocated control system itself, where a model of the structure to be controlled is needed and, even in the best situation, it is a discretization of a continuous structure. Moreover, one must consider that the root locus of a non-collocated system can pass from the left part of the complex plane to the right one (and vice versa), so the control system can be very sensitive to any distortion from the nominal design situation.

These two problems (spillover and non-nominal working conditions) can, however, be addressed quite efficiently with modern robust control techniques. For example, with μ-synthesis techniques a robust control design can be performed taking into account the unmodelled high dynamics and the possible variation of some parameters in bounded intervals. With this technique one accepts that the nominal gain is no longer the optimal one (so we lose a little in efficiency in the nominal situation), but in exchange one is mathematically sure that the system will remain at least stable in the range of variation of the parameters (and is usually quite efficient, too).

Another important question is: what happens if a sensor or an actuator fails?

Assuming that a sensor fails, two cases can be considered:

- the signal falls to zero value;
- the signal assumes a static value (for example, 1 or any other saturated value).

In principle, the control system can be designed to bypass the signal coming from the bad sensor (Casciati and Rossi 2004). In a collocated control system the corresponding actuator could be switched off, while in the non-collocated control strategy a new control algorithm avoiding that signal can be adopted.

A more difficult situation must be faced when the sensor is not responding or is delivering a wrong signal due to mismatch of gain, an offset, noise corruption, and so on. In this case it is very difficult for the control system to detect the sensor fault. But a system must remain robust, i.e., the overall behaviour of the control system must to remain stable even in the presence of faults and errors.

One strategy for strengthening robustness could be the use of redundancy measurements (Noltingk 1996) (which is common practice in nuclear power plants, for example) in order to accept that some sensors can give wrong values. Three measures can be taken for each quantity and the mode value can be assumed as the right one. In this case it is sufficient that only two sensors are measuring the right value. With three sensors it is also possible to control the failure of any sensor: if the mean value of two sensors is quite close to the value of the third, all is going well; on the contrary, one or more sensors have surely failed. An alternative approach is illustrated in (Faravelli and Rossi 2003).

2.6.2 Performance

Collocated control systems can be very efficient when they are used to provide supplementary damping to structures. From a theoretical point of view, however, they cannot reach the high performances of non-collocated systems. A non-collocated control system, as already mentioned, needs to have a properly designed model of the structure: this means that the level of optimization that can be

reached is considerably higher than in a collocated case in which the control system does not take into account the global behaviour of the structure, but only the very local one. This is especially true in positioning control problems, where the whole of the structure must assume a given configuration.

2.6.3 Realization Aspects

It is very difficult to deal with realization aspects if both the structure, where the control system will be applied, and the control system itself are not yet chosen. Since a very large number of variables are involved, no preference can be given a priori to a collocated or non collocated strategy from the point of view of practical realization.

A collocated system is generally easier to implement. For programming the controller, in fact, it is not necessary to have a complete model of the structural system, but just a rough idea about the interesting frequencies involved.

2.6.4 Simplicity

Mounting the actuators and sensors in a real environment is always an important and expensive task.

With a non-collocated control strategy, both actuators and sensors must be put in communication with one or more computers where the control law is implemented. It may be a problem to install the transmission cables inside the structure, because proper locations must be found in order to avoid vandalism or weather damages. Wireless solutions are currently being pursued (Casciati et al. 2003a; Faravelli and Rossi 2003; Casciati and Rossi 2004).

On the contrary, a collocated system can be very compact and complete in itself, in the sense that the actuator,

the sensor and the processor can be integrated in a single device. In this case there is no longer a need for cable connections and the mounting phase consists only of some mechanical operations, but no electronic connections must be arranged.

The amount of electrical power required by the device is related more to the type of control than to the adopted strategy:

- for semiactive control a low-power electrical supply is sufficient;
- for active control systems a large amount of electrical (or hydraulic) supply is needed.

This influence the realization, so semiactive device are much easier to install than active ones.

2.6.5 Economical Aspects

An a priori comparison between collocated and non-collocated control system costs is very difficult. The required implementation time makes a difference. As already explained, usually non-collocated systems need a deeper design, so they should be more expensive. Moreover the production of collocated systems can be easily industrialized, so the unit price should decrease. However, at the moment, only a few standard products are available on the market oriented to civil engineering applications.

The cost problem is much more related to the issue of efficiency and robustness than to the collocated or non-collocated structure. If one uses very precise sensors and actuators, in fact, one can achieve better results, but at a higher cost. However, the precision of sensors must be compatible with the accuracy of the actuators and vice versa.

2.7 A NUMERICAL COMPARISON

The control problem of a shear-type frame structure subject to dynamic loads such as earthquakes or strong winds is addressed here from the point of view of a comparison between collocated and non-collocated control strategies. The core of this comparison is to answer the following questions:

1. Which approach has the best performance (for example, comparing the resulting transfer function)?
2. Which is the most robust approach (for example, when any sensor fails)?
3. Which is likely to be the best compromise between these two possibilities?

As will be shown, even in the simple case of a 10-storey building with an equal distribution of masses, stiffnesses and dampings, a general answer to these questions cannot be given.

The structure taken into consideration is the n-storey building of Figure 1.1 with an equal distribution of masses, stiffnesses and dampings at each storey.

Only the case of decentralized control is considered, so that each actuator works on its own. Even in the case when there is an actuator at each storey, they work independently of each other. In the following $A1$ denotes the actuator placed at storey 1, $A2$ the actuator placed at storey 2, and so on.

There is only one sensor at each storey, giving displacement, velocity or acceleration, and, in analogy with what was defined for actuators, $S1$ denotes the sensor placed at floor 1, and so on.

Preliminarily, the possibility of having a single actuator at any storey utilizing a variable number of sensors was considered. This means that, by choosing the actuator placed at the first storey ($A1$), one has the possibility of controlling it by using the signal coming from the sensor placed at the first floor, or from the sensor placed at the second floor, or from the sensor placed at any floor of the building. There is also the possibility of feeding the control law with two signals coming from two different floors of the building, and so on, with every combination of sensors.

For a three-storey building one has the following choices:

$$\{S1;\ S2;\ S3;\ S1+S2;\ S1+S3;\ S2+S3;\ S1+S2+S3\}$$

because the actuator can use one of the three signals coming from the different storeys, or two of them, or eventually all of them.

The total number of combinations that can be found for a generic building is given by the following equation:

$$N=\sum_{k=1}^{n}\binom{n}{k} \tag{2.16}$$

where n is the number of storeys and k is the number of sensors that the actuator can use simultaneously. Given in Table 2.1 are the results of Equation (2.16) for various numbers of storeys.

It can be seen from Table 2.1 that the number of combinations grows very quickly, so the number of possibilities to

Table 2.1 Possible combinations N for a n storey building with an actuator feeded by a variable number of sensors

n	1	2	3	4	5	6	7	8	9	10	11	12
N	1	3	7	15	31	63	127	255	511	1023	2047	4095

explore becomes extremely high as soon as the number of storeys increases. Incidentally, some of these possibilities are feasible but, in practical applications, not useful.

The next step was to consider that the actuator could be at any storey of the structure, the number of possible combinations of actuator and sensor positions being given by the following equation:

$$N = n \sum_{k=1}^{n} \binom{n}{k} \tag{2.17}$$

In this case the number of possible combinations is given in Table 2.2.

The last step was to consider the fact that more than one actuator can simultaneously be present on the structure. In this case the equation that gives the total number of combinations becomes

$$N = \left[\sum_{k=1}^{n} \binom{n}{k} \right]^2 \tag{2.18}$$

The results for buildings up to 10 storeys are given in Table 2.3.

Table 2.2 Possible combinations N for a n storey building with an actuator placed somewhere and a variable number of sensors

n	1	2	3	4	5	6	7	8	9	10	11	12
N	1	6	21	60	155	378	889	2040	4599	10230	22517	49140

Table 2.3 Possible combinations N for a n storey building with a variable number of actuators and sensors

n	1	2	3	4	5	6	7	8	9	10
N	1	9	49	225	961	3969	16129	65025	261121	1046529

2.7.1 Case Study: A Five-storey Reinforced Concrete Building

Taking into account the preliminary discussion and moving towards a numerical comparison between collocated and non-collocated strategies in the case of a significant number of storeys (greater than three), only a restricted number of the previous combination sets were considered. In particular the study was restricted to the case in which there is an actuator at each storey that uses for its feedback control law:

- the only sensor located at the same storey;
- the sensor located at the same storey and two other sensors, one at the upper floor and the other at the lower floor;
- the sensors at every storey.

These three possibilities are quite realistic, because to use only one sensor for each storey is the cheapest way to achieve control and, in the meantime, is the case in which the sensors are collocated, one by one, with the actuators. The case of an actuator using the sensor placed on its own storey and the sensors immediately on the upper and lower ones is a straight generalization of the previous case. The case in which each actuator uses the information coming from all sensors is also interesting because, if the sensors are already placed on the structure, the additional cost and complexity can be compared with the potential benefits.

In this study these sensors are supposed to measure velocity and displacement, but the generalization to acceleration sensors is straightforward. This assumption was considered because a linear quadratic regulator (LQR) controller was designed and for this type of controller full state knowledge is necessary.

Figure 2.4 sketches the considered building, where storey 1 is the lower one. The three matrices of Section 1.3 are:

1. The mass matrix **M** (in kg):

$$\mathbf{M} = \begin{pmatrix} 95538 & 0 & 0 & 0 & 0 \\ 0 & 95538 & 0 & 0 & 0 \\ 0 & 0 & 95538 & 0 & 0 \\ 0 & 0 & 0 & 95538 & 0 \\ 0 & 0 & 0 & 0 & 95538 \end{pmatrix} \tag{2.19}$$

2. The stiffness matrix **K** (in kN/m):

$$\mathbf{K} = \begin{pmatrix} 300334 & -140086 & 0 & 0 & 0 \\ -140086 & 280568 & -140482 & 0 & 0 \\ 0 & -140482 & 276496 & -136014 & 0 \\ 0 & 0 & -136014 & 272775 & -136761 \\ 0 & 0 & 0 & -136761 & 136761 \end{pmatrix} \tag{2.20}$$

3. Assuming, as already stated, a damping value of 5% on the first and third modes, the following damping matrix **C** (in N s/m) can be obtained with the Raleigh method:[2]

$$\mathbf{C} = \begin{pmatrix} 573150 & -226670 & 0 & 0 & 0 \\ -226670 & 541170 & -227310 & 0 & 0 \\ 0 & -227310 & 534580 & -220080 & 0 \\ 0 & 0 & -220080 & 528560 & -221290 \\ 0 & 0 & 0 & -221290 & 308480 \end{pmatrix} \tag{2.21}$$

[2] We must recall that the Raleigh method, in a first step, provides the damping matrix that gives the requested damping on the first and the third modes and only in a second step can the inter-storey damping values be calculated. This second step must usually be performed in an approximate way, because, as in this case, the damping matrix can be a little different from the typical matrix configuration coming from shear-type behaviour.

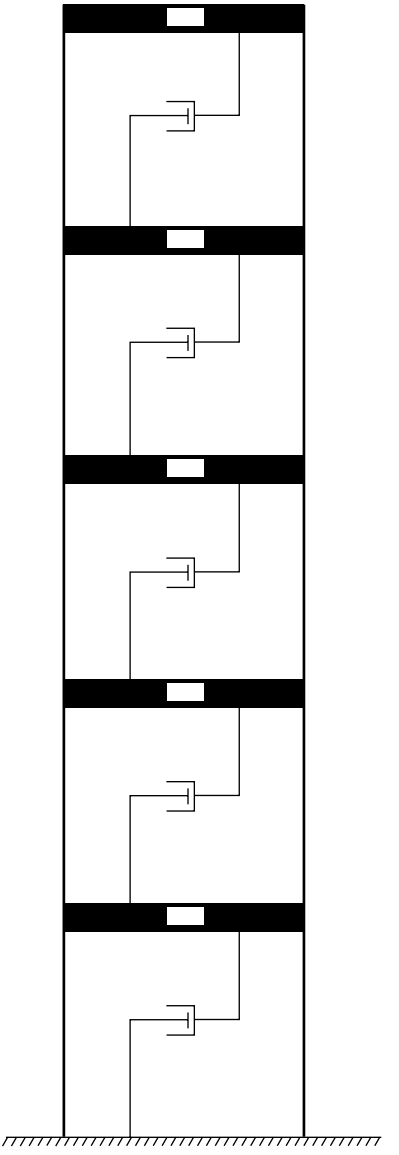

Figure 2.4 Sketch of the five-storey reinforced concrete building

From the above matrices, it is easy to calculate the five natural frequencies of the building (in Hz):

$$1.7715 \quad 5.1245 \quad 8.0646 \quad 10.2631 \quad 11.6678$$

and the corresponding modal shapes (each mode being normalized to 1):

	Mode 1	Mode 2	Mode 3	Mode 4	Mode 5
Storey 1	0.2539	0.6960	1.0000	0.9177	0.6557
Storey 2	0.5228	1.0000	0.3928	−0.6350	−0.9975
Storey 3	0.7469	0.5981	−0.8986	−0.3875	1.0000
Storey 4	0.9135	−0.2525	−0.6118	1.0000	−0.7120
Storey 5	1.0000	−0.9156	0.7708	−0.5250	0.2585

Moreover, using sub-matrices extracted by the global matrices above, a LQR controller was designed with $\mathbf{R} = 1$ and $\mathbf{Q}$ equal to the total energy[3] of the system (kinetic+elastic) and so equal to

$$\mathbf{Q} = \begin{pmatrix} \mathbf{K} & \mathbf{0} \\ \mathbf{0} & \mathbf{M} \end{pmatrix} \tag{2.22}$$

In any case, each actuator is designed to work independently of the others, the only difference among the three cases being the number of sensors it uses (Marazzi 2003).

[3] This is a possible choice, but several others could be performed in this example. The important thing to bear in mind is that the weighting function in the three cases must have a physical meaning in order to compare these different controlling schemes. Here the meaning of assuming the $\mathbf{Q}$ matrix equal to the total energy of the considered storey is to show that, if the energy of a larger number of storeys is taken into consideration, the results can be much improved.

2.7.1.1 Comparisons in the Frequency Domain

The transfer function of the uncontrolled structure versus the controlled one (with one sensor for each actuator, three sensors and all sensors) was analysed. The results are shown in Figure 2.5.

The dotted line represents the uncontrolled structure. The peaks relative to the five natural frequencies of the building are clearly shown: the sharpness of these peaks indicates that the natural damping is quite low. The dashed dot and the dashed lines represent respectively the controlled structure in which each actuator uses one or three sensors. It is clear that the behaviour of the controlled

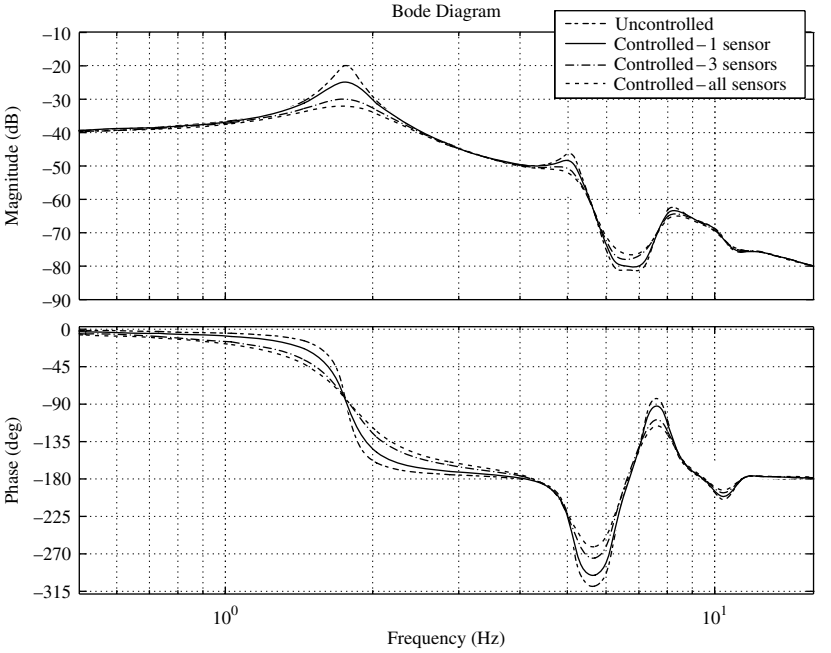

Figure 2.5 Comparison among transfer functions between ground acceleration and displacement at the fifth floor with different schemes of controlling action

structure is better by far than in the uncontrolled situation. The solid line represents the case in which each actuator has full information. This case is much better than the one-sensor case, but significant improvements are not obtained with respect to the three-sensor case. This fact suggests that the information coming from storeys far away from the actuator is not important, so it may not be useful to have full state feedback. This can also be physically interpreted by observing that the controllability of a storey decrease with its distance from the actuated floor, so, on the other hand, the vibration of a distant floor will not greatly influence the movement of the controlled storey.

The comparison in the frequency domain is very useful if a linear behaviour is expected from both the building and the actuating system.

2.7.2 Comparisons in the Time Domain

In case of non-linear effects, due for instance to sensor failures, time domain analysis must be performed. These simulations must be done skilfully, because the input must necessarily be a specific excitation time series and it may be that it does not excite the building in a critical way.

For this purpose, a Simulink® model was developed. In order to have a general scheme for testing a building with a chosen number of floors, the model is based on a physical balance of forces in which each storey is modelled independently from the others (see Figure 2.6).

The model of each storey forms a block with five inputs and two outputs. The five inputs are:

1. **Force:** this is the external force acting upon the storey. It can be an external force coming from wind, earthquakes or other environmental loads or a control force caused by an actuator or the resultant of the sum of the two.

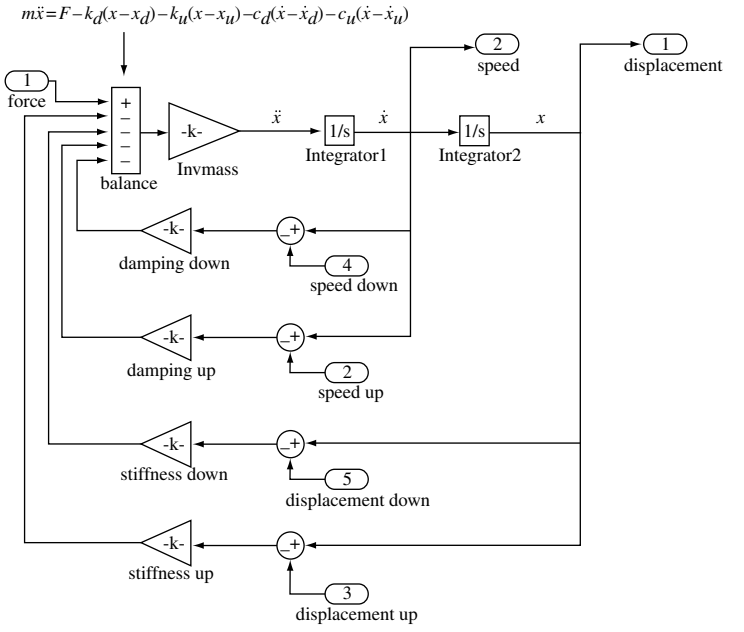

Figure 2.6 Simulink model of a single storey

2. **Displacement up:** this is the displacement of the upper storey. This signal, subtracted from the actual value of the displacement in the considered storey and multiplied by the stiffness value of the columns connecting the actual storey with the upper one, enters in the force balance
3. **Displacement down:** this is the displacement of the lower storey. Similarly to the previous case, it is subtracted from the actual value of the displacement in the considered storey and multiplied by the stiffness of the lower floor, and enters in the force balance.
4. **Speed up:** this is the velocity of the upper storey. This signal, subtracted from the actual value of the velocity in the considered storey and multiplied by the

damping value of the upper floor, enters in the force balance.

5. **Speed down:** this is the velocity of the lower storey. This signal, subtracted from the actual value of the velocity in the considered storey and multiplied by the damping value of the lower floor, also contributes to the force balance.

The two outputs are:

1. **Displacement:** this is the actual displacement of the storey.
2. **Speed:** this is the actual velocity of the storey.

A summation block subtracts the damping and elastic forces coming from the upper and lower storeys from the external force acting on the floor. The resulting signal is the inertial force of the storey. By dividing this signal by the mass value of the floor, the acceleration can be computed. The acceleration is then integrated once to obtain velocity and twice to obtain displacement.

As mentioned at the beginning of the section, the failure of sensors could become significant. As a result of the conducted time analysis (Marazzi 2003), the failure of one sensor is critical if it refers to the controlled storey, while the performance is not so badly affected if the failure refers to a sensor far away.

3
Semiactive Devices

3.1 THE BASIC IDEA AND A BRIEF HISTORY

This chapter presents the main types of semiactive devices conceived and implemented for civil engineering applications. This means that passive and active devices will not be mentioned here, even if some of the described devices can be seen as an adaptation of passive or active solutions.

It is worth noting that, from the semiactive control point of view, it does not make sense to speak of actuators (as in active control), because semiactive devices can only generate forces in a passive way, but they are unable to provide any force. The force that the semiactive devices generates is always related to the relative velocity and displacement of their ends.

As mentioned in Section 1.2, the basic idea of semiactive control is very simple: to change "on-line" the characteristics of a passive dissipation device. This requires a minimum amount of energy to turn the mechanical component devoted to the changing behaviour of the system (a valve, for example, or a bolt friction connection). The main advantage is to join the simplicity and reliability of a passive device to the adaptability of the active systems.

The semiactive control concept was introduced for the first time by (Karnopp et al. 1974) who proposed to modify

Technology of Semiactive Devices and Applications in Vibration Mitigation Fabio Casciati, Georges Magonette and Francesco Marazzi

the force of a fluid damper controlling the opening of a valve. They had automotive applications in mind, so their target was to obtain a better isolation of the vehicle from the roughness of the road.

The first proposal for semiactive control of civil structures can be found in (Hrovat et al. 1993). In that work the concept of semiactive control was extended to civil buildings, proposing a tuned mass damper that was connected to the main structure with a semiactive viscous damper. The proposed device was a variable-orifice damper.

Karnopp et al.'s idea was based on an anti-lock braking system (ABS), which, of course, is a technology closely related to the same automotive field. In the case of ABS braking, the main concern is the avoidance of sticking in a frictional interface while, in the case of semiactive damping, the main aim is to dissipate energy as quickly as possible. The two objectives are different but they are very much interconnected because both deal with the problem of allowing a relative movement of two parts. A sticking interface cannot dissipate energy, in fact. The optimal friction value is not constant, so the best device can adapt itself to these changes.

Since that time, many studies have been conducted from the point of view of both control strategies and implemented devices. New hardware and software capabilities allow the design of more sophisticated control laws, while, in addition, new materials such as magnetorheological liquids are now available to permit proper device design. In the next chapter the main control strategies present in the literature will be described, while the most promising devices are illustrated in the remainder of this chapter.

A variable-orifice damper can be achieved by using an electromechanical valve to alter the resistance to flow of a conventional hydraulic fluid damper. The valve enable such a device to deliver a wide range of damping level.

The size of the orifice can be modulated based on the measured response of the structure. As a result, the force–velocity relation in the damper is a variable function that can be controlled in real time.

Variable-friction dampers dissipate vibrational energy in a structural system by utilizing forces generated by surface friction. The ability of such devices to reduce drifts within high-storey buildings that are seismically excited has been successfully investigated. Furthermore friction-controllable systems are commonly employed in conjunction with seismic isolation systems.

Another type of semiactive device utilizes the motion of a sloshing fluid or a column of fluid to reduce the responses of a structure. These adjustable tuned liquid dampers are based on passive tuned sloshing dampers and tuned liquid column dampers.

Finally, one of the most promising classes of semiactive control devices is the magnetorheological (MR) damper. The outstanding characteristic of these fluids is their ability to change reversibly in milliseconds from free-flowing, linear viscous liquids to semisolids having controllable yield strength when exposed to a magnetic field.

3.2 VARIABLE VISCOUS DEVICES

This first class of devices is the oldest, but still frequently adopted. A viscous device can be obtained by a hydraulic piston in which a flux is allowed to pass from one chamber to the other. If the orifice that allows the flux between the two chambers has a constant opening, the device is a passive viscous damper, but if the flux intensity can be adjusted on-line by mean of a servo-valve orifice, the device assumes a semiactive nature. Note that, for a fixed position of the servo-valve, the behaviour of the device is

exactly like that of the corresponding passive version, but the advantage, in this case, is that the viscous coefficient characterizing the device can be adjusted on-line accordingly with a prescribed control law. This type of actuator is shown in Figure 3.1.

The phenomenological model of these devices is usually written in the form of a linear viscous element with controllable damping characteristics given by

$$F(t) = C_{adapt}(u)v(t) \quad \text{with} \quad C_{min} \leq C_{adapt} \leq C_{max} \tag{3.1}$$

where C_{adapt} is the actual damping value of the device (that is, a function of the control variable u), $v(t)$ is the velocity of device deformation (given by the difference between the velocities at the two ends of the device) and C_{min} and C_{max} are the minimum and the maximum damping value that the device can achieve with the orifice completely opened or closed.

Note that a linear opening of the valve does not necessarily reflect in a linear changing behaviour through C_{min} and C_{max}: a prior identification of the device is necessary properly to command the control signal u of the servo-valve. The reader is referred to (Karnopp et al. 1974; Karnopp 1990; Patten et al. 1994).

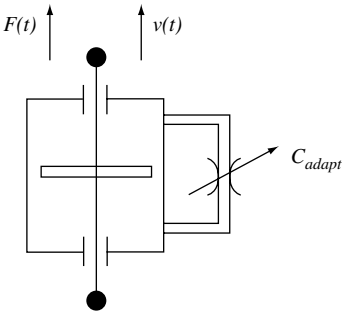

Figure 3.1 Variable-orifice damper

A special case of this continuous variable damping is the "on–off" device, in which the valve can only assume two values: completely open or completely closed. These types of devices are usually simpler than the continuous ones, but they have a lower performance.

If the device is equipped with a magnetorheological or electrorheological fluid (controllable fluid damper), the flux between one chamber and the other can be adjusted by changing the magnetic or electrical field around the bypass from one chamber to the other. This kind of device will be discussed later in the section devoted to magnetorheological devices.

3.3 VARIABLE STIFFNESS DEVICES

This class of devices was proposed to avoid, in real time, resonance phenomena: by varying the stiffness of the structure, it is possible to vary the natural frequency of the structure in order to have always a convenient response to external excitations.

The phenomenological model for these types of devices is given by

$$F(t) = K_{adapt}(u)[\delta(t) - \delta_0(t)] \quad \text{with} \quad K_{min} \leq K_{adapt} \leq K_{max} \tag{3.2}$$

where K_{adapt} is the actual stiffness of the device (that is, a function of the control variable u), and $\delta(t) - \delta_0(t)$ is the deformation of the device (given by the difference between the positions of the two ends of the device). K_{min} and K_{max} are the minimum and the maximum stiffness that the device can induce in a portion of the structure.

Also in this case the "on–off" device is a particular solution in which the stiffness can vary between two values: for

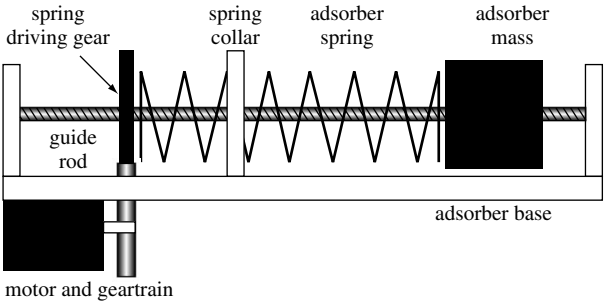

Figure 3.2 Variable tuned mass damper

example, a lower value in which a bracing system is ineffective and another value in which the bracing contributes to the structural stiffness.

One of the most common schemes for these devices consists in bracing that can vary its stiffness accordingly to a control law. This is usually achieved by means of hydraulic devices that can clamp the bracing to the structure. In this case the semiactive stiffness device is coupled to a semiactive damping device: the result is a varying viscoelastic device.

Another interesting way for varying stiffness is the adapted tuned mass damper scheme (Figure 3.2) in which the stiffness of an helicoidal spring can be modified by varying (thanks to an electric motor) the number of coils of the spring.

3.4 MAGNETORHEOLOGICAL DEVICES

Before describing these devices (Spencer and Sain 1997), some characteristics of magnetorheological fluids (compared with electrorheological ones) are reviewed.

In 1947, W. Winslow observed a large rheological effect (apparent change of viscosity) induced by the application

of an electric field to colloidal fluids (insulating oil) containing micrometre-sized particles; such fluids are called electrorheological (ER) fluids. The discovery of MR fluids was made in 1951 by J. Rabinow, who observed similar rheological effects by the application of a magnetic field to a fluid containing magnetizable particles. In both cases, the particles create columnar structures parallel to the applied field (Figure 3.3) and these chain-like structures restrict the flow of the fluid, requiring a minimum shear stress for the flow to be initiated. This phenomenon is reversible, very fast (response time of the order of a millisecond) and consumes very little energy. When no field is applied, the rheological fluids exhibit a Newtonian behaviour.

Typical values of the maximum achievable yield strength τ are given in Table 3.1. ER fluid performances are generally limited by the electric field breakdown strength of the fluid while MR fluid performances are limited by the magnetic saturation of the particles. Iron particles have the highest saturation magnetization. In Table 3.1, one can see that the yield stress of MR fluids is from 20 to 50 times larger than that of ER fluids. This justifies why most practical applications use MR fluids. Typical particle sizes are

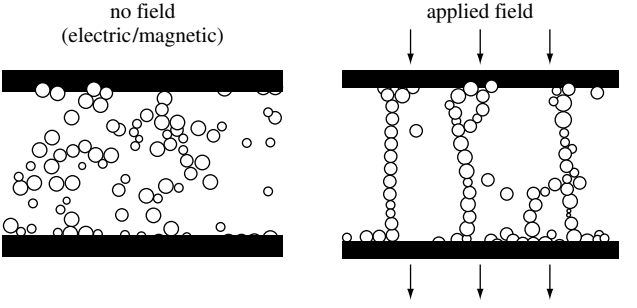

Figure 3.3 Chain-like structures formed under the external applied field

Table 3.1 Comparison of typical ER and MR fluid properties

Property	ER fluid	MR fluid
Yield strengh τ	2–5 kPa	50–100 kPa
Max. field	3–5 kV/mm	150–250 kA/m
Viscosity (no field, 25°C) η	0.2–0.3 Pa s	0.2–0.3 Pa s
Density	1–2 g/cm^3	3–4 g/cm^3
Response time	ms	ms
Viscosity/yield strength^2 η/τ^2	10^{-7}–10^{-8} s/Pa	10^{-10}–10^{-11} s/Pa

in the range from 0.1 to 10 μm and typical particle fractions are between 0.1% and 0.5%; the carrier fluids are selected on the basis of their tribological properties and thermal stability; they also include additives that inhibit sedimentation and aggregation.

The behaviour of MR fluids is often represented as a Bingham plastic model with a variable yield strength τ_y depending on the applied magnetic field H. The flow is governed by the equation

$$\tau = \tau_y(H) + \eta\dot{\gamma} \quad \text{with} \quad \tau > \tau_y(H) \tag{3.3}$$

where τ is the shear stress, γ is the shear strain and η is the viscosity of the fluid. Below the yield stress (at strains of order 10^{-3}), the material behaves viscoelastically:

$$\tau = G\gamma \quad \text{with} \quad \tau < \tau_y(H) \tag{3.4}$$

where G is the complex material modulus. This model is also a good approximation for MR devices (with appropriate definitions for τ, γ and η). However, the actual behaviour is more complicated and includes striction and hysteresis.

Figure 3.4 shows the three operating modes of controllable fluids: valve mode, direct shear mode and squeeze mode.

The valve mode is the normal operating mode of MR dampers and shock absorbers; the direct shear mode is that of clutches and brakes.

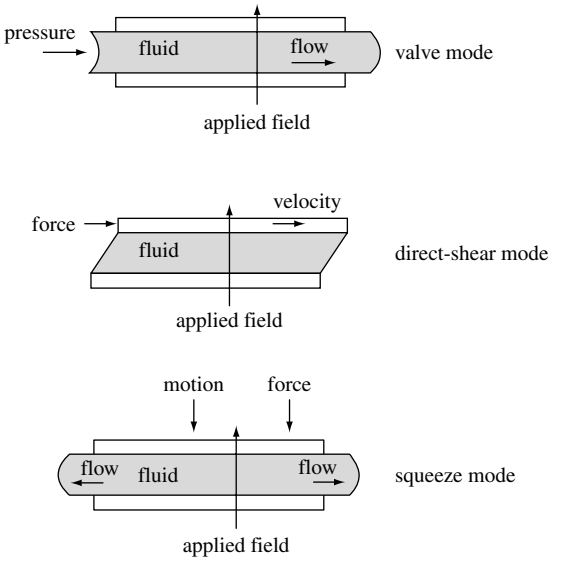

Figure 3.4 Operating modes of controllable fluids

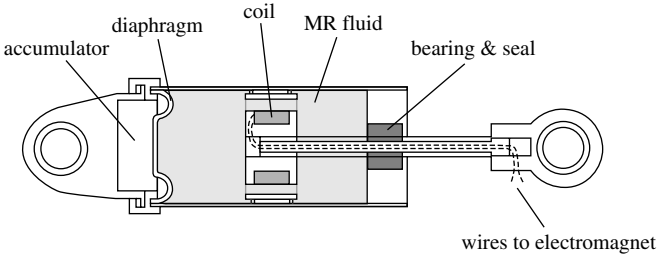

Figure 3.5 An example of MR damper

Figure 3.5 shows an example of a MR device. It can be seen that it consists of a common viscous damper, but instead of oil it is filled with a MR fluid. The current passing into the coil placed on the rod head generates a magnetic field that is able to polarize the metallic particles of the fluid in order to increase its viscosity.

The cost of the MR fluid contributes significantly to the total cost of the MR device. In order to bring this cost down by reducing the amount of fluid encapsulated, foam devices have been introduced where the MR fluid is constrained in an absorbent matrix by capillarity, without seals.

3.5 FRICTION DEVICES

3.5.1 Semiactive Joint Connections

In his PhD thesis, Nitsche (Nitsche 2001) noticed that, in many present-day structures, the previously described variable stiffness method is no longer practicable to avoid the excitation of resonance. This happens because the excitation covers a broad frequency band, and there is limited scope for adjusting the mass or stiffness properties of a structure in order to shift the resonance frequencies.[1] Because he referred his work mainly to aircraft vibration protection, he affirms that the situation mentioned above is exacerbated in his case studies by the low mass and by the all welded construction methods often used, which result in low inherent structural damping.

The problem is how to insert damping into the structure. This can be done by adding special high-damping materials or by using high-damping alloys, but these methods were, in Nitsche's opinion, usually expensive and the damping is often frequency and temperature sensitive. He then observed that, because about 90% of inherent damping in most structures arises in the structural joints, it would seem sensible to endeavour to influence the damping in

[1] He has in mind the classical passive means of changing natural frequency commonly used in mechanical engineering.

a structure by means of the joints. This can be achieved by controlling the joints' clamping forces and hence the relative interfacial slips.

Nitsche's suggestion was that frictional damping should be deliberately increased and controlled in some structural joints so that the inherent structural damping was increased, thereby reducing the dynamic response, stress and noise. The energy dissipation mechanism arising from relative interfacial slip in a joint is a complex process, which is largely influenced by the interface pressure. With low joint clamping pressures, sliding on a macro scale takes place. If the joint clamping pressure is increased, mutual embedding of the surfaces starts to occur. Sliding on a macro scale is reduced and micro slip is initiated, which involves very small displacements of an asperity relative to its opposite surface. A further increase in the joint clamping pressure will cause greater penetration of the asperities. The pressure on the contact areas will be the yield stress of the softer material. Relative motion causes further plastic deformation of the asperities.

In most joints he studied, the previously described mechanisms were working. The relative significance of these mechanisms depends on the joint conditions and the magnitudes of the forces. In joints with high normal interface pressures and relatively rough surfaces, the plastic deformation mechanism is significant. Many joints have to carry great pressures to satisfy structural criteria, such as high static stiffness. A low normal interface pressure would tend to increase the significance of the slip mechanisms. An improvement in the quality of the surfaces in contact will also facilitate the slipping. With the macro slip mechanism, the dissipated energy is proportional to the product of an interface shear force function and the relative slip. Under high pressure the slip is small and under low pressure

the shear force is small: between these two extremes the product becomes a maximum.

Then Nitsche introduced the "semiactive intelligent bolt". In order to set and maintain the normal force, a clamping arrangement more elaborate than simple bolts or rivets may be necessary, although this may only mean the addition of an active washer. In any event, the force and moment transfer mechanisms, as well as the damping in structural joints, must be understood if an efficient structure has to be designed. A piezoelectric stack disc is used as a washer to control in real time the normal force in the friction interface based on feedback from sensor outputs. If a voltage is applied to the piezoelectric washer, the stack disc tries to expand, which results in increasing the normal force. This idea of semiactive friction damping in joint connections has been patented by Gaul (Gaul and Nitsche 2001; Gaul and Lenz 1998).

3.5.2 Friction-controllable Sliding Bearing

The idea of this type of device is this: the friction between the bearing and the ground can be controlled by adjusting the pressure between the two sliding surfaces. For example, as shown in Figure 3.6, the fluid pressure in the chamber can be increased or decreased in order to diminish or augment the forces coming from the superstructure and acting on the sliding surfaces (Feng et al. 1993).

In this case the computer calculates an appropriate signal to control the fluid pressure based on the observed structural response, such as response acceleration and sliding displacement, and transmits it to the pressure control device.

The system can be a passive sliding isolation system as long as the pressure of the bearing chamber, and thus the friction, is kept at a constant value. But the pressure is not

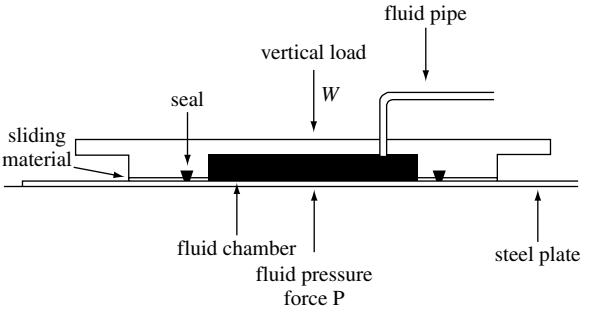

Figure 3.6 Idealised view of friction controllable sliding bearing

constant because it can be changed at little energy expense, so the device can be classified as semiactive. This has the great advantage that the device can become operative also at a low excitation level while maintaining high performance for stronger excitations.

One important point concerns the time response of the system: for practical application a very fast control algorithm should be used together with a good pumping system in order to avoid excessive delays.

3.5.3 Semiactive Slip Bracing System

This device incorporates the initial work done by (Akbay and Aktan 1991). More recent efforts are described in (Dowdell and Cherry 1994). Figure 3.7 shows the device: it dissipates energy by allowing slippage to take place along a Coulomb friction interface. The load F_f at which this interface slips is controlled by the clamping force N following the equation

$$F = \mu N(u)\texttt{sign}(v_{rel}) \tag{3.5}$$

where v_{rel} is the relative velocity among moving parts.

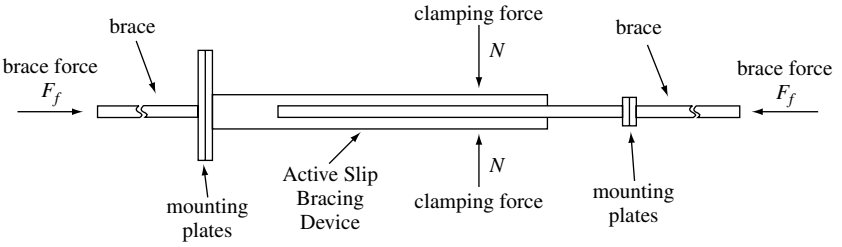

Figure 3.7 Operating principle of the semiactive slip bracing system

It is envisioned that the typical use is to mount the device on a lateral bracing system. The device will allow a brace's axial elongation or contraction through slippage when the brace loads reach the clamping force times the friction coefficient at the interface.

By installing this kind of device, a brace's strength can be altered independently of its stiffness. The other advantage of this device with respect to a passive one is that it can become operational also for small forces (that is, small earthquakes or winds) but maintain good performances also for stronger solicitations.

This device was called the "Active Slip Bracing Device" by (Kannan et al. 1995) because the clamping force can be varied by means of an actuator. Then, in the paper describing its characteristics, the authors say that the device should be classified as hybrid because it monitors and actively alters the energy dissipation of the building structure during its response to vibration excitation. Following the definitions given in Section 1.2, however, the most proper category in which the device should fall is the semiactive class, because it is a passive device in which the characteristics can be modified on-line according to some measurements and a control law.

3.6 TUNED LIQUID DAMPERS

In recent years, tuned liquid dampers (TLDs) have proved to be a successful control strategy for addressing a multitude of dynamic loading conditions (Abe and Fujino 1994; Sun et al. 1995). A frustum–conical TLD was also proposed as an alternative to the traditional rectangular, cylindrical or annular tank. Compared with the cylindrical reservoir, the cone-shaped TLD allows calibration of its natural frequency through varying liquid depth, which makes it suitable for a semiactive implementation, and seems to attain the same level of performance with a smaller mass, at least for small fluid oscillations (Figure 3.8). A linear model can interpret TLD behaviour for small excitations. For larger amplitudes, strong non-linearities occur and the linear model is no longer predictive. Consequently, for a frustum–conical

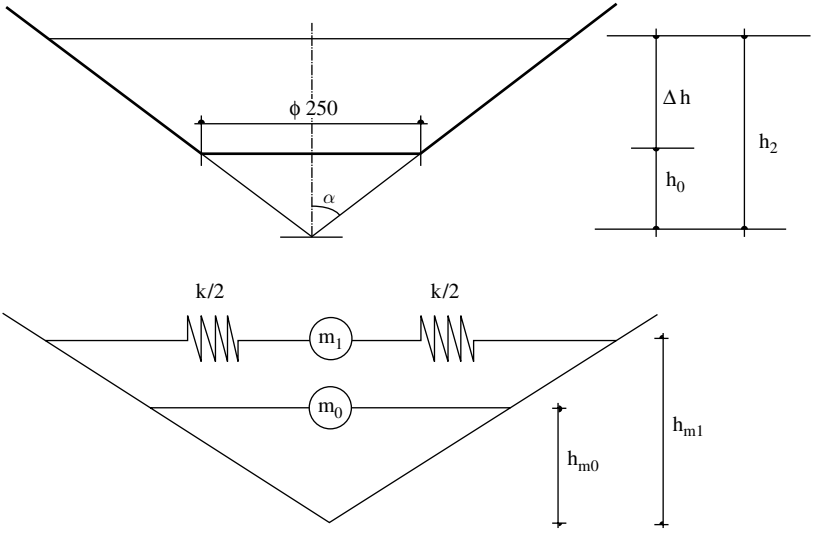

(a) liquid in fixed mass and moving mass

Figure 3.8 Conical tanks: scheme of functioning

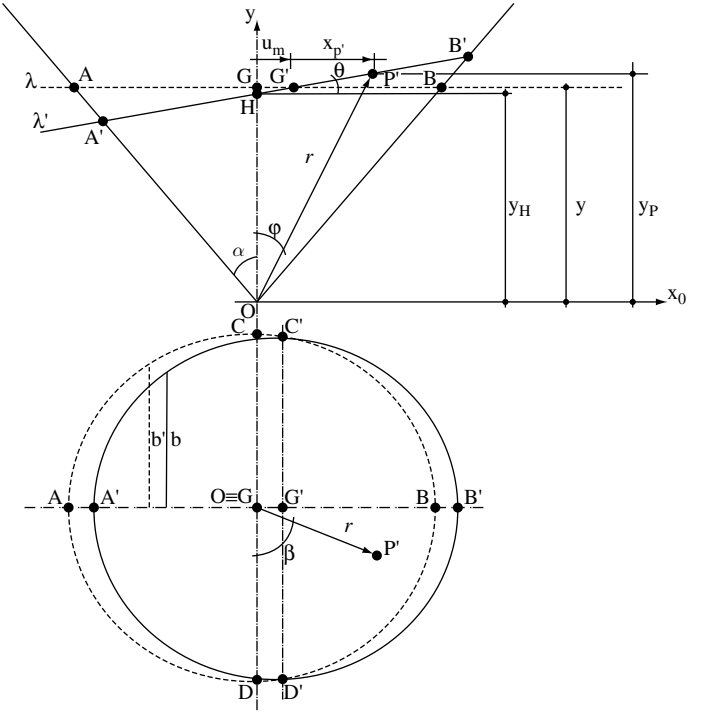

(b) liquid motion

Figure 3.8 (Continued)

TLD subjected to harmonic excitations, a single degree-of-freedom (SDOF) tuned mass damper (TMD) analogy is established in which the TMD parameters vary with the excitation amplitude (Casciati et al. 2003b).

The most practical way of addressing the non-linearity of a physical model is by substituting the real TLD system with an equivalent ideal TMD with parameters (mass, frequency and damping) varying with the excitation amplitude (besides depending on the geometry of the tank). There exist manifold criteria for the choice of optimally fitted TMDs, some of them based on time integration of the reaction force signal multiplied by tank base

displacement or velocity. In (Casciati et al. 2003b), a more elementary method is applied: for each TLD configuration (that is, for each value of h), and for each excitation amplitude, the mass, frequency and damping of the equivalent TMD are directly chosen as those able to reproduce best the experimental curve of force versus frequency (Figure 3.9).

In this search for the best fitting non-linear TMD, a further simplification seems to be legitimate, which enables one to consider the effective mass as equal to the total mass of the liquid. Actually, as far as a linear behaviour is concerned, one of the most favourable aspects of conical TLDs, compared with cylindrical ones, is the greater percentage of the mobile mass to the total mass of liquid, which allows smaller total masses for an identical level of performance.

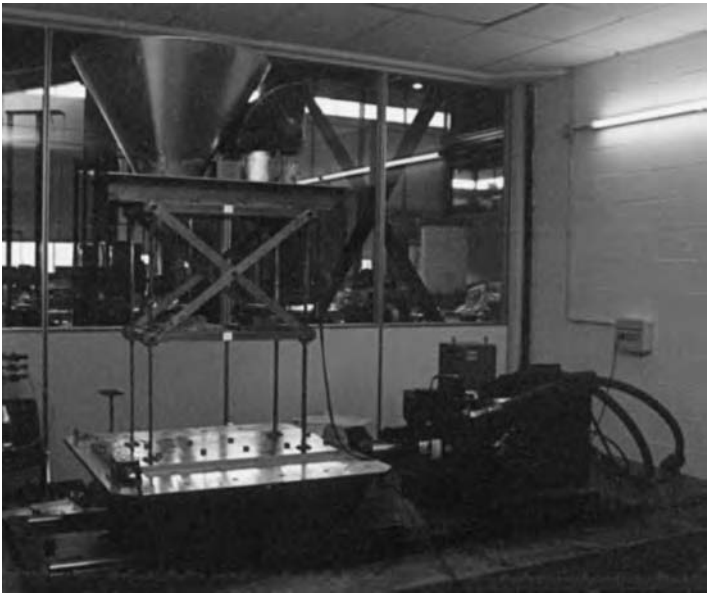

Figure 3.9 Testing environment in the University of Pavia laboratory

This aspect, together with the observation (Sun et al. 1995) that the effective mass for a cylindrical TLD approaches the total mass when the amplitude increases, helps to explain why, for a conical TLD, the best value for the effective mass corresponds quite well to the total mass of liquid, even for amplitudes that are not too large. This physical benefit has the additional advantage of reducing the unknown parameters to frequency and damping alone. In each case, in fact, the mass has been assumed identical to the total mass of liquid in the tank. The TMD frequency then is normalized to the value provided by the linear theory (respectively $f_0 = 1.22,\ 1.33,\ 1.38\,\text{Hz}$ for $h = 3,\ 4.5,\ 6\,\text{cm}$), which turns out to be a good estimator of TLD natural frequency for small oscillations. As the excitation increases, the fundamental frequency increases too (hardening-spring-type behaviour) but accordingly robust behaviour is appreciable near resonance (the frequency response functions grow flatter and wider), which makes the analogy conservative and some prediction errors acceptable. Once the mass is proved to coincide with the total mass of the liquid and the frequency is shown to increase slightly with respect to the value derived from the linear theory, the only a priori unknown and hardly predictable parameter is the damping of the equivalent TMD, which is easily obtainable from a fitting procedure. It turns out to increase significantly with the amplitude of the excitation. This fact is responsible for the decrement of the frequency response for the normalized force, but should not be looked upon as an unfavourable property. As is well known since Frahm's undamped oscillator in 1909, a small damping for a TMD (which corresponds to a high peak of the frequency response function for the reaction force) minimizes the structural response at its original resonance but creates two new resonance frequencies at certain distances. If the response is to be minimized on a large bandwidth, the optimum damping

(in case the condition of optimum tuning holds) depends on the mass ratio in a manner which is approximately given by the classical Den Hartog formula:

$$\xi_{opt} = \sqrt{\frac{3\mu}{8(1+\mu)}} \tag{3.6}$$

which suggests, for a usual mass ratio of 1%, an optimal damping of 6%, which is approximately the value experimentally obtained for a harmonic excitation amplitude of 10 mm.

3.7 ELECTRO-INDUCTIVE DEVICE

The paper by (Battaini et al. 2002) considers an electro-inductive solution which could result in a 30% reduction of the total length of common fluid dampers used in bridge technology. Such a device can be easily made into a semi-active device. The interesting feature is that the behaviour of this class of devices can be studied by simply investigating the response of an electric motor controlled to have zero speed (Figures 3.10 and 3.11).

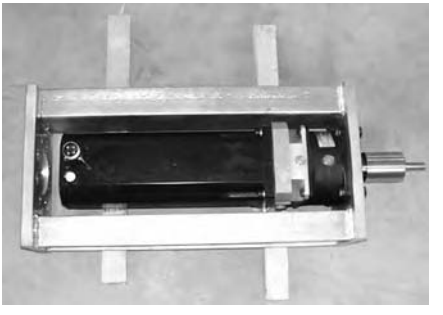

Figure 3.10 Electric engine

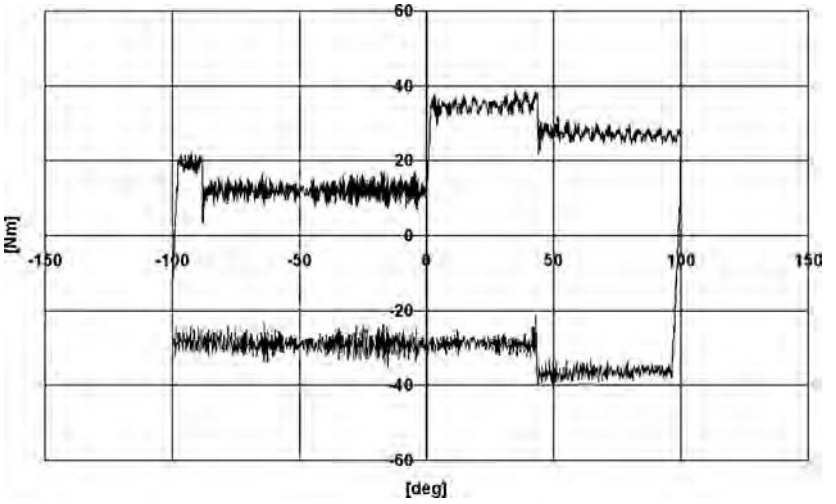

Figure 3.11 A moment-rotation diagram where the control current moves from 4 A down to 1 A in a single cycle. The frequency is 0.06 Hz.

Important aspects of using electro-inductive devices instead of fluid dampers are:

1. The response behaviour is practically independent of the external temperature because the device operating temperature is always higher than the air temperature and it is reached in few seconds.
2. The device maintenance is reduced because there is no ageing or leakage effects as in the fluid dampers.

3.8 AIR-JET ACTUATORS

Air-jet actuators were introduced in structural control as a fascinating answer to the classical objection that power could not be available when necessary if not preliminarily

stored. Among other possibilities, the preliminary compression of fluids could be exploited. Then pulses of relatively short duration from suitable nozzles, each of them requiring a relatively low amount of energy, could be used to control the structures.

When the fluid is air, the air is stored in a tank and flows towards a semi-rigid pipe to the final actuator jets, simply realized as nozzles (Figure 3.12). The flow through

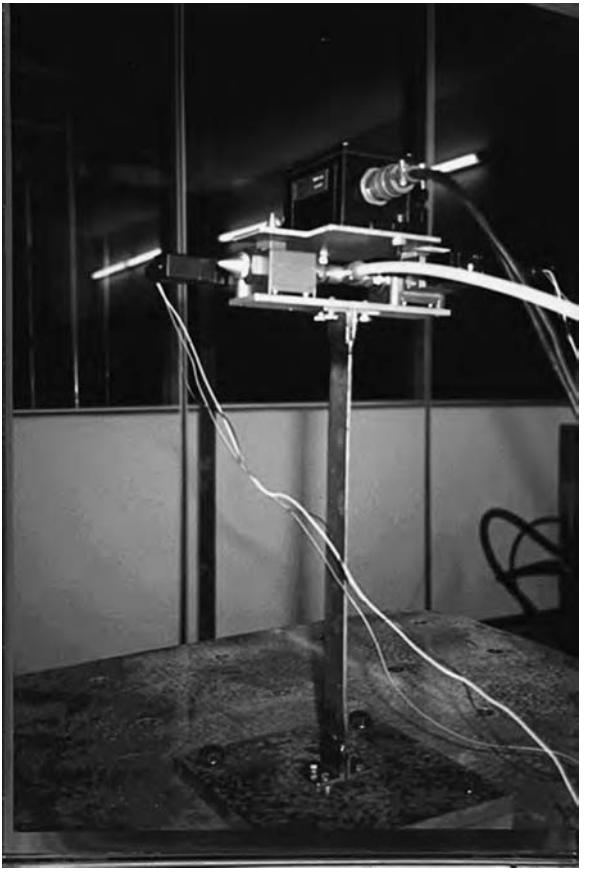

Figure 3.12 Testing air-jet actuators on the shaking table

each nozzle is controlled by an on–off electrical valve, and the system response is monitored by accelerometers which provide feedback. The actuator force is supplied by the flow of compressed air: it applies a force to the jet-supporting structure thanks to the principle of momentum preservation. The paper by (Brambilla et al. 1998) focuses on the experimental investigation of some of the practical issues encountered in the development of actuators based on mass-ejection techniques.

When the environment allows it, the exploitation of water as the fluid provides a much better efficiency. This is the case with structures belonging to the offshore drilling technology.

3.9 SMA ACTUATORS

Shape memory alloys (SMAs) were intensely investigated for possible exploitation in civil engineering (Auricchio et al. 2001). They are commonly adopted for the realization of passive devices, while the different (and long) reaction times to cooling and heating prevented their adoption in semiactive devices. In areas different from civil engineering, however, SMAs were conveniently incorporated into suitable devices and the reader is referred to (Kohl 2004) for a review of the main ideas. Future adaptations for civil engineering purposes can be easily foreseen.

4
Semiactive Control Laws

4.1 CONTROL STRATEGIES AND ALGORITHMS FOR SEMIACTIVE DAMPING

Several approaches were proposed in the literature (Dyke et al. 1996; Dyke and Spencer 1997; Carter 1998; François et al. 2000), some originating from an adaptation of active control laws, others originating directly from physical considerations.

With a semiactive control device, the energy can only be dissipated (and so removed from the system). These kinds of devices could be seen as passive dampers with changing characteristics to be adjusted on-line.

4.1.1 Open-loop Control

In the open-loop mode of operation no feedback is necessary. The control law is set a priori and no knowledge of the state variables is necessary. The damping characteristic of the devices can vary continuously or by steps, depending on the operating conditions. Typically, the variable dampers work in a bi-state (on–off) manner. This

Technology of Semiactive Devices and Applications in Vibration Mitigation Fabio Casciati, Georges Magonette and Francesco Marazzi

means that the device can be considered as a common passive element in which the dissipative properties can be switched from a net value to another one. This is the simplest and cheapest way to implement a control law and can be used very usefully for vibration isolation of rotating machines. Such a technique is used, for example, for washing machines: one value of damping (high) is used when the drum is at low speed (that is, during acceleration or deceleration), while a lower damping value is used for high speed (Figure 4.1). An automatic switch changes the damper's properties when a pre-set speed is reached.

This type of control is useful when the system to be damped has very well-known dynamic characteristics and loading conditions.

In some cases the different level of damping is chosen by the user, as in the case of the semiactive suspension of vehicles.

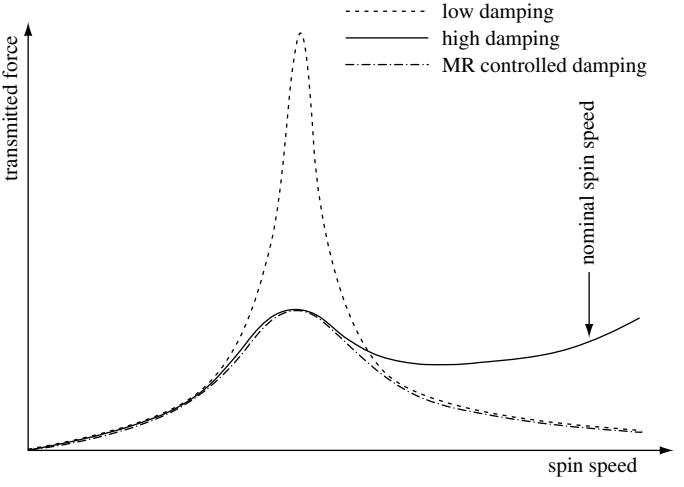

Figure 4.1 On–off open-loop strategy

4.1.2 On–Off Skyhook Control

In on–off skyhook control, the damper is controlled by two damping values. This control law was developed in order to obtain the lower vibration amplitude of the body mass (the upper one, see Figure 4.2). Illustrated in Figure 4.3, these values are referred to as high-state and low-state damping.

The choice between a damper adjusted to its high state or low state is made using the following control law. Depending on the product of the relative velocity v_{rel} across the damper (Figure 4.3) and the absolute velocity $\dot{z}_b$ of the system body mass attached to that damper, a damping value is chosen. If the product is positive or zero, the damping value c_s of the damping device is adjusted to its high state; otherwise, c_s is set to the low state.

This concept is summarized by

$$\begin{aligned} \dot{z}_b \times v_{rel} \geq 0 \quad & c_s = high\ state \\ \dot{z}_b \times v_{rel} < 0 \quad & c_s = low\ state \end{aligned} \tag{4.1}$$

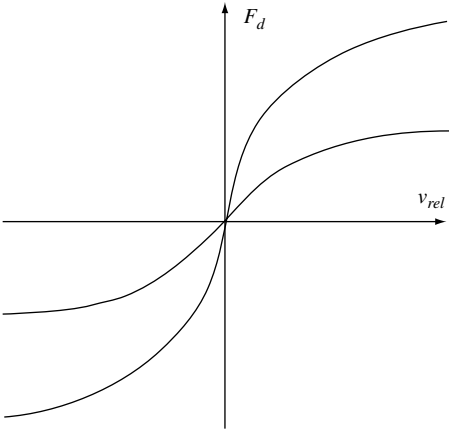

Figure 4.2 Typical semiactive damper curves

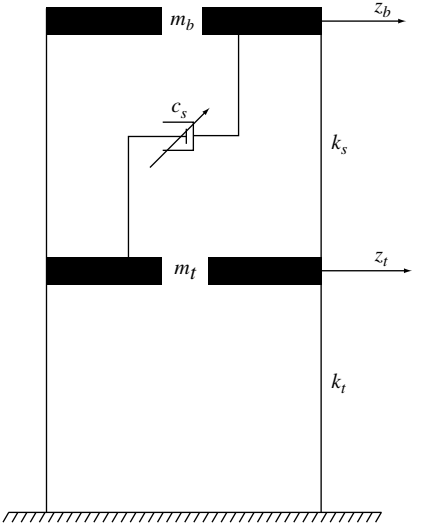

Figure 4.3 Suspension system model equipped with a variable damping device

where $v_{rel} = \dot{z}_b - \dot{z}_t$. The logic of the on–off skyhook control policy is as follows. When the relative velocity of the damper is positive, the force of the damper acts to pull on the system body mass; when the relative velocity is negative, the force of the damper pushes the body mass. Thus, when the absolute velocity of the body mass is negative, it is travelling to the left and the maximum (high-state) value of damping is required to push the body mass, while the minimum (low-state) value of damping is required to continue pulling on the body mass.

However, if the absolute velocity of the body mass is positive and the body mass is travelling to the right, the maximum (high-state) damping value is required to pull the body mass, while the minimum (low-state) damping value is required to push the mass further to the right (Figure 4.4).

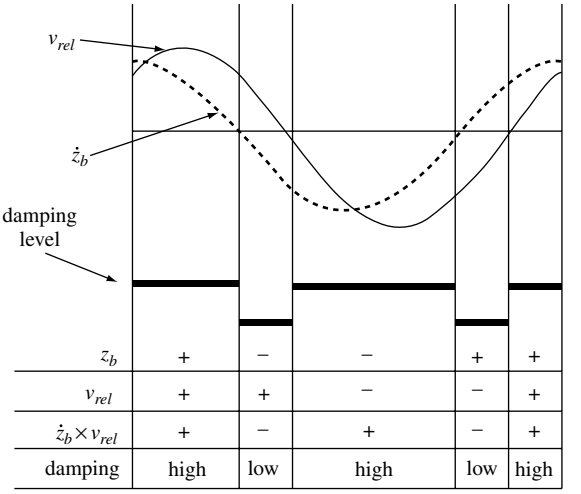

z_b	+	−	−	+	+
v_{rel}	+	+	−	−	+
$\dot{z}_b \times v_{rel}$	+	−	+	−	+
damping	high	low	high	low	high

Figure 4.4 Semiactive damping with continuous skyhook control

4.1.2.1 Physical Interpretation

In order to clarify the above-mentioned concepts, a physical interpretation of Equations (4.1) is given below.

Without loss of generality, $\dot{z}_b$ and $\dot{z}_t$ can be considered positive if the body mass and lower mass m_t (see Figure 4.3) are moving to the right. It can also be observed that $v_{rel} < 0$ when m_t and m_b are approaching each other, while if $v_{rel} > 0$ the two masses are going away from each other.

The following four cases can therefore be found:

1. The two masses are moving away from each other and the m_t is moving to the right (product is positive): high damping is required in order to try to keep the body mass left.
2. The two masses are moving away from each other and m_t is moving to the left (product is negative): low damping is required in order to try to reduce the pulling effect

of m_t moving to the left. If the damping is high, the body mass would move to the left faster, in this case.

3. The two masses are approaching each other and m_t is moving to the left (product is positive): high damping is required in order to keep the two masses as far apart as possible.
4. The two masses are approaching each other and m_t is moving to the right (product is negative): low damping is required.

In conclusion, a high damping value is used only when needed; the lowest possible damping value is used when damping is not needed.

The on–off skyhook semiactive policy emulates the ideal body displacement control configuration of a passive damper "hooked" between the body mass and the "sky", as shown in Figure 4.5.

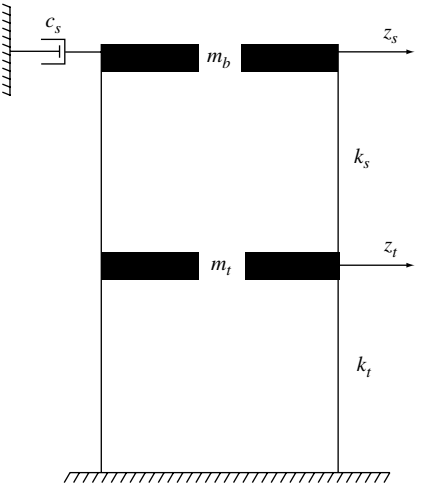

Figure 4.5 Passive damping representation of skyhook control

4.1.3 Continuous Skyhook Control

In continuous damping, a "high" and a "low" damping state can be defined as in the on–off damping control policy described previously. However, now, the damping values are not limited to these two states alone; they may exist at any value within the two states. As illustrated in Figure 4.6, the high and low states serve as the maximum and minimum damping values, with the intermediate (shaded) area including all possible damping values between the maximum and minimum.

Equations used for on–off skyhook control still apply, except for the definition of the high- and low-state damping. In on–off skyhook control, the high and low states were defined as constant damping values. In continuous skyhook control, the low state remains defined by a constant damping value, while the high state is set equal to a constant gain value g multiplied by the absolute velocity of the system body attached to the damper,

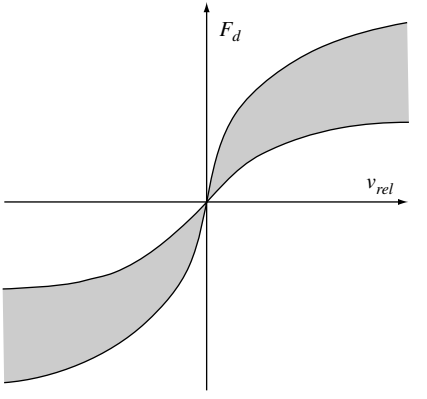

Figure 4.6 Semiactive damping with continuous skyhook control

not exceeding the corresponding high- and low-state limits:

$$\begin{array}{ll} \dot{z}_b \times v_{rel} \geq 0 & c_s = \alpha \\ \dot{z}_b \times v_{rel} < 0 & c_s = low\ state \end{array} \tag{4.2}$$

with $\alpha = \max\{low\ state, \min[(g \times \dot{z}_b),\ high\ state]\}$.

4.1.4 On–Off Groundhook Control

In this case the determination of whether the damper is to be adjusted to its high state or its low state depends on the product of the relative velocity across the damper and the absolute velocity of the lower mass m_t attached to that damper.

Contrary to the skyhook control strategy, this control law was developed in order to have the lower vibration amplitude on m_t. The control law is as follows:

- if the product of the relative damper and the absolute lower mass velocity $\dot{z}_t$ is negative or zero, the damper is adjusted to its high state;
- if this product is positive, the damper is adjusted to its low state.

Putting this into the equations gives:

$$\begin{array}{ll} \dot{z}_t \times v_{rel} \leq 0 & c_s = high\ state \\ \dot{z}_t \times v_{rel} > 0 & c_s = low\ state \end{array} \tag{4.3}$$

The reasoning behind the on–off groundhook control policy is similar to the on–off skyhook control policy, except that control is based on the unsprung mass. When the relative velocity of the damper is positive, the force

of the damper acts to pull on m_t; when the relative velocity is negative, the force of the damper pushes on m_t. However, when the absolute velocity of m_t is negative, it is travelling to the left and the maximum (high-state) value of damping is required to pull m_t, while the minimum (low-state) value of damping is required to continue pushing on m_t. But, if the absolute velocity of m_t is positive and so m_t is travelling to the right, the maximum (high-state) value of damping is required to push m_t, while the minimum (low-state) value of damping is required to pull m_t further to the right. The on–off groundhook semiactive policy emulates the ideal low mass displacement control configuration of a passive damper "hooked" between the lower mass m_t and the "ground", as shown in Figure 4.7.

The continuous groundhook control strategy can be derived directly from the continuous skyhook control simply by changing the chosen condition on the damping value, so it will be omitted.

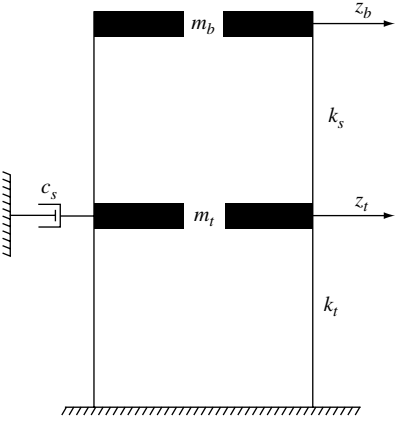

Figure 4.7 Passive damping representation of groundhook control

4.1.5 Clipping Control

A class of controls is grouped under this denomination. Their common characteristic is the fact that these laws have a two-stage architecture, that is the controller design can be divided into two parts.

The first step consists of designing an active control law assuming that an ideal active device is present. The second step involves the design of a clipping controller allowing the semiactive damper to develop the force that the active device would have removed from the structure.

This means that, for the first step, every kind of control law design can be chosen (optimal control, integral force feedback control, H_2 or H_∞ control) because the second step is independent of it. To clip the active control law to a semiactive one the following rule is usually used: when the magnitude of the force F_d produced by the damper (that is, the control force f in this case) is smaller than the required target force f_c, and the two forces have the same sign, the voltage applied to the current driver is increased to the maximum level, so as to match the required control force; otherwise, the command voltage is set to zero. This strategy is usually called "clipped on–off" and has a formula appearing as

$$v = V_{max} H\left[(f_c - f)f\right] \tag{4.4}$$

where v is the command signal,[1] $H[.]$ is the Heaviside step function, V_{max} is the maximum voltage applicable on the semiactive device to obtain the maximum damping, and

[1] This command signal can act on the excitation coil of a magnetorheological device, or on the position controller of an hydraulic device or the position of a valve closing an orifice.

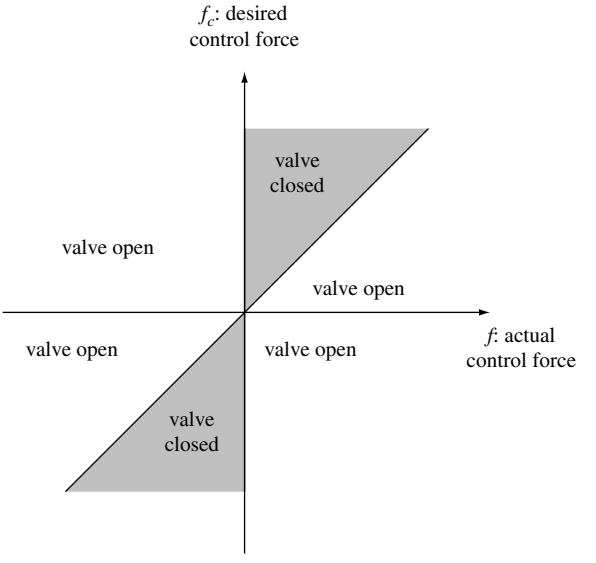

Figure 4.8 Clipping control strategy

f and f_c are the measured and required control forces. Figure 4.8 illustrates this strategy graphically.

4.1.6 Direct Lyapunov Control

This approach requires the use of a Lyapunov function $V(\mathbf{x})$, which must be compatible with the following conditions:

i. be a positive definite function of the states of the system, $\mathbf{x}$;

ii. have a negative time derivative for all trajectories from any initial state in the neighbourhood of the origin.

$$V(\mathbf{x}) = \frac{1}{2}\mathbf{x}^T\mathbf{P}\mathbf{x} \tag{4.5}$$

where $\mathbf{P}$ is a real, symmetric, positive definite matrix, found by solving the Lyapunov equation[2]

$$\mathbf{A}^T\mathbf{P} + \mathbf{P}\mathbf{A} = -\mathbf{Q} \tag{4.6}$$

with a positive definite $\mathbf{Q}$ matrix (ensuring $\dot{V}(\mathbf{x}) = -\frac{1}{2}\mathbf{x}^T\mathbf{Q}\mathbf{x} < 0$).

For a linear system with control forces $\mathbf{f}_{cf}$

$$\dot{\mathbf{x}} = \mathbf{A}\mathbf{x} + \mathbf{B}\mathbf{f}_{cf} \tag{4.7}$$

the derivative of the Lyapunov function becomes

$$\dot{V}(\mathbf{x}) = -\frac{1}{2}\mathbf{x}^T\mathbf{Q}\mathbf{x} + \mathbf{x}^T\mathbf{P}\mathbf{B}\mathbf{f}_{cf} \tag{4.8}$$

The second term containing $\mathbf{f}_{cf}$ can be directly affected by a change in the control voltage. The control law that will minimize $\dot{V}$ is

$$\nu_i = V_{max}H(-\mathbf{x}^T\mathbf{P}B_i f_{cf_i}) \tag{4.9}$$

where $H(.)$ is the Heaviside step function, f_{cf_i} is the measured force produced by the i^{th} semiactive device, and B_i is the corresponding column of $\mathbf{B}$.

4.1.7 Fuzzy Logic Control

Fuzzy logic control of semiactive dampers is another example of continuous control. The output of the controller determined by the fuzzy logic may exist anywhere between the high and low damper states. Fuzzy logic is used in a number of controllers because it does not require an accurate model of the system to be controlled. Fuzzy logic

[2] In the case of a linear system with state matrix $\mathbf{A}$, see also (1.1).

works by executing rules that correlate the controller inputs with the required outputs. These rules are typically created through the intuition or knowledge of the designer regarding the operation of the system being controlled. No matter what the system is, there are three basic steps that are characteristic of all fuzzy logic controllers. These steps include the fuzzification of the controller inputs, the execution of the rules of the controller, and the defuzzification of the output to a crisp value to be implemented by the controller. These steps can be briefly explained as follows:

- Step 1: fuzzification. This step is accomplished through the construction of a membership function for each of the inputs. This is the main point, because the possible shapes of these functions are infinite, though very often a triangular or trapezoidal shape is used. Once the membership functions are chosen, the input, read as a crisp value, is transformed into a fuzzy value by intersecting each component of the membership function with this value. This must be done for all inputs of the controller.
- Step 2: execution of the rules. In order to create the rulebase of the controller, the membership function of the output must first be defined. Once these functions have been defined, a table of combinations can be stated. In this table a linguistic value of output is defined for each possible combination of two inputs. These rules can be described as a series of "IF–THEN" statements.
- Step 3: defuzzification. These fuzzy outputs now go through the defuzzification process in which a single, or crisp, controller output value is obtained. Some common methods of defuzzification include the max or mean-max membership principles, the centroid method and the weighted average method. To give an example, the weighted average method is described in Section 4.2. In

this case the crisp output value is obtained as the sum of the product of each weighting function (to be chosen arbitrarily) with the maximum value of its respective membership value and dividing it by the sum of the weighting functions.

These three steps must be repeated for each input point to obtain continuous outputs.

4.1.8 Modulated Homogeneous Friction Control

This control strategy was developed originally for a variable-friction damper. In this approach, at every occurrence of local extremes in the deformation of the device (that is, when the relative velocity between the ends of the semiactive device is zero), the normal force applied to the frictional interface is updated to a new value. At each local minimum or maximum in the deformation the normal force $N(t)$ is chosen to be proportional to the absolute value of the semiactive device deformation. The control law is written as

$$N(t) = g\,|P[\Delta(t)]| \tag{4.10}$$

where g is a positive gain and the operator $P[.]$ (referred to the prior-local-peak operator) is defined as $P[\Delta(t)] = \Delta(t-s)$ where $s = \{\min x \geq 0 : \dot{\Delta}(t-x) = 0\}$ defining $\Delta(t-s)$ as the most recent local extreme in the deformation.[3]

Because this algorithm was developed for variable-friction devices, the following modifications are needed

[3] This definition is quite ambiguous, as will be explained in Section 4.2.

when applying it to other kind of semiactive devices (for example, magnetorheological or variable-orifice devices):

1. There is often no need to check if the force is greater than the static friction, because some semiactive devices have no static friction.
2. A force feedback loop is used to induce the semiactive damper to produce approximately the frictional force corresponding to the required normal force. Thus, the goal is to generate a required control force with a magnitude

$$f_c = \mu g \, |P[\Delta(t)]| = g_n \, |P[\Delta(t)]| \tag{4.11}$$

where the constant g_n has units of stiffness.

The resulting control law is

$$v = V_{max} H(f_c - |f|) \tag{4.12}$$

where $H[.]$ is the Heaviside step function. An appropriate choice of g_n will keep the force f_c within the operating envelope of the semiactive damper most of the time, allowing the device force closely to approximate the required force.

4.1.9 Bang–Bang Control

Bang–bang control is used mainly for dissipative devices in order to increase their capabilities in dissipating energy with respect to a classical passive device. It provides a simple and yet often effective approach.

When the relative displacement and the relative velocity of the two ends of the damping device are in the same

direction, bang–bang control acts in the direction of increasing the friction forces in the device to a maximum value. In this way it works as a brake, thus allowing the dissipation of energy. On the other hand, when the relative displacement and the relative velocity of the ends of the device are in opposite directions, this control law decreases the friction forces to a minimum in order to make the device movement as easy as possible.

If the maximum value of the friction forces is obtained when the control signal is u_{max} and the minimum one when the control signal is u_{min}, the control law can be written as follows:

$$u(t) = u_{max} \quad \text{if } \text{sign}(x) = -\text{sign}(\dot{x}) \tag{4.13a}$$

$$u(t) = u_{min} \quad \text{if } \text{sign}(x) = \text{sign}(\dot{x}) \tag{4.13b}$$

The control parameter u_{min} should be set at as small a level as possible, to reduce the dissipative forces to a minimum, making the device telescope as much as possible. The control parameter u_{max} should be at the optimal value, that is a value which provides the maximum energy dissipation.

4.1.10 Instantaneous Optimal Control

In the instantaneous optimal control strategy the command signal $u(t)$ is determined by minimizing the following time-dependent objective function $J(t)$ at every time instant t for the entire duration of the excitation:

$$J(t) = q_d x^2(t) + q_f f^2(t) + r u^2(t) \tag{4.14}$$

in which x is the relative displacement. The normalized friction force f indirectly represents the amount of response acceleration and also serves as a measure of the transfer of induced force to the structure. The weighting coefficient q_d and q_f are non-negative and r is positive. They indicate the relative importance in the control objectives of relative displacement, response acceleration and control signal, respectively. The basic objective of the control is to provide a device that dissipates the biggest amount of energy within an acceptable range and at the same time minimizes the transferred force.

Without entering into details, an explicit Newmark method can be used for implementation to solve the involved equations numerically.

4.2 IMPLEMENTATION SCHEMES

4.2.1 Open-loop Control

This control strategy is very easy to implement, because no knowledge of the states is needed. In the case of a washing machine, for example, the control law can be implemented following these steps:

1. When the machine begins to spin-dry, the damping value is set to the maximum one and a time counter is reset to zero.
2. When the time counter reaches a pre-selected value, that is after a fixed time, the damping value is switched to the minimum one.

The same procedure can be applied when the washing machine finishes the spin-drying phase and decreases the drum speed.

4.2.2 On–Off Skyhook Control

The flowchart summarizing the subroutine applying the on–off skyhook policy of damping control is shown in Figure 4.9.

It is immediately evident that to implement this control strategy is very simple: it needs only to measure two quantities (d_{rel} and d_{abs}) and then to act on some device switching the dissipator from one state to another. High and low damping values are those given by the dissipation device when, for example, a valve is completely open or closed, so they cannot be modified once the device has been

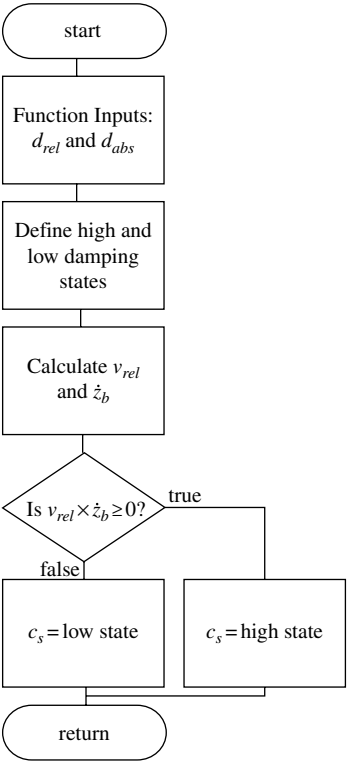

Figure 4.9 Flowchart of the on–off skyhook subroutine

Algorithm 1 On–off skyhook control strategy

Require: $\Delta t > 0$, $\xi_h \neq 0$, $\xi_l \neq 0$ and $\xi_h \geq \xi_l$
  $d^v_{rel} \Leftarrow \bar{d}_{rel}$
  $d^v_{abs} \Leftarrow \bar{d}_{abs}$
  repeat
    acquire d^n_{rel}
    acquire d^n_{abs}
    $v_{rel} \Leftarrow (d^n_{rel} - d^v_{rel})/\Delta t$
    $\dot{z}_b \Leftarrow (d^n_{abs} - d^v_{abs})/\Delta t$
    if $v_{rel} \times \dot{z}_b \geq 0$ **then**
      $c_s \Leftarrow \xi_h$
    else
      $c_s \Leftarrow \xi_l$
    end if
    $d^v_{rel} \Leftarrow d^n_{rel}$
    $d^v_{abs} \Leftarrow d^n_{abs}$
  until stop condition

designed. The only change that the control law can induce into the device is to switch from one value to another.

In algorithm 1 the quantities $\xi_l \neq 0$ and $\xi_h \neq 0$ are respectively the low damping state of the device and the high damping state. With the Lord® magnetorheological device, for example, the first state is reached when the supply current is 1 A, while the second one is achieved for 0 A current. The quantity Δt is the time step of acquisition. The algorithm checks at the beginning that the needed parameters are meaningful, then executes the procedure.

In the algorithm, $\bar{d}_{rel}$ and $\bar{d}_{abs}$ are the starting values for d_{rel} and d_{abs}, the indices ^{n} and ^{v} standing for ^{new} and ^{old}, respectively: the old values come from the previous calculation, while the new values are the just calculated ones.

It must be noted that this procedure is reduced to its base bones: in real implementations it is necessary to take into account also the fact that, under some conditions, for example when $v_{rel} \times \dot{z}_b \approx 0$, the control action can continuously switch from the first to the second state. This can consume energy and can also lead to damage of the device. To avoid this effect it is necessary to model a relay behaviour: the switching command does not trigger exactly when the product $v_{rel} \times \dot{z}_b$ becomes zero, but slightly later, so avoiding an oscillatory switching if one of the two quantities v_{rel} or $\dot{z}_b$ is moving around the zero.

4.2.3 Continuous Skyhook Control

The flowchart summarizing the subroutine applying the continuous skyhook policy of damping control is shown in Figure 4.10.

It must be noted that, as in Figure 4.9, Figure 4.10 also represents one single step of control: the continuous skyhook subroutine is called at each calculation step. This fact can lead to some optimizations, as shown in the corresponding algorithm: for example, it is not necessary to define high and low damping states at each step, but to define them once and for all when the semiactive control algorithm is started.

The continuous skyhook algorithm implementation is much more complex than the on–off one at least for three main reasons:

1. The coefficient α must be calculated at each step.
2. The correlation between the α coefficient and the command signal to the semiactive device could be highly non-linear.

3. The semiactive device must be complex enough to allow little modification of its properties.

The first point is not very important if the calculation power is high enough: in this case the algorithm will be very fast even with some more complex calculations.

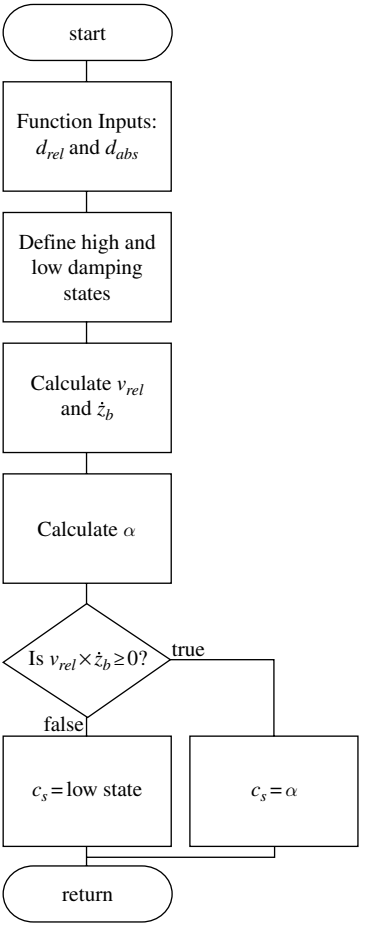

Figure 4.10 Flowchart of the continuous skyhook subroutine

Algorithm 2 Continuous skyhook control strategy

Require: $\Delta t > 0$, $\xi_h \neq 0$, $\xi_l \neq 0$, $\xi_h \geq \xi_l$ and g
  $d^v_{rel} \Leftarrow \bar{d}_{rel}$
  $d^v_{abs} \Leftarrow \bar{d}_{abs}$
  repeat
    acquire d^n_{rel}
    acquire d^n_{abs}
    $v_{rel} \Leftarrow (d^n_{rel} - d^v_{rel})/\Delta t$
    $\dot{z}_b \Leftarrow (d^n_{abs} - d^v_{abs})/\Delta t$
    if $v_{rel} \times \dot{z}_b \geq 0$ **then**
      $\alpha \Leftarrow \max\{\xi_l, \min[(g \times \dot{z}_b), \xi_h]\}$
      $c_s \Leftarrow \alpha$
    else
      $c_s \Leftarrow \xi_l$
    end if
    $d^v_{rel} \Leftarrow d^n_{rel}$
    $d^v_{abs} \Leftarrow d^n_{abs}$
  until stop condition

The second point can also be solved if a characterization testing campaign is conducted on the semiactive device. In this way it is possible to define a calibration curve correlaton: for example, the required value of damping with the necessary amount of voltage needed.

The last point means that only special kinds of devices can perform this control strategy, such as the MR devices, because the response time is only some milliseconds. In the case of mechanical arrangements, it is much easier to switch between two values (for example, clamped and unclamped) than to pass through all the intermediate states.

The flowchart of Figure 4.10 is then translated into algorithm 2, where Δt, ξ_h, ξ_l, d_{rel}, d_{abs} have the same meaning

as before, while g is a fixed gain chosen at the beginning of the algorithm.

4.2.4 On–Off Groundhook Control

The flowchart summarizing the subroutine applying the on–off groundhook policy is shown in Figure 4.11. It looks very similar to Figure 4.9, except for the chosen condition on the device damping value.

The flowchart of Figure 4.11 is then translated into algorithm 3.

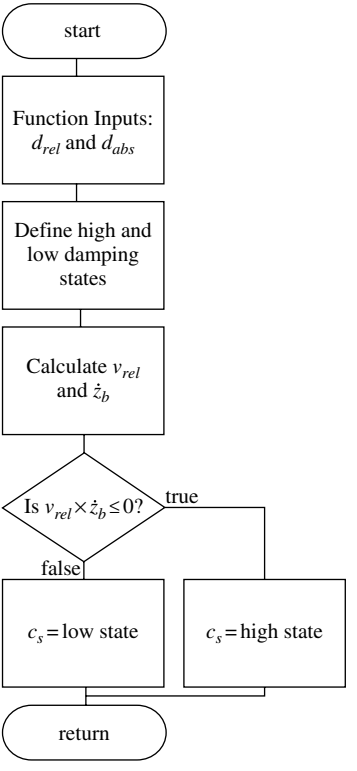

Figure 4.11 Flowchart of the on–off groundhook subroutine

Algorithm 3 On–off groundhook control strategy

Require: $\Delta t > 0$, $\xi_h \neq 0$, $\xi_l \neq 0$ and $\xi_h \geq \xi_l$
  $d^v_{rel} \Leftarrow \bar{d}_{rel}$
  $d^v_{abs} \Leftarrow \bar{d}_{abs}$
  repeat
    acquire d^n_{rel}
    acquire d^n_{abs}
    $v_{rel} \Leftarrow (d^n_{rel} - d^v_{rel})/\Delta t$
    $\dot{z}_b \Leftarrow (d^n_{abs} - d^v_{abs})/\Delta t$
    if $v_{rel} \times \dot{z}_b \leq 0$ **then**
      $c_s \Leftarrow \xi_h$
    else
      $c_s \Leftarrow \xi_l$
    end if
    $d^v_{rel} \Leftarrow d^n_{rel}$
    $d^v_{abs} \Leftarrow d^n_{abs}$
  until stop condition

4.2.5 Clipping Control

From an implementation point of view, this control strategy seems to be the most direct one because it can take advantage of the great amount of experimental and practical studies that have been conducted on active control strategies. The clipping control can be viewed, in fact, as a control strategy in which the actuator can operate only resisting forces and not act directly on the structure. So the active control law applies when the device is subjected to forces and turns into a constant value when it should act. The corresponding flowchart is shown in Figure 4.12, where ν is as defined in (4.4).

Only a little modification can lead to a continuous clipping control strategy. When the active control law requires

a negative damping (that is, it requires that the device acts on the structure) there is nothing better to do than set the device at its minimal resistance force. For the shaded region in Figure 4.8 a continuous value of the damping coefficient can be achieved if a proportional valve is actuated on the semiactive device or if a MR fluid is subjected

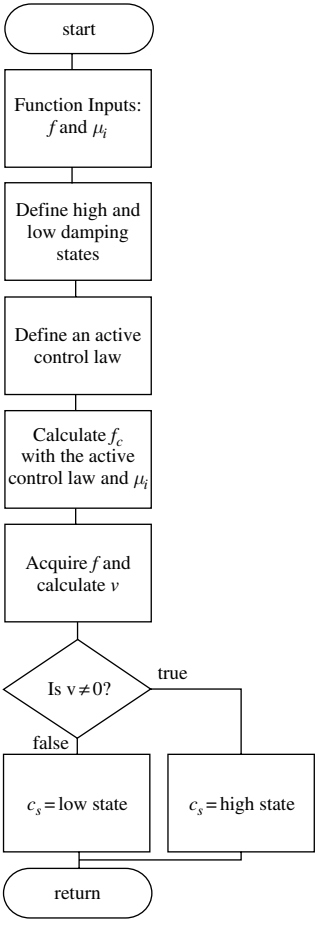

Figure 4.12 Flowchart of clipping control strategy subroutine

Algorithm 4 Clipping control strategy

Require: V_{max}, f_{max}, $\xi_h \neq 0$, $\xi_l \neq 0$ and $\xi_h \geq \xi_l$
Require: an active control law with the corresponding measured variables μ_i
Require: the Heaviside step function $H[.]$
  repeat
    acquire f
    acquire μ_i
    calculate f_c accordingly with the active control law and μ_i
    $\nu \Leftarrow V_{max} H[(f_c - f)f]$
    if $\nu \neq 0$ **then**
      if on–off control **then**
        $c_s \Leftarrow \xi_h$
      else
        if $f_c \geq f_{max}$ **then**
          $c_s \Leftarrow \xi_h$
        else
          c_s proportional to f_c
        end if
      end if
    else
      $c_s \Leftarrow \xi_l$
    end if
  until stop condition

to a magnetic field proportional to the active law required force. The control must be designed in this case to manage saturation on the semiactive device: too high a value of command voltage to the magnetic coil can lead to damage.

The flowchart is then detailed as algorithm 4 for both the on–off and the continuous clipping control strategies.

The clipping control strategy is more a class of strategies than a specific technique because every type of active control law can be used. For this reason it is very difficult to compare it with the other approaches mentioned above. The computing time required is just a little more than the one corresponding to the active implementation, because a few more "IF–THEN" statements must be evaluated. A general criticism of this class of methods, however, is that there is no way of assessing if a good active control law can also give good results when turned into a clipped one. Because of the inherent non-linearity, the clipping strategy cannot be assessed with a frequency domain technique, but time domain analysis must always be performed with several types of excitations and at different intensity levels.

The Heaviside step function is implemented in algorithm 5.

Algorithm 5 Heaviside step function

Require: f_1, f_2
  if $(f_1 - f_2)f_2 > 0$ **then**
    $H[.] \Leftarrow 1$
  else
    $H[.] \Leftarrow 0$
  end if

4.2.6 Direct Lyapunov Control

As mentioned before, the Heaviside step function is very easy to implement (see algorithm 5). The real task for implementing the direct Lyapunov control method is then to obtain all the values that must be fed into the Heaviside step function. In fact:

- **x** must be known at each step: enough sensors must be placed on the structure to be controlled;
- **P** is calculated once and for all at the beginning: the Lyapunov equation must be solved once only, even if this is usually not easy;
- B_i is constant for a given device;
- f_{cf_i} must be measured at each step.

The most critical value to be obtained is the matrix **P**, because the effectiveness of the final algorithm depends on it.

4.2.7 Fuzzy Logic Control

The flowchart summarizing the subroutine applying the fuzzy logic policy to a damping control is shown in Figure 4.13.

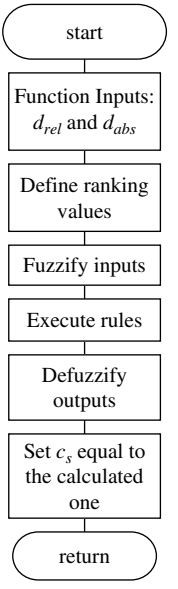

Figure 4.13 Flowchart of the fuzzy logic subroutine

Algorithm 6 Fuzzy logic control strategy

Require: $\Delta t > 0$, $c_s \neq 0$
Require: Input membership function, rule table, output membership function
  $d^v_{rel} \Leftarrow \bar{d}_{rel}$
  $d^v_{abs} \Leftarrow \bar{d}_{abs}$
  repeat
    acquire d^n_{rel}
    acquire d^n_{abs}
    $v_{rel} \Leftarrow (d^n_{rel} - d^v_{rel})/\Delta t$
    $\dot{z}_b \Leftarrow (d^n_{abs} - d^v_{abs})/\Delta t$
    $\mathbf{v}^{fuzzy}_{rel} \Leftarrow$ intersect v_{rel} with input membership function
    $\dot{\mathbf{z}}^{fuzzy}_b \Leftarrow$ intersect $\dot{z}_b$ with input membership function
    $\mathbf{c}_s \Leftarrow$ execute the rule table for each input combination
    combine the fuzzy values $\mathbf{c}_s$
    $c_s \Leftarrow$ convert $\mathbf{c}_s$ to a crisp output value
    $d^v_{rel} \Leftarrow d^n_{rel}$
    $d^v_{abs} \Leftarrow d^n_{abs}$
  until stop condition

In more detail, the flowchart is translated into algorithm 6. At each step, a fuzzification–defuzzification takes place. This may result in a long calculation time, so researchers have placed great emphasis on the design of a dedicated chip for fast on-line calculation (Faravelli and Rossi 2002).

In Figure 4.14(a) there is an example of an input membership function with three linguistic variables: N (short for Negative), P (Positive) and Z (Zero). Figure 4.14(b) shows an example of an output membership function where the linguistic output variables are defined as

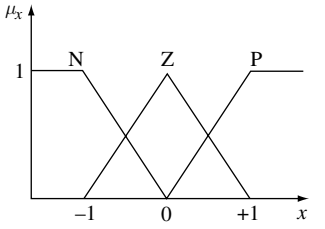

(a) Input Membership Function

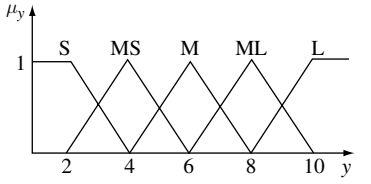

(b) Output Membership Function

Figure 4.14 Examples of input and output membership functions for a fuzzy controller

follows:[4] *S* (Small), *MS* (Medium Small), *M* (Medium), *ML* (Medium Large), *L* (Large). Obviously, the rule table can be described only after the output membership function has been defined. An example of a rule table is shown in Table 4.1.

The main advantage of fuzzy control, that is the fact that it is based on verbal rules (and so very close to common sense practice), is also its main drawback. In fact it is impossible to obtain the optimal solution automatically or to check mathematically if the elaborated solution is stable or not. So simulations and

[4] This definition is similar to that given for clothes sizes: XXXS ← XS, S, M, L, XL → XXXL.

Table 4.1 Example of a rule table for a fuzzy controller

$x_2 \backslash x_1$	**N**	**Z**	**P**
N	S	MS	S
Z	M	M	M
P	L	ML	L

experimental tests must be conducted to assess the control law.

4.2.8 Modulated Homogeneous Friction Control

The implementation scheme is similar to the one described for the clipping control strategy. The main difference here is that the required control force is not calculated with an active control algorithm, but with Equation (4.11).

The flowchart is shown in Figure 4.15. The real point is to implement the operator $P[.]$ because its given definition is appropriate if the device behaviour is similar to a smooth "go and return" around the zero position: only in this case does it make sense to speak of the "recent local extreme in the deformation". When the deformation record is a very noisy signal, it must be filtered in order to have a smoother behaviour.

Algorithm 7 describes in more detail what is shown in Figure 4.15.

4.2.9 Bang–Bang Control

The bang–bang control strategy is easy to implement in real-time algorithms to control operations since the control

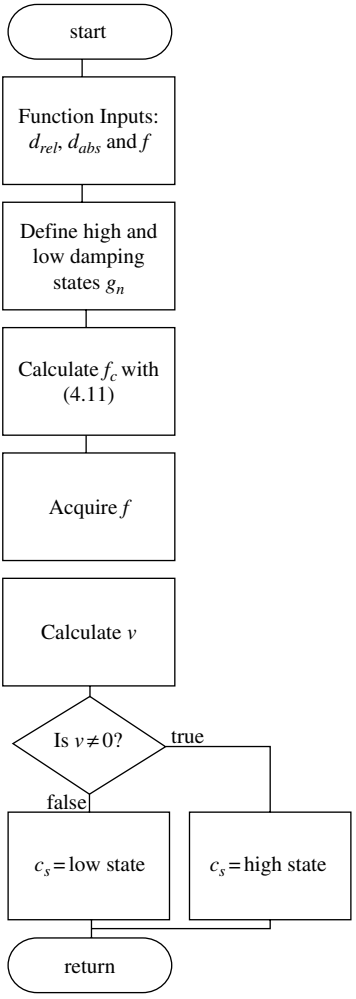

Figure 4.15 Subroutine flowchart of the modulated homogeneous friction control strategy

Algorithm 7 Modulated homogeneous friction control strategy

Require: $\Delta t > 0$, V_{max}, g_n, $\xi_h \neq 0$, $\xi_l \neq 0$ and $\xi_h \geq \xi_l$
Require: the Heaviside step function $H[.]$
  $d^v_{rel} \Leftarrow \bar{d}_{rel}$
  repeat
    $v^n_{rel} \Leftarrow (d^n_{rel} - d^v_{rel})/\Delta t$
    if $(v^v_{rel} > 0 \,\text{AND}\, v^n_{rel} < 0) \,\text{OR}\, (v^v_{rel} < 0 \,\text{AND}\, v^n_{rel} > 0)$ **then**
      $d_{max} \Leftarrow d^n_{rel}$
    else
      no change in d_{max}
    end if
    acquire f
    $f_c \Leftarrow g_n |P[d_{max}]|$
    $\nu \Leftarrow V_{max} H[(f_c - |f|)]$
    if $\nu \neq 0$ **then**
      $c_s \Leftarrow \xi_h$
    else
      $c_s \Leftarrow \xi_l$
    end if
    $d^v_{rel} \Leftarrow d^n_{rel}$
    $v^v_{rel} \Leftarrow v^n_{rel}$
  until stop condition

signal switches between two values and only the relative displacement needs to be measured by a sensor and fed back to the control signal. The function sign(x) can be obtained by the relative displacement signal and does not need to measure the velocity.

5

Implementation of Semiactive Control Strategies

5.1 INTRODUCTION

The implementation of a semiactive control system includes components of a different nature (mechanical, electrical, electronic). Furthermore the control architecture can be oriented towards the realization of a centralized or non-centralized system, as illustrated in Chapter 2. In the development of their medium- and large-scale testing facilities the authors were confronted by many implementation problems regarding the hardware and software needed to realize prototype testing set-ups. Some useful approaches for facing these problems are presented hereafter to familiarize the reader with equipment already available on the market and with possible hardware configurations that are easy to realize by using standard components.

Technology of Semiactive Devices and Applications in Vibration Mitigation Fabio Casciati, Georges Magonette and Francesco Marazzi

5.2 HARDWARE CONTROL IMPLEMENTATION

Specific control products are commercialized but most of them appear as "black boxes" difficult to use for the realization of prototype control systems enabling easy access for software modifications and implementing new algorithms, as well as for the addition of particular hardware interfaces needed for communication or instrumentation. An alternative choice is possible by selecting standard PC components and building, around an open architecture, the proper hardware and software. This flexible approach is especially appealing for implementing innovative solutions and realizing prototype systems.

5.2.1 Architecture

The proposed hardware scheme is optimized for centralized control and consists of three main parts:

1. The master processor board.
2. One or several slave processor boards.
3. The communication bus connection (Figure 5.1).

5.2.1.1 Master

The master board (Figure 5.2) is a powerful PC board, equipped with a fast processor, memory and Ethernet communication. It collects data from the slaves, runs the centralized control algorithm and provides the target displacements or forces to the slaves. The master/slave communication is achieved through a passive ISA bus.

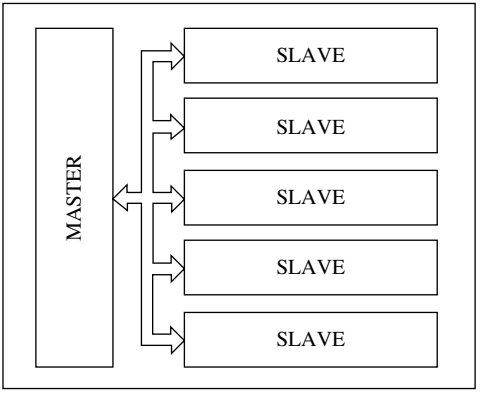

Figure 5.1 Scheme of controller architecture

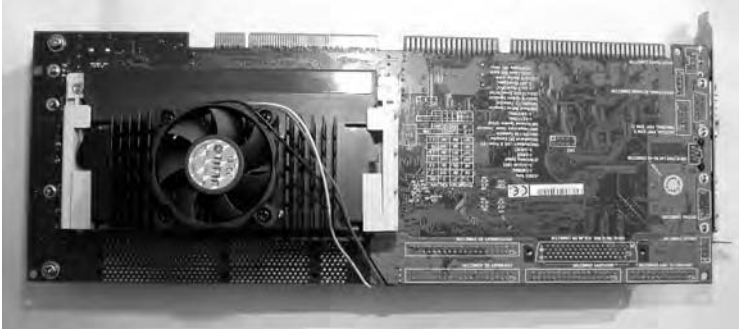

(a) front side

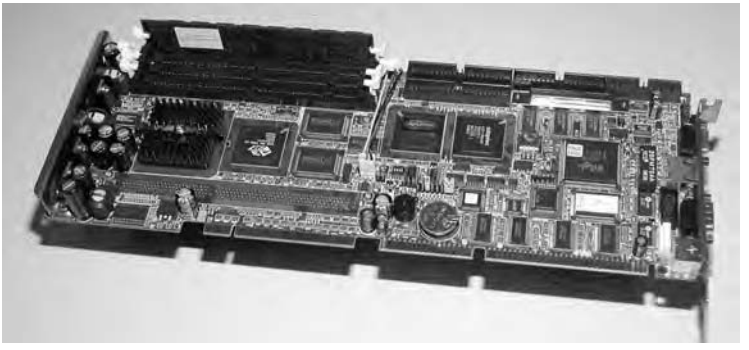

(b) back side

Figure 5.2 Photographs of the master card

5.2.1.2 Slave

The slave board is shown in Figure 5.3. It consists of three main components, all based on the PC104 bus architecture:

1. A processing unit card.
2. One or two digital and analogue input/output cards specifically selected for the application.
3. A dual-port memory card enabling high-speed access and easy sharing of data between the local PC104 bus and the ISA bus connected to the master.

5.2.1.3 Passive Bus

The ISA passive bus connects the master and slaves boards following a common standard. In the current configuration it connects the master board up to four slave boards, but with minor modifications a larger number of slaves could be supported. Figure 5.4 shows an assembled controller with its power supply and adjunct tools such as hard and floppy drives. These modular computers (master

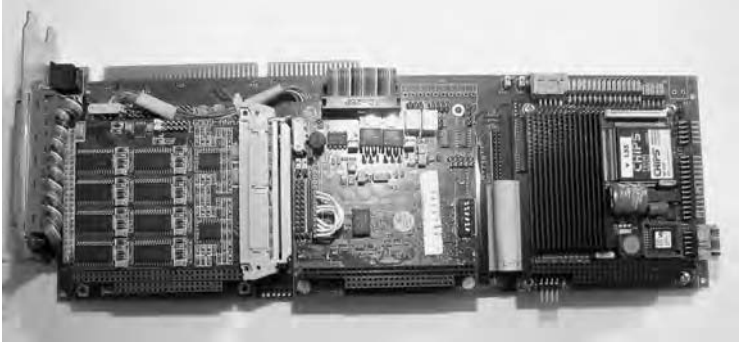

Figure 5.3 Photographs of the slave card with components

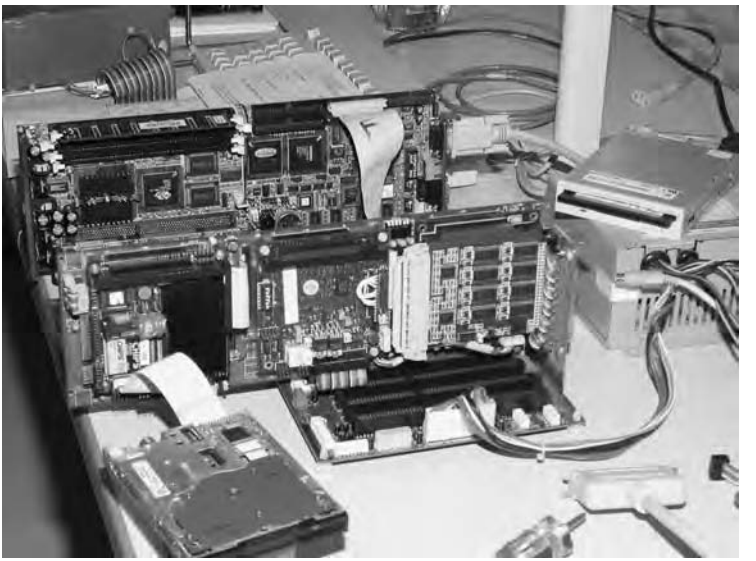

Figure 5.4 Photograph of the passive bus equipped with a master card and a slave card

and slaves) can be easily inserted into a rack and connected to standard LCD screens and keyboards.

5.2.1.4 Remarks

Following this succinct description of the control equipment architecture used for prototypes development, an explanation of the choices is due. This architecture was selected for three main reasons:

1. It is quite good in term of modularity and flexibility. The hardware and software configurations remain the same for many different applications in the field and the number of slave boards can be modified for best adaptation to the complexity of the development. In

this way implementation and technician training remain easy to conduct.

2. It is optimal to achieve many conventional tests that can be performed in a laboratory, such as pseudodynamic tests or cyclic tests involving the use of many synchronized actuators. In such common applications it is necessary that all actuators are well coordinated by a central algorithm in charge of computing the target displacements or forces to apply to the tested structure. Furthermore it integrates a large number of data acquisition channels and can be easily adapted to drive electric or servo-hydraulic actuators;
3. It presents an ideal configuration for implementing either centralized or decentralized control strategies in dynamic structural control. When a centralized strategy is desired, the master executes the control algorithm and sends the target signals to the slaves. Their only duty is to reach the target values (displacement or forces) via specific control laws. When a decentralized control strategy is requested, the master's only duty is to synchronize the slaves, to collect and save the internal control values, and to process these values for display or for checking security levels.

5.2.2 Hardware Details

The technical characteristics of a typical hardware configuration are listed below. Obviously this list must be updated as regards the fast evolution of this technology, but the essential functions remain the same.

The master board is a vertical processor board available on the industrial PC market. It is a complete PC that plugs onto the passive AT-ISA bus to communicate with

the slave boards, through a dual-port RAM. Substantially it includes:

- CPU Pentium III chip of 800 MHz or higher;
- 512 MB DRAM;
- real-time clock + watchdog;
- floppy disk and AT-IDE hard interface;
- USB serial bus interfaces;
- Ethernet network connection;
- LPT1, COM1, COM2 communication interfaces;
- AT keyboard;
- VGA/LCD video interface;
- AT-ISA bus connector.

Systems based on the PCI bus, instead of on the old AT-ISA bus, can also be envisaged, but they are much more difficult to manage for quickly designing the dedicated hardware and software often needed during prototype development. Furthermore hard real-time software is delicate and complex to implement on such systems, while its higher computation capabilities are not really needed for the application in which we are interested here.

The slave board is equipped with standard PC104 modules as shown in Figure 5.5. It integrates three PC104 connectors for PC104 mounted modules and interfaces the PC104 bus to one of the two access ports of the dual-port memory. The other port is accessible through the AT-ISA bus. The dual-port memory enables very fast synchronized communications between master and slaves. Figure 5.6 illustrates the slave board without PC104 modules.

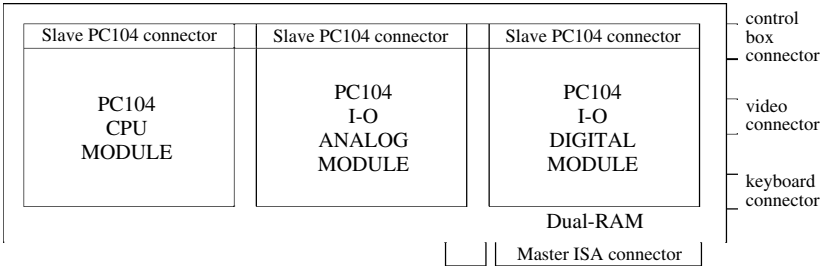

Figure 5.5 Scheme of a slave board

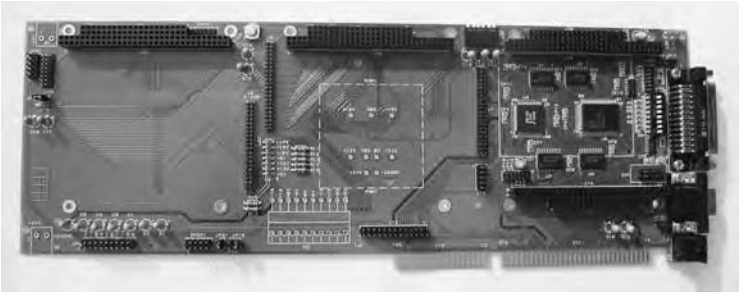

Figure 5.6 Slave board without modules (the dual RAM is visible on the left side)

A typical slave configuration includes:

- a PC104 processing unit module (Figure 5.7);
- PC104 analogue input/output modules equipped with AD and DA converters (Figure 5.8);
- PC104 modules usually specially designed for a particular application and including specific interfaces such as the one needed for reading digital sensors or for generating servo-valve or electric motor commands (Figure 5.9).

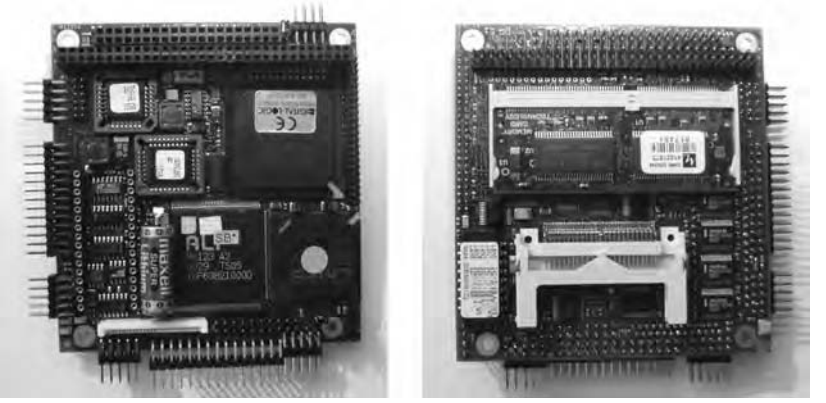

(a) front (b) back

Figure 5.7 Slave CPU module

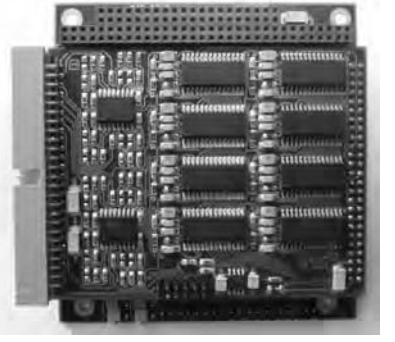

Figure 5.8 Slave analogue I/O module

The PC104 processing unit module is equipped with:

- CPU 486 DX4, 100 MHz or higher;
- 32 MB DRAM;
- solid-state disk (>2 MB);
- real-time clock + watchdog;

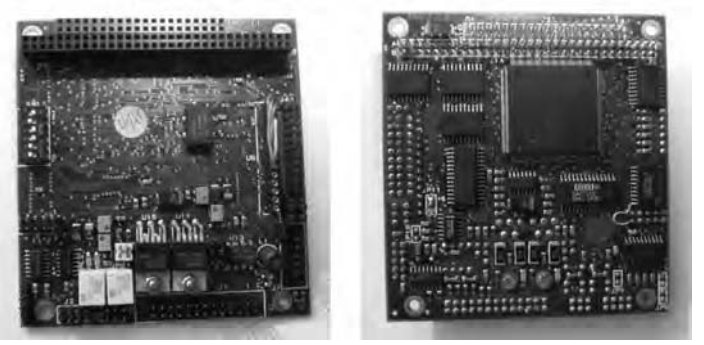

(a) front (b) back

Figure 5.9 Slave I/O module equipped with servo-valve drivers

- floppy disk and AT-IDE hard interface;
- LPT1, COM1, COM2 communication interfaces;
- AT keyboard;
- VGA/LCD video interface;
- PC104 bus connector.

The PC104 analogue input/output module includes:

- 16 ADC channels with 16-bit resolution;
- 2 DAC channels with 16-bit resolution;
- 24 digital input/output channels;
- 3 counter–timers, 24-bit resolution;
- voltage reference.

The specific PC104 module integrates:

- two SSI serial interfaces for "Temposonic" transducers;
- two serial interfaces for incremental digital displacement transducers;

- two hydraulic servo-valve drivers;
- eight digital input/output channels for alarm and safety signal management.

The slave board is designed to read a wide variety of signals, for ulterior local processing or master processing. It is equally able to generate a large set of signals to drive different types of actuation systems. For easy management of the interconnections of the many signals coming from the external environment to the system, it is recommended to interpose, between the slave connectors and the external signals, an interconnection box dispatching all the signals to a BNC connector panel for easy verification and checking.

5.3 REAL-TIME SOFTWARE

The main requirement of the control software is to be robust, flexible and easy to use. It must be modular and structured in such way that it can be easily adapted to different tasks or to different applications. It must give access to an easy programming procedure to insert new algorithms or modifications and must provide also easy access to the external signals in reading from as well as in writing to the controlled system. The master as well as the slave software used here was written in C++. This homemade software runs under one of the many real-time kernels currently available on the market. Hard real-time software functions cannot be achieved with the commonly used MS-DOS® or Windows NT® operating systems. These last platforms are not conceived to manage fast interrupts with re-entrant capabilities and to process tasks switching at a rate higher than 1 kHz.

5.3.1 Real-time Kernel Selection

The real-time kernel was selected taking into account the following two items:

- Reduced and fixed latency time. When an interrupt signal triggers the processor, the latency time must be constant and very short (a few microseconds). In a non-real-time system, such as Windows NT, a variable latency time is observed because it is not possible to obtain absolute priority and some internal tasks need to be completed before the task switching is accepted.
- The kernel software must be well structured, robust and easy to learn. The real-time platform is programmed at two levels: the user level and the kernel level. The user level is easy to manage but the kernel level is quite complex and requires skilful programmers. Once the general architecture is configured at the kernel level by a specialist, the user-level access is made as easy as possible. Tasks and priorities can be assigned easily and are guaranteed to be respected.

The advanced C++ program language is currently used to program the applications at the user level.

5.3.2 The Application Software

The application software reflects the hardware architecture: A central master program communicates synchronously with several slave programs. For the sake of simplicity the following description concerns a single slave but can be easily extended to several slaves. Both master and slave tasks run inside the background process or the foreground process.

The background process is devoted to the management of several services that are used during control. They include mainly:

- keyboard access;
- uploading of control parameters;
- display refreshing;
- hard disk management;
- Ethernet LAN operation.

Since these services are not strictly necessary to ensure the process control itself, they have a lower priority and can be interrupted at any moment.

The foreground process is the core of the control software. It performs at a fixed sample rate and the control tasks including mainly:

- data acquisition and signal processing;
- control algorithm computation;
- command variable generation;
- alarms and safety management tasks;
- foreground/background communication.

These true real-time tasks must be completed inside the time gap between two successive interrupts. For this reason they cannot be interrupted (delays cannot be accepted in the control loop) and must have absolute priority over the background tasks. The actual time taken by these tasks is an essential factor in the process of validation.

Bearing Figure 5.10 in mind, the interactions between the foreground tasks running on the master and on

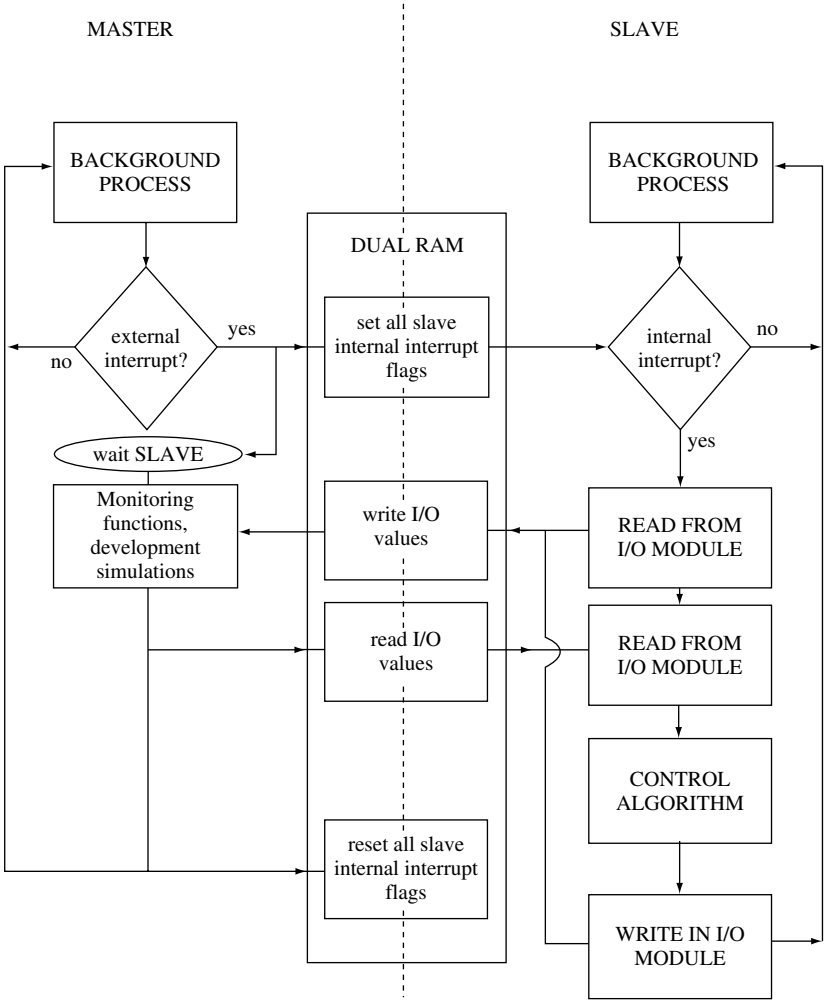

Figure 5.10 Flowchart of the application software

the slave boards can be described in the following way:

- A real-time clock (fixed frequency pulse generator) generates pulses at a sampling rate of 1 kHz. These pulses

are used to generate interrupt signals applied to the master processor and activate its foreground software. This means that the control algorithm as well as the master/slave data exchange must be completed within 1 ms, before the next interrupt signal. On the occurrence of the interrupt signal, the master sets the slave internal interrupt flag in the dual-port memory and waits for completion of the slave-first operation.

- This flag generates an internal interrupt on the slave processor that starts its foreground process.
- The slave reads its input modules, filters the acquired signals and writes their values to the dual-port memory, then points the end of these operations to the master and enters into a wait state.
- The master collects the data from the dual-port memory and executes the specific data processing and control algorithm. At completion of the computation the results are passed to the slave. Note that in the case of a collocated control strategy, the control algorithm may be solved by the slave processor only; then the master performs mainly monitoring and safety functions and slave coordination.
- The slave reads the master data, performs its own computation (when necessary) and sends the command values to its output interface. After conversion into analogue signals, these command values drive the controlled device. Then the slave returns to its background process.
- In the meantime the master resets the slave internal interrupt flag (that will be ready for the next step) and returns to its background process.

It must be noted that the architecture presented here is ideal for the development and debugging of controllers or

devices. After development, the control algorithm may be implemented in an embedded system or in an industrial computer.

5.3.3 Windows NT Software

As explained in the next section, it is possible to interface the real-time application software to a remote NT station; that is, from a common PC station, a remote user can enter commands or read data for analysis, monitoring or storage. To this end an Ethernet LAN is used to link the NT remote station and the master board. Two remote interfaces have been developed so for: the "acquisition" program and the "generator" program.

5.3.3.1 The "Acquisition" Program

The acquisition control panel is shown in Figure 5.11. This interface allows the user to perform remote data acquisition

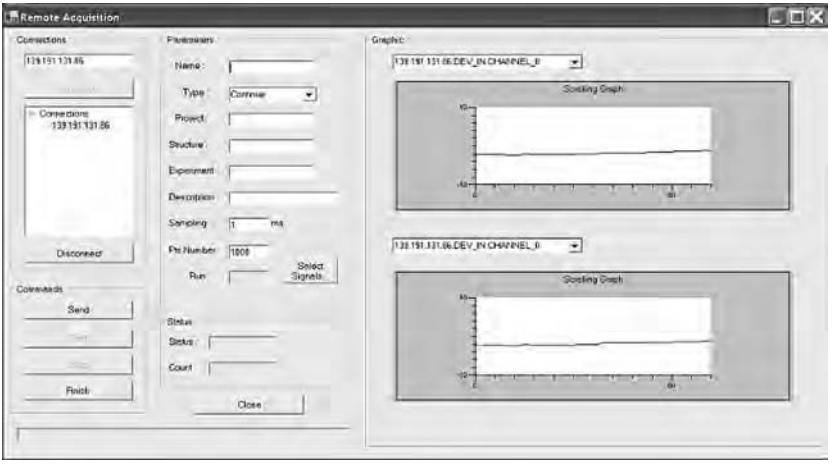

Figure 5.11 External acquisition control panel

by entering the parameters defining the acquisition process. Control panel fields must be filled with data including master address, project name, sampling time, acquisition length, transducer type, conversion factors, etc., and selection of the measured signals for monitoring and storing in a database. The data acquisition is then started by an external trigger signal.

5.3.3.2 The "Generator" Program

The generator control panel (Figure 5.12) was created to generate common (sinusoidal, square) or specific (user-defined)

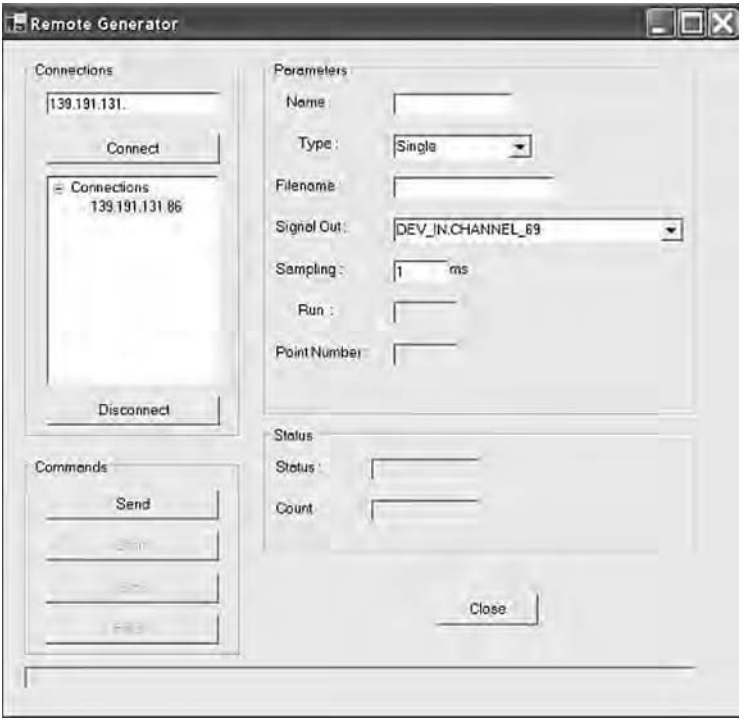

Figure 5.12 Generator control panel

waveforms from an NT station using a friendly interface. These signals are then downloaded to the master and used as target or reference signals in the control loop. They can be easily distributed on different slaves. Once again control panel fields must be compiled with data relative to master address, sampling time, etc., and the number of times the signal must be sequentially repeated. Arbitrary signals can be read from any software as far as they have been generated in binary double-precision format.

5.3.4 Real-time Software Tools

The software in support of the real-time controller program is included under this name. These tools were developed in order to integrate better the controller software with commonly used commercial software and for making data storage easy, faster and reliable.

5.3.4.1 Exchanging Master/Slave Variables

Internal variables are used and exchanged by both master and slave processes. These variables include measured values, target values, monitoring data, control parameters, conversion factors, command values. Depending on the priority of the task requiring such variables, the exchange can be handled by a foreground or by a background process. From the remote NT workstation it is often required to access these values for modification or storage. An exchange process was created under NT. It interfaces with the master background process and provides an easy way to monitor most control variables as well as a robust way to modify parameters. Furthermore, access to the master control variables from NT Windows is of great interest for interfacing application programs such as MATLAB® which are very often used to analyse control systems.

5.3.4.2 DCOM Technology

This technology was widely used in the development of the tools created here under Windows. It consists of a standard procedure developed by Microsoft Corporation to realize easy interfaces between several applications eventually designed by different users.

Figure 5.13 illustrates the basic scheme of several software applications interfaced together by applying the DCOM technology.

In this illustration the database can be directly connected to the data acquisition program via the DCOM technology. Although the programs are separate entities, the data flow between them is managed following the DCOM technology to build an integrated package. After having provided the test description and specification, the master variable read by the acquisition program can be sent directly to

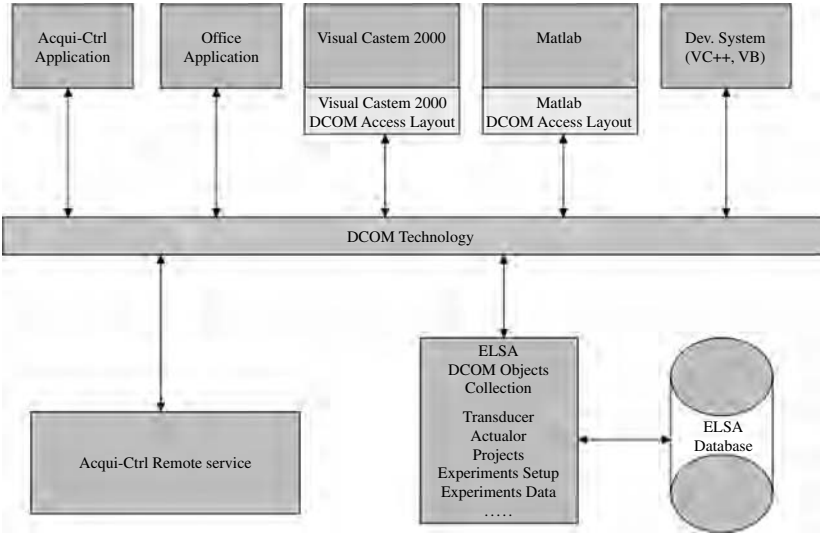

Figure 5.13 DCOM technology

the database under the proper project name and test directory.

5.4 NON-CENTRALIZED CONTROL VERSUS COLLOCATED SYSTEMS

When working with a focus on a very specific target, the market must be deeply investigated in order to identify the best components, each with properties consistent with there of others when interfaces among them are required.[1] As a result, the main task covers system architecture design and implementation.

5.4.1 Commercial Hardware and Software

5.4.1.1 Sensors

Analogue sensor devices range from the old FBA-11 uniaxial force–balance accelerometer by Kinemetrics to the new uniaxial and triaxial EpiSensor model produced by the same company.

The FBA-11 device (Figure 5.14) is a high-sensitivity, low-frequency device characterized by rugged construction and proven reliability. It is housed in a watertight cast aluminium case and is suitable for a variety of seismic, structural and commercial applications. Its quality is given by the maximum sensitivity (1.25 V/g) and a low noise density (350 ng/$Hz^{1/2}$–18 bit).

Digital sensor devices belong to the class of MEMS (Micro-Electronic Mechanical Systems). Among them are

[1] The authors thanks Dr Roberto Rossi of Paviasystem, Pavia, who was so kind to assemble and review the material summarized in this section.

(a) FBA-11 (b) EpiSensor

Figure 5.14 Accelerometer sensors by Kinemetrics

the high-sensitivity LF series Crossbow triaxial accelerometers (Figure 5.15) with the regulated voltage (-R) option. The full-scale acceleration is either $1g$ or $2g$ on every axis. The response is DC to 50 Hz, so they also measure the acceleration of gravity. These accelerometers feature an excellent offset stability over temperature and a low noise

Figure 5.15 Crossbow accelerometer sensor

density in the range of 70 $\mu g/Hz^{1/2}$ and maximum sensitivity (2 V/g). Internally, a bulk micromachined sensing element and ASIC electronics provide low noise and high stability. Common applications include seismic vibration, tilt/sway and orientation measurements. Thanks to the (–R) option, these accelerometers operate on a 6–30 V DC unregulated single supply.

5.4.1.2 Acquisition Modules

National Instruments® offers a large variety of acquisition modules working in conjunction with the LabView® software. The LabView® program uses the technique of graphical programming. This type of coding is referred to as G-Code (for graphical code). The program developed by National Instruments is widely used in industry for a variety of applications. One of these important applications is the automation of information gathering.

But one can also rely on other acquisition modules, such as, for instance, the Advantech PCL-818 data acquisition cards (Figure 5.16).

These cards feature 16 single-ended or 8 differential analogue inputs, 100 kHz 12-bit AD conversion and programmable gain for each input channel (up to 1000). The boards include a special wiring board (PCLD-8115) with a DB-37 connector and CJC (Cold Junction Compensation). This combination allows low-level thermocouple signals to be measured without an external signal conditioning board. The conversion time is 8 μs.

5.4.1.3 Software

In addition to LabView, it is useful to have access to the interactive MATLAB environment for simulation, data processing and control design.

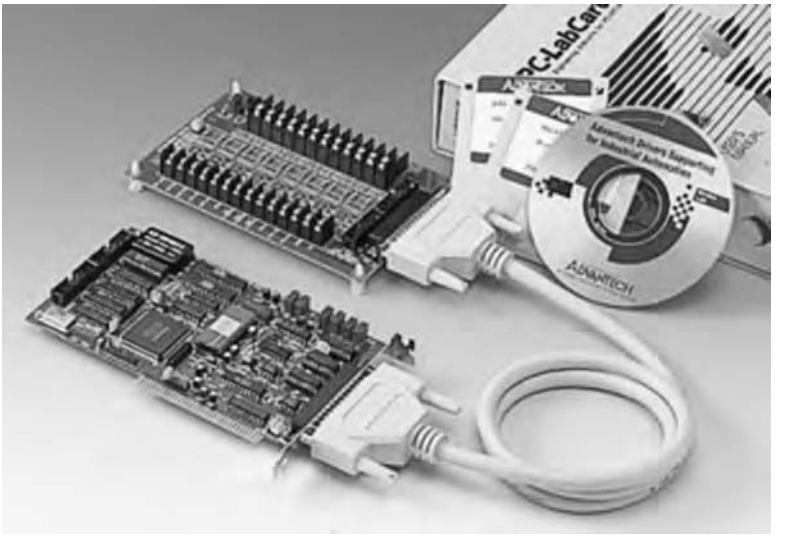

Figure 5.16 Advantech PCL-818 data acquisition card

MATLAB is a high-level technical computing language and interactive environment for algorithm development, data visualization, data analysis and numerical computation. Using MATLAB, one can solve technical computing problems faster than with traditional programming languages, such as C, C++ and Fortran. A key function is given by the functions for integrating MATLAB-based algorithms with external applications and languages, such as C, C++, Fortran, Java, COM's and Microsoft Excel®.

5.4.1.4 Wireless Technology

The 24XStream (Figure 5.17) is MaxStream's longest range, low-power OEM RF (Original Equipment Manufacturer[2]

[2] OEM means that the item is sold without a box to labs which assemble components.

Figure 5.17 24XStream card

Radio Frequency) module developed for worldwide use (2.4 GHz). Here is a list of its features:

- Plug-and-communicate (default mode – no configuration required).
- True peer-to-peer network (no need to configure a "Master" radio).
- Transparent mode supports existing software applications and legacy systems.
- Addressing capabilities provide for point-to-point and point-to-multipoint networks.
- Uses standard AT commands (which is *de facto* the standard language for controlling modems and is recognized by virtually all PC modems) and/or fast binary commands for changing parameters.
- Native RS485/422 (multi-drop bus) protocol support.
- Support for the RS232 protocol.

- Retry and acknowledgements of packets provide guaranteed delivery of critical packets in difficult environments.
- Networking features allow up to seven independent pairs (networks) to operate in close proximity.
- Multiple low-power modes including shutdown pin, cyclic sleep and serial port sleep for current consumption as low as 26 μA.
- Host interface baud rates from 1200 to 57600 bps.
- Signal strength register for link quality monitoring and debugging.
- Ninth-bit parity support (None, Even, Odd, Mark, Space).

AirborneDirect is a family of fully integrated 802.11b wireless LAN bridge products designed specifically to provide wireless LAN and Internet connectivity to industrial, scientific, medical and automotive applications. The highly integrated hardware and software enables plug-and-play capability. This significantly reduces the complexity of wireless system deployment and network connectivity.

With an AirborneDirect serial bridge (Figure 5.18), one creates a connection between an 802.11b wireless LAN device and a serial port. The bridge transparently conveys data between the device with a RS232, RS422 or RS485 interface and a wireless LAN. The bridge opens up the world of remote device monitoring and management, connecting data loggers, medical and industrial monitors, data acquisition and control systems, programmable controllers and a host of other applications to the LAN or Internet.

Figure 5.18 DPAC AirBorne bridge

5.4.1.5 Microprocessor

At the heart of the board is a C8051F007 microcontroller from Cygnal Integrated Products Inc. It is an 8051-based microprocessor with on-chip peripherals (ADC (Analogue Digital Converter), DAC (Digital Analogue Converter), UART (Universal Asynchronous Receiver/Transmitter), etc.) and flash memory. The maximum clock frequency is 25 MHz, which is perfectly suited to processing signals whose spectrum ranges from 0 to 25 Hz. It has 32 KB in-system-programmable flash memory plus on-chip RAM in excess of 2 KB.

The 8051 architecture is very widely used in the industry and is very flexible in that it supports any type of peripheral. Many 8051-based microcontrollers exist on the market with different features. Those from Cygnal Integrated Products were among the first to implement a high-speed core capable of executing most of the instructions in a single clock cycle, as opposed to the standard 8051 core that executes most of its instructions in no less than 12 clock cycles. Moreover, at the time this board was designed, these microcontrollers were those with the greatest amount of on-chip flash memory.

Microcontrollers based on the 8051 core are standard and can be programmed using standard and well-tested C compilers available from many vendors. This is the main reason why they have been chosen for this board. The C8051F007 has a peak 25 million instructions per second, which is sufficient for implementing a fuzzy controller as well as a linear controller. Although this board has been mainly designed with fuzzy control in mind (Faravelli and Rossi 2002), it is suitable for hosting any type of controller as long as no more than 25 million instructions per second are required.

5.4.2 Assembled Boards

This section describes some of the boards which were designed and implemented at the University of Pavia (Faravelli and Rossi 2002).

5.4.2.1 Controller

Figure 5.19 shows the top-level board diagram of the fuzzy controller board. The microcontroller is connected to the input channels, the output channel, the RS232 interface and the JTAG (Joint Test Action Group – IEEE Standard 1149.1-1990) interface. The input channels perform offset voltage cancellation by means of a simple first-order high-pass filter made up of a capacitor and a resistor. The corner frequency of the high-pass network is 0.016 Hz. This means the phase distortion introduced at 0.5 Hz is 1.8 degrees, while the amplitude distortion is less than 0.005 dB. The same figures at 1 Hz are 0.9 degrees and 0.001 dB, respectively. This means the amount of distortion introduced in the signal band (that is, $0.5\,\text{Hz} < f < 25\,\text{Hz}$) is negligible.

The output channel has the same offset cancellation filter and, in addition, has the capability of setting the DC

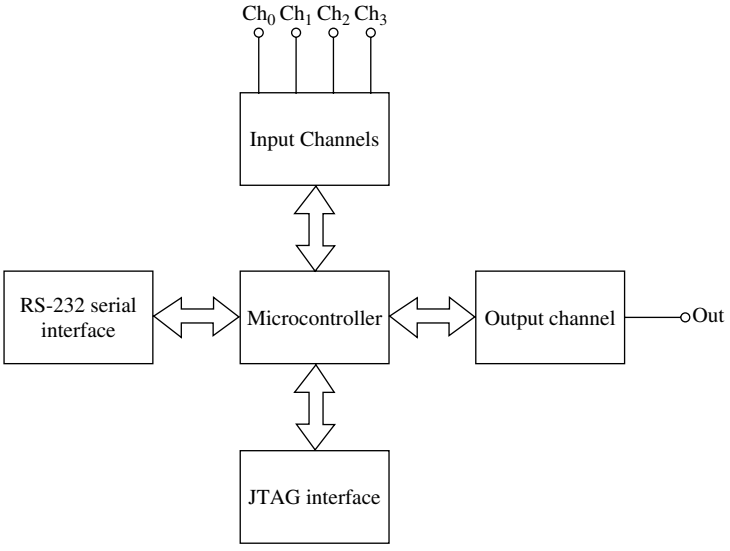

Figure 5.19 Top-level board diagram

output value either to 0 V or to 5 V. This way, two output ranges are possible: 0 V to 10 V and 5 V to +5 V. Output range selection is carried out through software. The RS232 interface allows the board to communicate with a computer or with another board of the same kind or even with a different peripheral, such as a radio modem or another kind of wireless transceiver. The board needs a dual ±15 V power supply or higher. Voltage regulation is carried out on-board. In case the output channel is not used, the board can function from a simple 9 V battery. In this case, only the input channels and the serial port will be operational. With suitable software, in this mode the board could, for example, still work as a controller and drive an actuator through a wireless link (for example, a radio modem connected to the serial port). The microcontroller works from a 3.3 V power supply. A 25 MHz quartz crystal provides the chip with a stable and accurate clock source. Finally, the

JTAG interface is used for downloading the software into the flash memory of the chip and for debugging purposes. A software tool from Cygnal, along with a serial-to-JTAG converter (a small and inexpensive black box), provides programming and in-system real-time debugging facilities. Figure 5.20 is a photograph of the fuzzy controller board.

5.4.2.2 Wireless Module

This printed circuit board hosts a microcontroller, a RF transceiver, a RS232 interface and some analogue signal conditioning hardware. The microcontroller is an Analog Devices ADuC812 or any other pin-compatible device, such as the newer fast core version, which is 12 times faster. The microcontroller embeds some flash memory, which allows

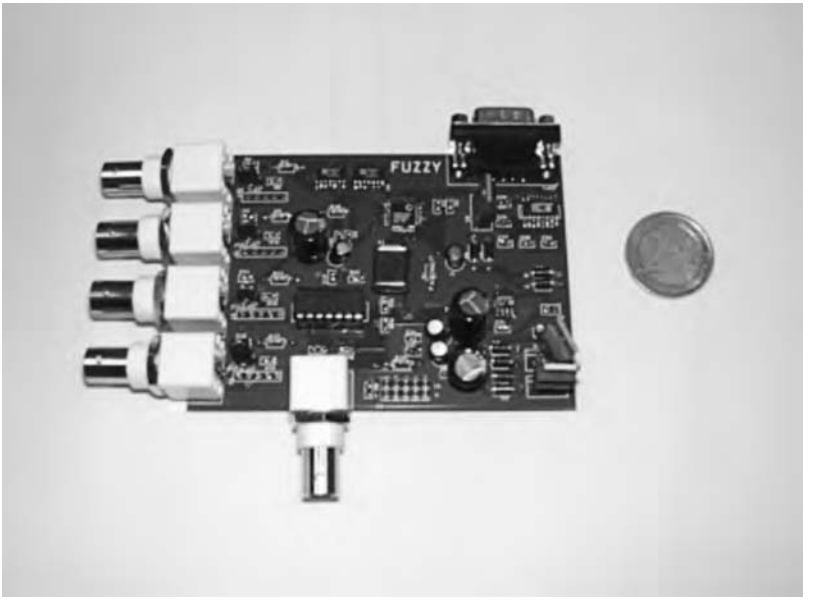

Figure 5.20 Photograph of the board

in-field firmware downloading. The RF transceiver is an Aurel XTR-869 hybrid module. This module is a low-level radio module that provides access to a wireless channel in the 869 MHz frequency band (ISM (Industrial, Scientific and Medical) band). Use of this band is licence-free. The peak over-the-air bit rate is 100 kbps, but the module requires balancing zeros and ones in the range from 20% to 80%, or the receiver will not be able properly to demodulate the incoming signal. The simplest way to accomplish this is to use Manchester encoding, which ensures a 50% balance between zeros and ones. Unfortunately, this also means a 50 kbps over-the-air bit rate. Some analogue conditioning hardware is on-board and allows software-selectable anti-alias filtering thanks to digital potentiometers that can alter the filters' passbands.

6
Experimental Verification

6.1 INTRODUCTION

In spite of the significant progress achieved in the dynamic analysis of structures in recent years, there remains a strong need for the experimental evaluation of structural performance. This chapter presents meaningful developments performed in laboratory testing of large structures under dynamic loads and attempts to recognize the major research trends in this area. Emphasis is given to earthquake engineering applications but most considerations can be easily extended to the wider field of vibration mitigation.

Experimental testing of structures is undergoing deep changes motivated by a variety of reasons. Progress in advanced seismic design specifications is certainly one of them. Performance-based design requires that engineers have a comprehensive knowledge of the structural system performances and notably gain access to complete data on material behaviour in the non-linear range and on energy dissipation mechanisms. This approach addresses a shift towards a more scientifically oriented design process with

Technology of Semiactive Devices and Applications in Vibration Mitigation Fabio Casciati, Georges Magonette and Francesco Marazzi

emphasis on more accurate characterizations and predictions, often based on a higher level of technology than has been used in the past.

Another key element that strongly pushes research towards non-traditional areas is the rapid advancement of technologies related to earthquake and wind engineering. Many new approaches to hazard mitigation based on novel equipment are in progress and need to be endorsed. Smart materials and intelligent structures, advanced sensors, remote sensing, supercomputing power, wireless communication, structural control technologies, etc., provide not only an unprecedented opportunity for improving vibration risk control, but also some new tools for solutions to better understand damage that cannot be solved by traditional approaches. To this end many research programmes have been extended to support the development of new technologies to prevent adverse vibration effects and more generally to control the movements of large structures such as building and bridges. Relevant contributions are currently made in full/large-scale testing of structures effectively protected by base isolation or energy dissipation devices.

More recently, the introduction of semiactive devices has stimulated the development of advanced on-line testing techniques with substructuring able to validate their dynamic characteristics as well as to verify the overall performance of their control laws applied to a realistic structure. Semiactive devices, as their name implies, fill the gap between purely passive and fully active vibration control systems and offer the reliability of passive systems, yet maintain the versatility and adaptability of fully active devices. Many of these systems can operate on battery power alone, providing advantages during seismic events when the main power source to the structure may fail. Also, because semiactive devices cannot inject energy into the

structural system, they do not have the potential to destabilize the system. Recent works have indicated that semiactive control systems, when appropriately implemented, achieved significantly better results than passive control systems and demonstrate significant potential for controlling structural responses to a wide variety of dynamic loading conditions. These factors explain the considerable interest in the practical implementation of these systems for protection of civil infrastructures against earthquake and wind loading or, more generally, for vibration mitigation.

As illustrated in Chapter 3, examples of semiactive devices include variable-orifice dampers, variable-friction dampers, adjustable tuned liquid dampers and controllable fluid dampers:

Many applications combine passive and semiactive systems. A typical example is the hybrid isolation system consisting of friction pendulum sliders or Teflon sliders and semiactive fluid viscous dampers. The semiactive dampers behave as linear viscous dashpots in which the damping coefficient may be continuously modulated between an upper and lower bound. The dynamic response of the building structure is monitored and utilized within a feedback control system to determine the optimal value of the damping coefficient.

6.2 THE CHALLENGES OF PERFORMANCE-BASED DESIGN IN STRUCTURAL TESTING

There is a widespread consensus about the need for developing design methods based on performance objectives rather than on strict practical rules (Pinto et al. 2004). A performance-based approach defines the performance required for a structure, as opposed to prescriptive

approaches, which describe one design solution considered acceptable. In a prescriptive approach, the detailing is specified for each part of the structure, so that the resulting structural assembly does possess some minimum (yet not explicitly defined) performance attributes. On the other hand, the performance-based approach is concerned with what a structure is required to provide, rather than prescribing how it should be designed, detailed and constructed. In other words, the performance-based approach is the practice of thinking in terms of objectives as opposed to means. Performance-based approaches are best suited to the interests of the owners, because performance, in terms of loss of property, contents and operation, is the only requirement the owners are able and willing to look at.

Moreover, there is a general conviction about the fact that a fully performance-based approach would result in more economic structures (where economy includes, besides the cost of construction, the costs associated with damage and limitation/disruption of occupancy), without limiting the possibility of adopting new materials, technologies and design methods.

The European scientific community can already rely on a suite of norms, such as the Eurocodes, which explicitly state the fundamental requirements in terms of performance. However, even though based on performance-based fundamental requirements, the Eurocodes are still far from allowing for a fully performance-based design. In earthquake engineering, for instance, four performance levels are generally thought necessary to characterize the structure fully in terms of performance, whereas Eurocode 8, the Eurocode dealing with the seismic design of structures, explicitly accounts for only one level (life safety). Another level is referred to in the objectives, namely the objective of limiting structural and non-structural damage resulting

from frequent seismic events. This level, however, is considered only by limiting the overall deformations. Moreover, most of the design process is still based on strength rather than deformations, in spite of the generally accepted evidence that deformations, rather than forces, affect the behaviour of buildings and structures. The main reason for the discrepancy between the objectives (which are, even though not in a quantitative fashion, expressed in terms of performance) and the design rules (which are almost exclusively specified in terms of prescriptions) remains with insufficient knowledge of the performance parameters and criteria.

The scientific community is currently tackling the definition, harmonization and cross-correlation of standard and new performance parameters, so that requirements could eventually be specified in terms of those parameters, and new design methods could be developed. In the meantime, prescriptive design rules are maintained, and practice and experience, rather than explicitly quantified performance criteria, control the design process. Even though the situation is acceptable in the case of normal structures, this is certainly not the case for structures with special devices, for which practice and experience are not sufficient to justify prescriptive rules and to drive the engineer in the design process. For these structures, the definition of performance parameters and criteria is more urgent, and this can only come from a research effort based on experiments. However, new problems arise when conducting experiments to meet the requirements of investigations aimed at the definition of performance criteria.

Research activities are based on a combined use of numerical simulation and experimental data. If not available in the literature, experimental data must be obtained by means of appropriate testing activities. For typical structural problems, the data that are needed are usually limited

to a particular phenomenon which is not sufficiently understood, or to a single structural component which is innovative, or designed and detailed with new methods. The experimental set-up can therefore be limited to a simple component or subassembly, in general with no need to test a complete structure. In such cases, the choice of the experimental technique is not particularly important, and the simplest solution, to perform a cyclic test, does meet the scope.

This is not the case for most of the problems relating to performance-based design. For such problems, the performance parameters can hardly be defined at the different levels (cross-section, component, storey or subassembly, complete structure), and their correlation is a substantial part of the problem to be tackled. For this reason, the minimum set-up is quite often a large mock-up, or even the complete structure. Unfortunately, for structures which cannot be treated as a single degree of freedom, cyclic testing can hardly be used. The adoption of more advanced testing techniques, such as shaking table or pseudodynamic (PsD) testing, often becomes necessary (Williams 2001). The choice of the most appropriate testing techniques could become even more difficult when the structure is equipped with special devices, because of the conflicting requirements for testing the structure itself and the device. The possibilities offered by the substructuring capabilities of the PsD method are considered below.

6.3 BASE-ISOLATED BUILDINGS AND BRIDGES

As engineers move towards the acceptance of performance-based seismic design specifications, they are more likely to consider the application of advanced technologies for protecting their structures.

To a limited degree, this has already occurred for passive structural control systems. In particular, a number of structures use passive fluid dampers for absorbing seismic energy either within the framing of the structure or within a base isolation system (Sorace and Terenzi 2001).

The concept of introducing a base isolation system to reduce the vibration transmitted to floors and neighbouring equipment is well established (Figures 6.1 and 6.3). It is one of the most widely implemented and accepted seismic protection systems (Naeim and Kelly 1999). This technique mitigates the effects of an earthquake by essentially decoupling the structure and its contents from potential dangerous ground motion, especially in the frequency range where the building is most affected. The aim is simultaneously to reduce inter-storey drifts and floor accelerations to limit or avoid damage, not only to the structure but also to its contents, in a cost-effective manner.

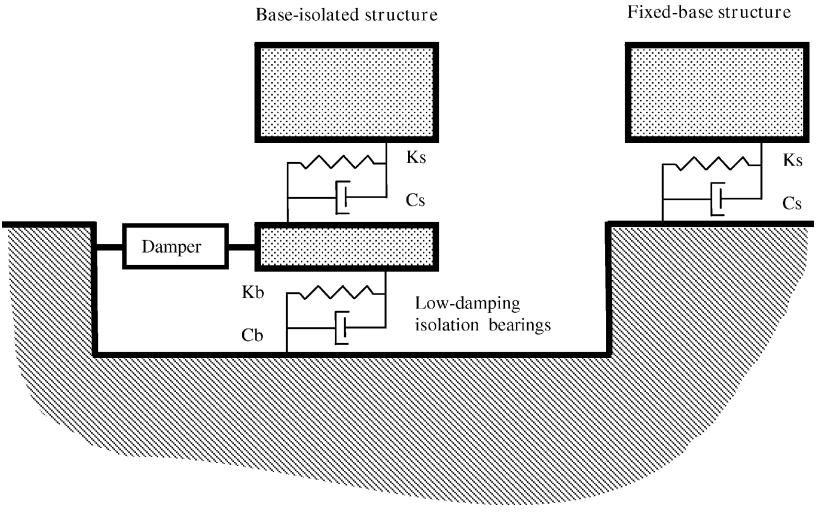

Figure 6.1 Building structure protected by a hybrid seismic isolation system

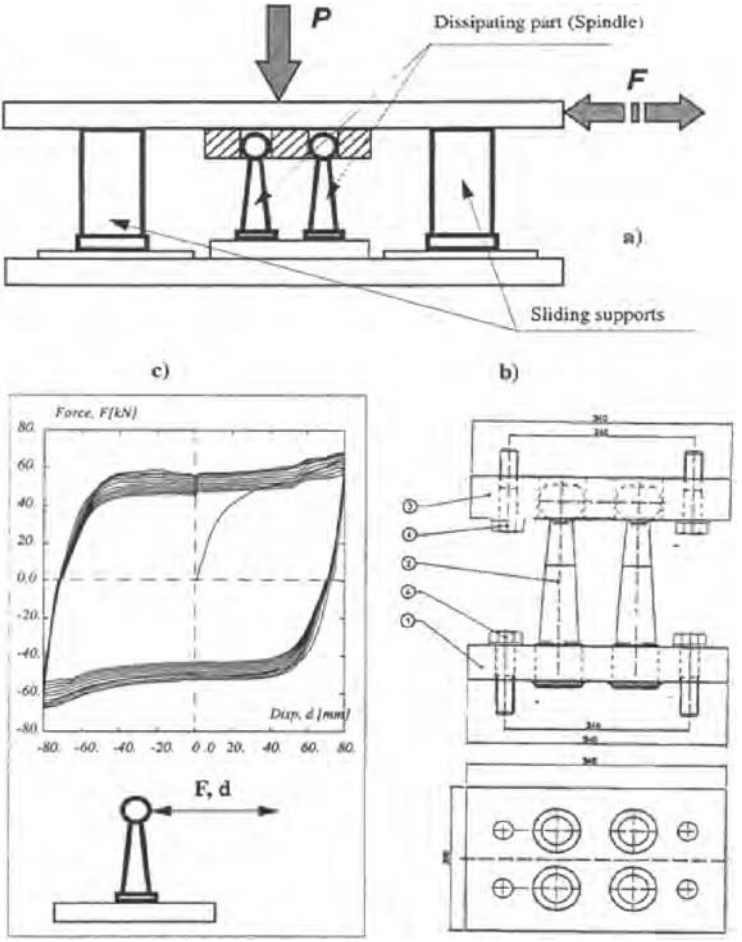

Figure 6.2 Bridge protection system (installed at the top of the piers)

Typically the basic elements of a practical system include (Figure 6.2):

1. A flexible mounting (passive sliding isolation bearings) so that the period of the total system is increased sufficiently to reduce the response.

2. A damper or energy dissipater so that the relative displacement between the structure and the ground can be controlled to a practical level.
3. A method of providing rigidity under low service loads, for example wind and minor earthquake.

Such systems offer a very reliable and cost-effective approach to mitigate the effects of strong earthquake-induced ground motion. In principle they are quite effective for controlling the response of structures since the

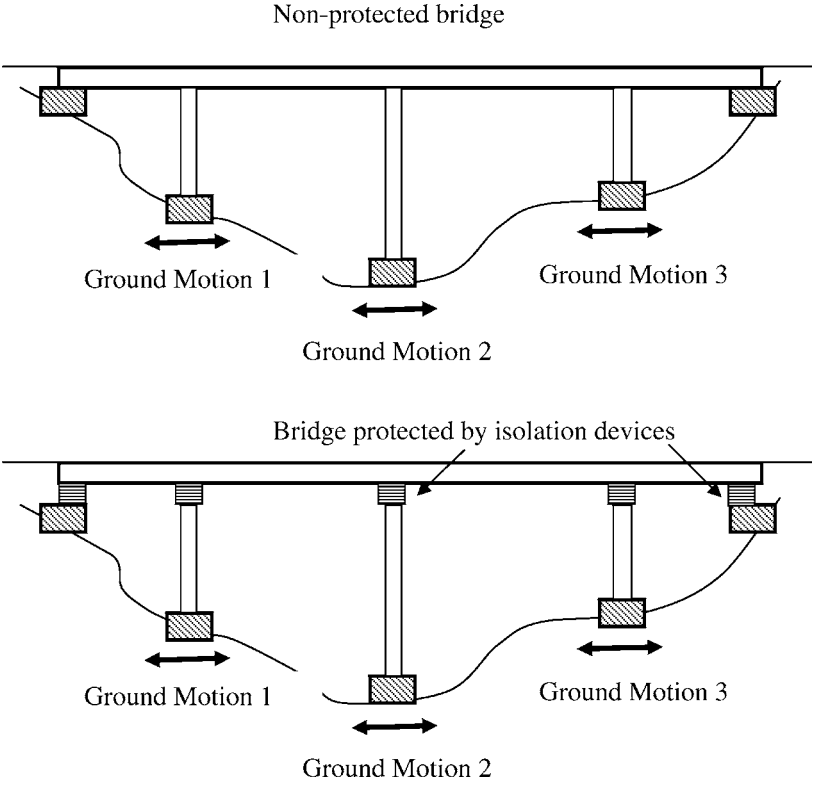

Figure 6.3 Bridge equipped with protection devices

bearings increase the fundamental period of vibration, resulting in a reduction of spectral acceleration, while the dampers limit the displacement response at the isolation level. However, concerns about the effectiveness of passive base isolation systems under various types of seismic excitations have prompted further interest in controllable base isolation (Spencer et al. 2004).

In fact, passive systems may not perform well under a variety of earthquakes. As for the performance issue, it is apparent that passive isolation systems are limited in their ability to respond in an optimal fashion to a wide variety of earthquake ground motion characteristics. For example, a structure may be prone to typical short-period ground motion from a far-field source and to long-period pulse-like ground motion from a near-field source. These two ground motions induce significantly different demands on the seismic isolation system. Another aspect is reported by (Johnson et al. 1998): when isolated structures are designed for extreme earthquake events, the isolation may be much less effective for more frequent moderate earthquakes. An isolation system that can adapt in an optimal fashion to different types of ground motions may exhibit superior performance compared with a passive isolation system that has been designed with a particular type of ground motion in mind. Studies by (Makris 1997) have demonstrated the potential advantages of a semiactive seismic isolation system for near-field pulse-like ground motion. In addition to the near-fault problem, researches by (Sadek and Mohraz 1998a) have indicated that the acceleration response of multi-storey structures with semiactive hybrid isolation systems can be reduced while simultaneously limiting the displacement response.

Because an optimal design of base isolation systems depends on the magnitude of the design-level earthquake that is considered, ideally, to be effective during a wide

range of seismic events, an isolation system should be adaptable. Isolation based on semiactive devices has been shown effectively to protect structures against large earthquakes, without sacrificing performance during the more frequent, moderate seismic events. Further advantage of using variable dampers acting at the isolation interface derives from the observation that beyond certain damping values, increasing the isolation damping value increases the superstructure response. Therefore, a controlled damping system, according to an optimization criterion, may produce better reduction effects. There are currently a wide variety of semiactive control elements for application within hybrid seismic isolation systems (for example, see (Symans and Constantinou 1998)).

These base isolation systems are typically composed of:

1. conventional low-damping elastomeric bearing or Teflon–stainless-steel bearings, operating as sliders; and
2. semiactive dampers, such as variable-orifice fluid dampers, magnetorheological fluid dampers (Spencer and Sain 1997) or friction dissipation devices (Dorka et al. 1998; Taucer 2005).

The latter are connected to the base floor to provide optimal control of the superstructure response in terms of maximum drifts and accelerations. The real-time structural parameter adjustment is applied according to an optimal control algorithm monitoring the system state from an *observation* and *sensory* system.

Bridges for elevated roads and rail tracks are essential parts of the lifelines in a country; their protection against loads that could cause catastrophic collapse is of paramount importance. Quite often a bridge is designed such that it does not collapse after a severe event, while the associated damage may prevent the use of the bridge

for a long period of time. This usually has a dramatic effect on transportation and communications within the affected region and, more often, on crucial emergency response. Modern vibration control technology, especially in the form of semiactive control, offers the possibility of keeping bridges serviceable, even after very strong earthquakes.

A research programme on bridge protection with semiactive devices was undertaken in the framework of the EC-ECOLEADER TASCB Project (HPRI-CT-1999-00059) and is documented in (Dorka 2003; Rodellar et al. 2003; Rodellar et al. 2004). In this study a 150 m, three-span bridge was considered. At the joints between the columns and the superstructure, controllable friction devices (CFDs), designed by Dorka, were applied in parallel to elastomeric bearings. The control objective was to attenuate transversal vibrations of the structure by means of these devices. The CFD used during the experimental testing campaign was made up of a friction element consisting of two steel plates and a set of bronze inserts. One of the steel plates serves as a guide for the bronze inserts, while the other plate represents the sliding surface, sand-blasted and in contact with the inserts. Although the device itself has an ideal elasto-plastic behaviour, elastic joint stiffness after sliding is guaranteed by parallel elastomeric bearings. An easy adjustment of the friction force is accomplished by gas pressure. Quite different force–displacement characteristics, including viscous damping, can be achieved. The gas pressure can be manipulated by a control algorithm. Since no external energy is needed for controlling the dynamic behaviour of the structure, other than for the adjustment of the gas pressure, this concept belongs to the family of semiactive control devices. This application is better documented at the end of this chapter.

6.4 SUPPLEMENTAL DAMPING DEVICES

Some types of structural protective systems may be implemented to mitigate the damaging effects of natural hazards. The basic role of passive energy dissipation devices when incorporated into a structure is to absorb or consume a portion of the input energy, thereby reducing energy dissipation demand on primary structural members and minimizing possible structural damage. Unlike seismic isolation, however, these devices can be effective against wind-excited motions as well as to earthquakes. These systems work by absorbing a portion of the input energy that would otherwise be transmitted to the structure itself.

Consider the following energy conservation relationship:

$$E = E_k + E_s + E_h + E_d \tag{6.1}$$

where

E is the total input energy from environmental forces;
E_k is the absolute kinetic energy;
E_s is the recoverable elastic strain energy;
E_h is the irrecoverable energy dissipated by the structural system through inelastic or other inherent forms of damping;
E_d is the energy dissipated by structural protection systems.

One can see that the demand on energy dissipation through inelastic deformation can be reduced by using structural protection systems. As a consequence, many innovative concepts for structural protection have been suggested and are at various stages of development. Such supplemental damping devices protect a structure by increasing its energy dissipation capacity. They work by absorbing a portion of the input energy to a structure, thereby reducing energy dissipation demands and preventing damage to the

primary structure. This effect is achieved either by conversion of kinetic energy to heat or through the transfer of energy among vibration modes.

A first method commonly used to protect a structure utilizes a brace frame system to resist external forces such as wind and seismic activity. A common configuration consists of a preloaded friction shaft rigidly connected to the structural bracing. Operation in the brace is controlled by the preload on the friction interface, which in turn can be actively regulated through commands generated by the controller during earthquake or severe wind excitation. In another possible configuration, all forces and loads acting on the building will be transferred through the beams through the "K" braces to base resistance (see Figure 6.4).

A second method of energy dissipation incorporates dynamic vibration absorbers, such as tuned mass dampers (TMDs), tuned sloshing dampers (TSDs) or tuned liquid column dampers (TLCDs). As in a TMD, the TSD uses the liquid in a sloshing tank to reduce the resonance of the

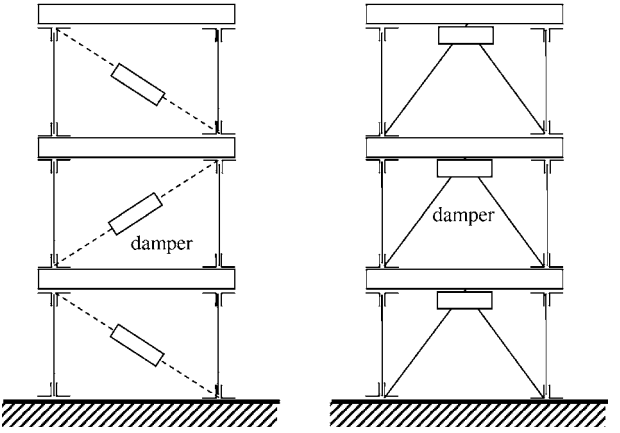

Figure 6.4 Structures protected by a brace frame system to resist external forces

structural system; the length of the sloshing tank is altered to change the natural frequency of the liquid damper. Similarly, in a TLCD, the moving mass is a column of liquid that is driven by the vibration of the structure; the damper works by maintaining an optimal damping condition using a variable orifice in the tuned liquid column.

In the design practice, an earthquake with predicted intensity is usually assumed, and a passive damper system is designed according to this intensity. As a result, the dampers may perform well under earthquakes of the predicted intensity, but may not perform well under others. It is for this reason that the concept of variable dampers is introduced to improve the performance of the whole structural system. For example, a friction damper provides a structure with the damping effect in response to the displacement. Since the damping effect is given by forming a hysteresis it is of great significance how to set the damper slipping or yielding level. In this respect it is desirable to alter the slipping level so as to form an appropriate hysteresis regardless of the intensity of seismic excitation. The slipping level is therefore to be properly controlled by regulating the clamping force applied on the interface of the friction damper in real time, so that the damper may be activated for earthquakes with arbitrary intensities.

Recently, efforts to develop these concepts into workable technology have increased significantly and semiactive control systems have attracted a great deal of attention.

6.4.1 Implementation Issues

A wide variety of issues must be addressed to achieve the successful implementation of a semiactive protection system, but an essential topic to cover from the beginning of the study is the need for clear demonstrations of significant performance enhancements over that which can be

achieved by passive isolation or energy dissipation systems. Passive systems, such as the ones illustrated at the beginning of this chapter, are generally capable of significant response reductions over conventional seismic design approaches. In addition, they are reputed for their reliability in the sense that they have no hydraulic, mechanical or electrical power requirements. As a result of these properties, passive systems are quiet well accepted within the structural engineering community as evidenced by their relatively diffused use within buildings and large infrastructures. Once the performance levels of semiactive systems are shown clearly to exceed that of passive systems, a number of other implementation issues must be faced. Examples of some of these issues include:

1. Experimental characterization and development of a numerical model to simulate and study in detail the semiactive systems.
2. Development of robust control algorithms for operation of the semiactive system.
3. System integration issues where by the protected structure, the semiactive system, the sensor responses and the control hardware/software are considered as a whole in the design process.
4. Reliable and long-life power sources for operation of the semiactive control elements.
5. Development of robust semiactive control elements that will correctly react when called upon after remaining dormant for extended periods of time.

These issues must be considered inside a general process that aims to assess the behaviour of a complete structure by taking into account the study of those components

that are critical in controlling and determining the structural response. For example, in building structures, the behaviour of beams and columns in the vicinity of joints plays a key role in determining earthquake response, while protection devices, when used, can control the overall seismic performance of the structure. In this context, we will examine below the experimental researches that are currently under development to establish adequate and efficient procedures to test protection devices without dissociating them from the protected structure.

6.5 EXPERIMENTAL METHODS IN STRUCTURAL DYNAMICS

For each type of civil structure (reinforced concrete, masonry, steel/concrete composites, etc.) it is intended to identify and fully characterize the minimum number of materials/elements from which a realistic structure can be built: beams, columns, shear walls, infill panels, floor slabs, etc. Then, it is necessary to determine how these elements interact when used together in subassemblies, that is to characterize the behaviour of joints and connections. To this end, *basic tests* are conducted to capture the progression of damage and to obtain the information needed to model the behaviour of the subassembly in a computer program. They are performed to calibrate numerical models to be used to predict numerically the behaviour of the complete structure. Finally *global tests* are conducted to investigate the response of complete structures and demonstrate damage modes and failure propagation, with particular attention given to the energy absorption and margins available between first damage and ultimate collapse. At this level the application of protection techniques including passive or semiactive devices can be analysed in detail. Global

tests are generally needed to verify the adequacy of a complete structure, or of a particular construction method (for instance, with new materials, construction processes), or of a design method including supplementary protection devices or not. They will also be used to calibrate global computer models so that the test results can be supplemented by extensive sensitivity and parametric studies.

At each of the three levels of material/element, subassembly and full structure – it is required to identify the most appropriate tests and variables while reducing the possible range of parameter values to the minimum necessary. A survey of the techniques used in dynamic testing of structures is provided in (Williams 2001) including free-vibration tests, monitoring of ambient vibrations, harmonic excitation tests, shaking table tests, quasi-static tests and PsD tests.

Essentially, two complementary methods are currently applied to simulate the effect of earthquakes on structural mock-ups:

- Small- or medium-scale models are tested, in a laboratory environment, by using a shaking table. More information can be found in (Taucer 2005).
- Full-scale (or large-scale) models are tested in selected sites (in a region prone to either wind or earthquake excitation) or in a laboratory specially equipped with a large reaction wall and specialized in on-line testing or PsD methods (Taucer 2005; Negro and Magonette 1998).

Both approaches have their respective advantages and drawbacks. For earthquake testing a shaking table could, in principle, give the best simulation. The test on a shaking table has the advantage of being dynamically similar to a real earthquake event, but it suffers from at least two severe drawbacks. First, the amount of power needed to move

the mock-up and the table in real time is such that only reduced scale models can be tested, but making reduced models which have dynamic structural behaviour fully representative of real large-scale structures is unfortunately not possible. Scale effects are very important in civil engineering structures, primarily because of the material used. Thus the behaviour of reinforced concrete, particularly in the non-linear regime, is determined by, for example, the aggregate size and the cracking of concrete and the bond between it and the reinforcing steel bars; none of these factors can be scaled readily. Similarly, in steel structures difficulties arise when attempting to scale the behaviour of bolted or welded joints. Secondly, the test on a shaking table is essentially an open-loop process and does not allow following in time the degradation behaviour of the structure with sufficient accuracy.

Hitherto, full-scale dynamic testing of structures has been restricted to on-site measurements on real structures subjected to dynamic loading from, say, traffic excitation, a nearby explosion, a real earthquake or by means of an eccentric-mass vibrator. This may allow a direct measurement of the vibration eigen-frequencies, as well as (if the duration of the motion is sufficiently long) a rough assessment of the corresponding mode shapes. These techniques are generally used to monitor the progression of damage in endangered structures. The data obtained through the monitoring of ambient vibration are of little importance in earthquake engineering, owing to the difficulty in correlating the exciting actions with the recorded motion and to the low level of the actions themselves. However, since earthquakes are uncontrolled in terms of time, location, intensity and repeatability, it is not appropriate to include the measurements obtained from instrumented structures among the experimental techniques.

A reaction wall can be used for full-scale testing to apply only quasi-static cyclic loading because of the limited hydraulic supply rate of a typical system. Consequently, in order to simulate the dynamic inertia forces, special techniques, such as the PsD method, described in the next sections are required. In this context, rate-sensitive materials pose further problems for the PsD method because the tests are performed comparatively slowly; furthermore there is some load relaxation during a step. However, work is in progress towards improved algorithms and more continuous loading to smooth and accelerate the tests, thus reducing these errors.

6.5.1 Shaking Tables

Modern shaking tables are complex systems consisting of a platform which can move in all six degrees of freedom under the control of servo-hydraulic actuators. The prime function of a shaking table is to reproduce accurately, in the laboratory, the true nature of earthquake input to a structure, which is fixed to the table. The growing interest and sensitivity in structural dynamics (shocks, vibrations and earthquakes) called for new requirements to the experimentation and to the associated testing equipment, mainly with respect to the enhancement of the quality and reliability of the simulation. During the last few years many efforts were devoted to the enhancement of shaking table control by implementing advanced controllers to ensure an accurate reproduction of dynamic loads (Stoten 2002) and remove unwanted movements of the table, particularly the rotational (roll, pitch and yaw) components. Although small, they made a significant contribution to the response of the tested structure. This significant progress lies in the fact that economic provision of seismic resistance requires that use be made of energy-absorbing characteristics of the

construction materials. The structure is designed to follow a progressive deformation caused by failure of individual redundant members, but not to suffer either sudden or complete collapse.

The main specific field of application of shaking table testing refers to structural engineering research and to qualification of products. The main advantage of the shaking table resides in its inherent capability of reproducing the real dynamic phenomenon as it acts on the structure under study: that means real-time excitation of the structure and reproduction of the spectral distribution of the input. This aspect is in fact very important when considering the effects of a correct application of the dynamic load on the behaviour of materials or structural elements sensitive to the rate effect (for example, polymer isolation materials, viscous shock absorbers or many semiactive devices). Another appealing feature of most modern shaking tables is their capability to reproduce a dynamic load simultaneously in several directions. This allows, in many cases, a better reproduction of the excitation phenomenon. An ulterior element of peculiarity of the shaking table testing is the capacity to reproduce structural phenomena of fatigue, which is an important aspect, in general, in the study of the behaviour of construction materials, dissipation devices or in the qualification of industrial products. Owing to these specific features, the shaking table technique is currently widely utilized in the following areas:

- The area of civil constructions: in the most recent applications special attention was dedicated to the study and validation of design assumptions, of strengthening and repairing techniques for masonry and reinforced concrete structures, and to the characterization, qualification and validation of seismic isolation and risk mitigation

systems, obviously including, besides the classic passive devices, the most advanced semiactive protection devices.

- The area of industrial protection: shaking table testing is oriented both to the applied research in support of industries in the study, production and application of innovative materials and components, and to the qualification of the industrial products, as a tool for certifying their compliance with the technical and quality requirements imposed by standards and regulations. Among the most interested are the transportation, telecommunication, energy distribution and nuclear power industries.

Shaking tables are especially well adapted for the verification of structures equipped with semiactive protection. The algorithm controlling the semiactive device is based on the real response of the protected structure, and in particular on its displacement and velocity at the location where the control device is applied. Moreover the dissipation principle of the device is often based on a viscous mechanism, whose characteristics strongly change with time, being regulated at each instant by the opening of a valve orifice. Finally the intervention of the devices is affected by their coupling when two or more devices are applied to the same structure; the simulation of this working environment justifies the testing of a suitable physical model of the structure (Figure 6.5).

Concerning drawback and future trends, in most cases the size limitations of the table dimensions require the construction of physical test models with strongly reduced scale ratios compared with the prototypes. The reliability of the results, which could be extrapolated, is a matter of discussion as a consequence of the complex similitude laws, which necessarily must be adopted. The development

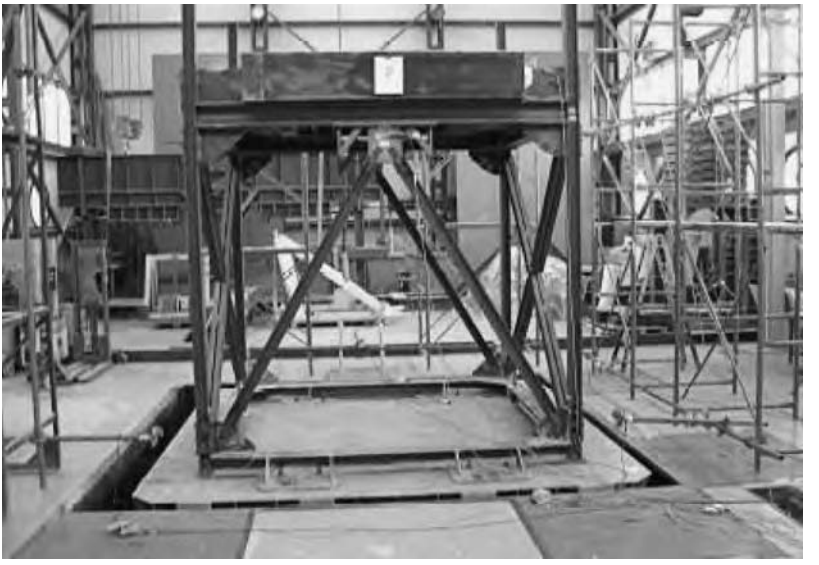

Figure 6.5 Protected mock-up tested on the NTUA-Athens shaking table

of new materials (namely, composite materials) and technologies (namely, seismic energy absorbers) with strongly non-linear behaviour, and the new design concepts recommended by the design codes which allow the use of materials working largely beyond their elastic limits, have further modified the needs of the experimental approach, making necessary a reorientation of the technologies towards the verification of the real structures and, therefore, obliging the abandonment of the model with strong scale ratios in favour of the full-scale prototypes.

6.5.2 On-line Testing

The on-line test method (commonly called the pseudodynamic test method) is a hybrid test technique which combines the numerical integration of the equations of motion

of a complex structure, condensed to a reduced number of degrees of freedom (DOF), and the experimental measurement of the reaction forces resulting from the application of this motion to the structure. The numerical simulation of the inertial forces allows a dynamic test to be performed in a dilated time scale and thus to use reduced hydraulic power. As a consequence, it is possible to determine experimentally the response of a full-scale specimen subjected to seismic loading. Because most of these tests can be carried out quasi-statically, the corresponding methodology is commonly designated as the pseudodynamic (PsD) test method.

Owing to their very large size, civil engineering structures of strong interest, such as bridges, seem to exceed the PsD capabilities. Continuous research efforts in recent years have made it possible to extend the PsD field of application – at least when the behaviour of a part of the structure can be represented analytically – by introducing the substructure technique. Taking advantage of the hybrid character of the PsD method, this technique combines the numerical simulation of the analytical parts of the structure, referred to as the analytical structure, with the effective laboratory testing of the remaining parts of the structure, referred to as the experimental structure. It is well suited for bridges since their largest component, the deck, can be modelled by most finite element software: only the piers, whose dimensions remain reasonable in many cases, are tested in the laboratory. A further advantage of the substructure technique, which is again well suited for bridges, is the possibility to study situations where the seismic excitation is asynchronous or of different intensity from pier to pier (Pinto 2002). However, in its original form the "conventional" PsD method suffers from an important limitation: the computed displacement at each time step is imposed by means of ramps followed by hold periods,

which means that the actuator motion is stopped when the test specimen reaches the target displacement so that the reaction force can be measured and the next target displacement computed. This procedure often introduces spurious relaxation in the structure because the hold period can be of the order of some seconds.

In the last few years, many laboratories have been involved in the development of the new "continuous" PsD testing method. The continuous PsD testing (PsD testing without the hold period) avoids the problem of load relaxation and consequently improves the quality of the results strongly (Pegon and Magonette 1999). Furthermore it allows a considerable reduction in the duration of tests carried out on large structures and is particularly well suited to perform high-speed (or real-time) tests with substructuring. This last property designates this technique as an ideal tool for semiactive device verification. Further details are given in the next sections.

6.5.2.1 The Conventional PsD Method

The basic assumption in the PsD test method is that a discrete-parameter model that has only a finite number of degrees of freedom can represent the dynamic behaviour of the structure. The equations of motion for such an idealized multi-degrees-of-freedom model can be expressed in terms of a system of second-order ordinary differential equations which, in matrix form, reads

$$\mathbf{M}\mathbf{a}(t) + \mathbf{C}\mathbf{v}(t) + \mathbf{r}(t) = \mathbf{f}(t) \tag{6.2}$$

where $\mathbf{M}$ and $\mathbf{C}$ are the mass and damping matrices, $\mathbf{a}(t)$ and $\mathbf{v}(t)$ the acceleration and the velocity vectors, $\mathbf{r}(t)$ the structural restoring force vector and $\mathbf{f}(t)$ the external force vector applied to the system.

Various types of loading can be used. Impact, hydrodynamic, aero-elastic and other loads may be considered by formulating the appropriate equations of motion. In the simplest case of seismic loading, a planar structure is excited by a single lateral ground acceleration, giving $\mathbf{f}(t) = -\mathbf{M}\{1\}\mathbf{g}(t)$ where $\{1\}$ is a vector of ones and $\mathbf{g}(t)$ is the ground acceleration. The equations of motion (6.2) are integrated on-line using a step-by-step numerical time integration method.

Generally the methods applied in PsD testing belong to the Newmark family. In the Newmark algorithms it is assumed that

$$\mathbf{M}\mathbf{a}^{m+1} + \mathbf{C}\mathbf{v}^{m+1} + \mathbf{r}^{m+1} = \mathbf{f}^{m+1} \tag{6.3}$$

$$\mathbf{d}^{m+1} = \mathbf{d}^{m} + \Delta T\mathbf{v}^{m} + \Delta T^2\left[\left(\frac{1}{2} - \beta\right)\mathbf{a}^{m} + \beta\mathbf{a}^{m+1}\right] \tag{6.4}$$

$$\mathbf{v}^{m+1} = \mathbf{v}^{m} + \Delta T\left[(1-\gamma)\mathbf{a}^{m} + \gamma\mathbf{a}^{m+1}\right] \tag{6.5}$$

in which $\mathbf{a}^{m+1}$, $\mathbf{v}^{m+1}$ and $\mathbf{d}^{m+1}$ are the acceleration, velocity and displacement vectors, respectively, at time equal to $(m+1)\Delta T$; and β and γ are parameters selected by the user for stability and accuracy. When β is zero the method becomes explicit, and by setting $\beta = 0$ and $\gamma = 1/2$, the popular central difference scheme can be recovered.

The formulation (6.2) permits tests to be performed with a single horizontal component of motion. The PsD method, however, can easily be extended to non-planar structures subjected to multiple-component fixed-base excitations (Shing and Mahin 1984). Inertia and viscous damping forces are modelled analytically, a relatively straightforward matter compared with obtaining the non-linear structural restoring forces which are measured experimentally because of the virtual impossibility of modelling them

accurately. The process automatically accounts for the hysteretic damping, due to inelastic deformation and damage to the structural materials, which is usually the major source of energy dissipation.

To simulate the earthquake response of a structure (see Figures 6.6 and 6.7), a record of the ground acceleration history of an actual or artificially generated earthquake is given as input data to the computer running the PsD algorithm. The horizontal displacements in the building floors (where the mass of the structure can be considered to be concentrated) are calculated for a small time step using a suitable time integration algorithm.

These displacements are then applied to the test structure by servo-controlled hydraulic actuators fixed to the reaction wall. Load cells on the actuators measure the forces

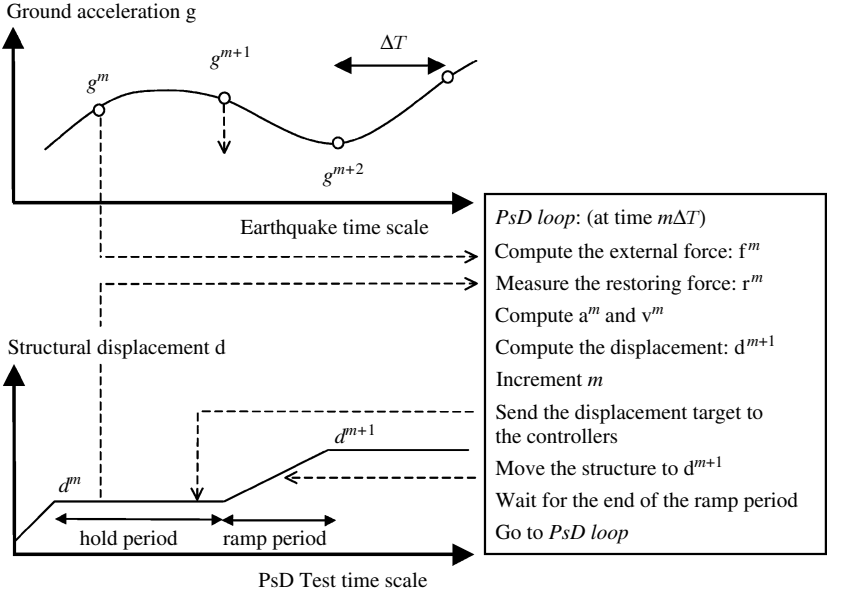

Figure 6.6 Schematic procedure of the conventional PsD method

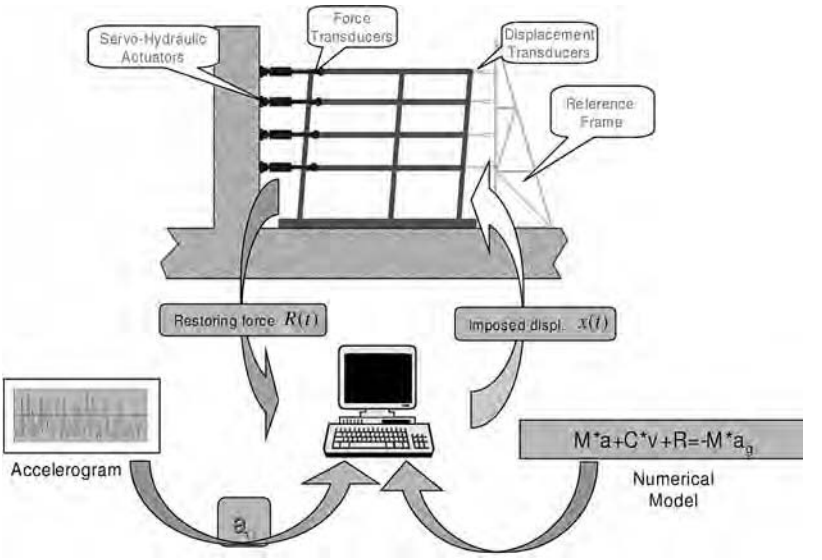

Figure 6.7 Implementation of the conventional PsD procedure

necessary to achieve the required storey displacements and these structural restoring forces are returned to the computer for use in the next time step calculation.

Because the inertia forces are modelled, there is no need to perform the test on a real time scale, and this allows very large models of structures to be tested with only a relatively modest hydraulic power requirement. In this sense, PsD tests are complementary to the more conventional shaking table tests that are done in real time but are restricted to components or small-scale models of large structures. The structural idealization that corresponds to the discretized model (6.2) is not expected to introduce severe limitations since the number of DOF can be large enough to capture the dynamic behaviour accurately. The dynamic properties can in fact be accurately modelled since a consistent mass formulation can be used. The only

concern is about the numerical representation of damping forces. In Equation (6.2) damping forces were introduced as purely viscous. In practical cases, damping forces do not depend on velocity alone and moreover no rational technique to compute a damping matrix exists. Compared with real-time testing techniques, the PsD method is therefore expected to allow only a crude simulation of viscous-damping forces. However, it has to be stressed that in the non-linear regime, most energy is dissipated through hysteretic damping – which is properly represented, since the actual restoring forces are measured in the specimen – so that the accurate representation of viscous-damping forces is no longer important (Shing and Mahin 1984).

The experience gained so far has shown that it is the attention to the PsD method's experimental implementation that ultimately leads to good results (Magonette and Negro 1998). The effects of experimental errors are much more severe in PsD testing than in other testing methods. The experimental feedback errors can in fact propagate in the numerical computations. Incorrect displacements imposed on a test structure result in erroneous force feedback, and the errors in the force feedback lead to erroneous displacements computed in the next step. As a consequence of error propagation, the results of a PsD test can become unreliable, even though the experimental errors produced at each time step are relatively small. Measurement and control errors tend to have a cumulative effect and in some cases these have been seen to dominate the response. In particular, systematic errors can induce unbounded error growth due to the spurious energy introduced into the system, which tends to excite artificially the higher vibration modes of the structure. Nevertheless, by applying modern control technologies, very accurate PsD tests can be achieved. Details on the implementation of the PsD technique

implemented at the European Laboratory for Structural Assessment (ELSA) of the Joint Research Centre (JRC) of the European Commission are given in (Magonette 1991).

A last concern is related to the strain-rate effects. The tests carried out according to the PsD method are performed on a much extended time scale: one spreads out over a long time period (more than 1 hour) the shocks generated in 10 seconds by a real earthquake. In a PsD test, the structure is loaded quasi-statically, that is at a speed low enough to neglect inertial effects. The time interval actually required to apply the displacement increment corresponding to each time step is subdivided into two phases: a ramp period and a hold period. During the hold period, the restoring forces developed by the specimen are measured and fed back to the algorithm to compute the response at the next time step. The expansion of the time scale – which is not constant, owing to the variability of the ramp period – is by two or three orders of magnitude. Such a controlled simulation makes it possible to implement complex models, reproducing with precision the conditions of an individual earthquake, and to observe progressively the distortions undergone by the structure, and in particular the appearance of cracks. It also offers the possibility to complement the experimental model with other structural parts modelled numerically and introduced in the control loop through a substructuring technique. This is very useful for testing very large civil engineering structures such as bridges for which it is unrealistic to build a complete model.

In principle, the behaviour of a structure in a PsD test differs from its actual dynamic response owing to the different rates of loading. Most structural materials exhibit strain-rate-dependent mechanical properties. These effects, however, vary from one material to another. Generally,

the larger the strain rate, the higher the strength. Since in PsD testing deformations are imposed quasi-statically, the structure is somehow made artificially weaker. Even though the behaviour of most materials at different strain rate has already been reported, the assessment of the importance of strain-rate effects in PsD testing is not straightforward. The most effective way to assess the importance of strain-rate effects is to carry out comparative tests. This is systematically done at ELSA whenever a large-scale test is being prepared. The means for this assessment is provided by a comparison of the records of the real-time snap-back tests (performed by pulling the test structure against the reaction wall) and of the PsD simulation of the free vibration. This exercise has been performed for steel structures, reinforced concrete structures, as well as masonry structures.

At this point, it must be emphasized that in spite of its limitation related to strain-rate effects, the PsD technique was applied successfully to the testing of a five-storey steel structure isolated by means of high-damping rubber bearings and of a two-storey reinforced concrete structure equipped with rubber viscoelastic dampers (Williams 2001). As regards seismic isolation by rubber bearings or energy dissipation by rubber devices, although the strain-rate effect cannot be taken into account at the experimental stage, it can be taken into account in the numerical part of the method. A standard procedure for the PsD testing of large-scale models of base-isolated structures has been developed and validated at ELSA. In the proposed procedure a correction function is inserted into the PsD algorithm to allow for strain-rate effects in the isolators. To this end, the measured force is multiplied at each integration step by a correction factor corresponding to a given percentage of the forces in the isolators.

6.5.2.2 The Continuous PsD Method

As stated before, the conventional PsD procedure requires considerable time to complete a test, because pauses in driving the test machines must be set to adjust the actuators to the right positions and to acquire instrument readings. Moreover, the pauses in driving produce discontinuities in the structural velocity and prevent the smooth movement of the structure.

The quality of the PsD tests achieved at ELSA has been improved by applying a technique called continuous PsD testing (PsD testing without hold period), which avoids the load relaxation problem and allows a considerable reduction in the test duration. In the conventional PsD test procedure, the actuator motion is stopped when the test specimen reaches the target displacement (hold period) so that the reaction force can be measured and the next target displacement computed. Instead of stopping the actuator, in continuous PsD testing, the servo-controller moves the actuator in such a way that the specimen follows very accurately the target displacement (due to the lack of discontinuities in the motion). The force is measured at every control sampling period and the equations of motion are integrated "on the fly" (without hold period) at the control sampling rate. The next displacement is determined and the motion proceeds without any interruption. This has been achieved by incorporating the central difference algorithm (to solve the equation of motion) into the digital controller of the electrohydraulic system in place of the displacement target generator.

One significant departure from the conventional PsD system is that in the continuous PsD technique (see Figure 6.8), for each g^m discrete value of the ground acceleration sequence (**g**) read from the acceleration file, a sequence of N acceleration values g_n^m is computed by interpolation

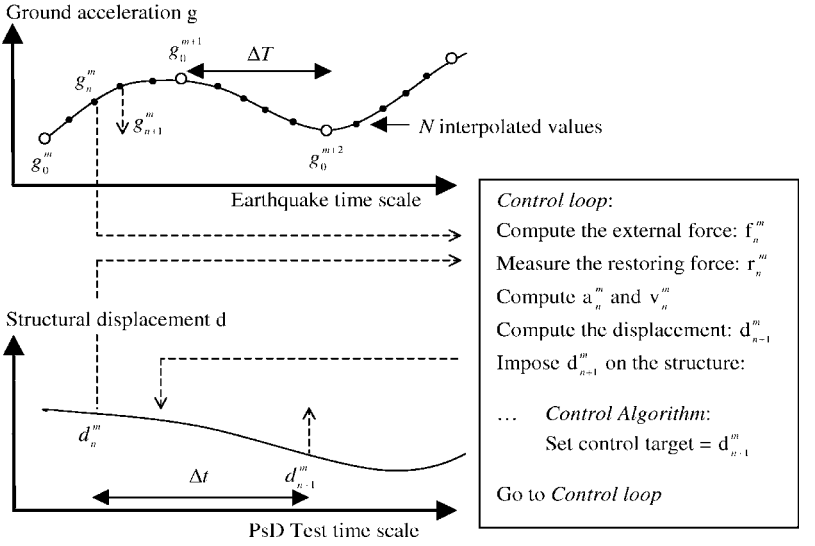

Figure 6.8 The continuous PsD procedure

between g^m and g^{m+1} (that is, $g_0^m, g_1^m, \ldots, g_n^m, \ldots, g_{N-1}^m$). After computation of these N intermediate acceleration values, the PsD procedure is computed N times at the sampling rate of the controller performing N sub-steps in one conventional PsD step. As shown in Figure 6.8, the basic sequence used in the continuous PsD test system remains the same as that used in the conventional PsD test. That is, at sub-step n of step m, this sequence proceeds as follows:

1. g_n^m is read and the external load is computed.
2. The restoring forces $\mathbf{r}_n^m$ are measured.
3. The equations of motion are solved by direct integration; the displacements are computed and used as target displacements by the control algorithm. The actuators drive the test structure to the target position.

4. Wait for the end of the control sampling time Δt (typically 2 ms), and then go to step 1.

Considering a base acceleration file recorded with a sampling time ΔT and a controller (solving the equations of motion and the servo-control algorithms) running with a sampling time Δt, the time scale expansion factor (λ) of the PsD test is given by: $\lambda = (N\Delta t)/\Delta T$. For a continuous PsD test performed on large-scale multi-DOF structures, one may have $N = 1000$, $\Delta t = 2\,\text{ms}$, $\Delta T = 5\,\text{ms}$ giving $\lambda = 400$, which means that 1 second of the real earthquake takes 400 seconds in the test.

In the PsD sequence described here, the reaction force vector is measured at the sampling rate of the controller (typically 500 or 1000 Hz). This procedure not only generates a smooth displacement of the structure, but also performs a noise filtering of the load measurements with respect to a conventional PsD test in which far fewer measurements enter in the algorithm. Moreover, the results of exploratory tests conducted on a three-storey, one-bay, full-scale (10.4 m high) steel frame (Figures 6.9 and 6.10) have shown that this procedure enabled the test speed to be improved by a factor ranging from 10 to 20 (depending of the inertial mass present in the test specimen). It should be noted that, in the PsD test under dynamic loading, the force measured by the load cell includes an inertial force λ^2 times smaller than the real inertial force so that it is usually disregarded. When the mass of the test structure is large, and λ lower than ≈ 10, this inertial effect should be taken into account when solving the equation of motion.

Continuous PsD testing increases the loading rate and drastically reduces stress relaxation phenomena. It is particularly useful for the study of structural

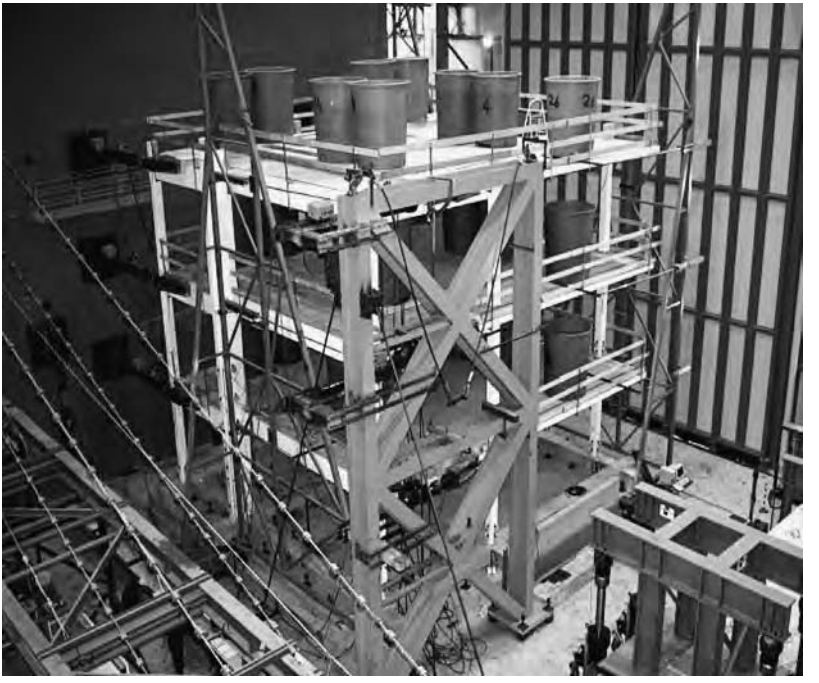

Figure 6.9 Multidimensional PsD tests on a three-storey, full-scale building at the European Laboratory for Structural Assessment (ELSA)

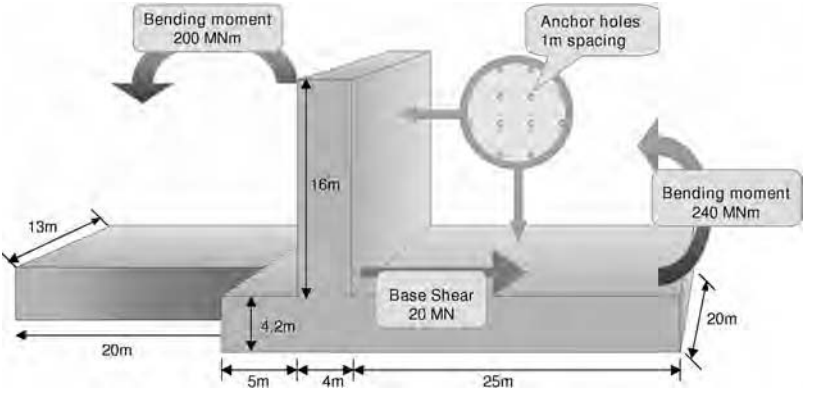

Figure 6.10 Large strong floor and reaction wall at ELSA

components made of materials exhibiting velocity-dependent behaviour.

6.5.2.3 The PsD Technique with Substructuring

In spite of the potential of the PsD technique, direct testing of very large civil engineering structures raises the problems of mock-up size and of the number of DOF to be controlled, so that one may exceed the experimental capabilities. In addition, the lateral load resistance of many structures is governed mainly by certain critical components that suffer the most severe inelastic deformations during a strong earthquake. In such cases, it may be inefficient, uneconomical and unnecessary to test the entire structure. It is, however, possible to overcome these difficulties with the PsD method by introducing the substructuring concept used in computational dynamic analysis. In this case, different portions of a structure are grouped into substructures that are treated separately for convenience in implementation as well as for computational economy. Considering that the PsD test is in fact a numerically controlled process based on equation (6.2), one can readily form the idea that only that part of the specimen which has complex hysteretic behaviour may be fabricated and tested in the laboratory, whereas the remaining parts are handled only within the computer. By means of substructuring techniques, the displacements that are imposed on the test structure are obtained by solving the equations of motion of the global system, while the restoring forces of the portions that are not subjected to experimental testing are provided by numerical models (see Figure 6.11).

In order to avoid iterative solutions and the corresponding load oscillations of numerical origin, explicit integration schemes are normally used to perform conventional

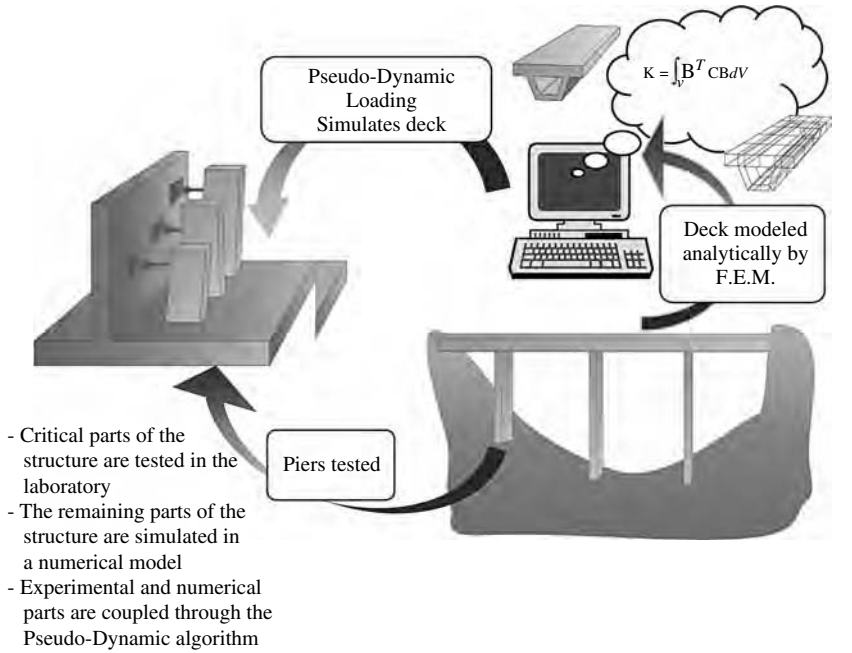

Figure 6.11 PsD testing with substructuring

PsD tests. In PsD substructuring, the number of DOF of the structure is likely to be large. Thus, when the explicit integration scheme is used the time interval applied has to be very small to meet the constraint of stability and this could make the experiment impracticable. Recently, several unconditionally stable implicit and mixed implicit–explicit integration schemes have been successfully implemented for substructuring tests (Nakashima 1999). Among them, it was found that the mixed explicit–implicit operator splitting (OS) method, originally proposed by (Hughe et al. 1979) and successfully implemented for substructuring PsD tests, is very suitable for incorporation into many existing dynamic response analysis codes using implicit integration procedures.

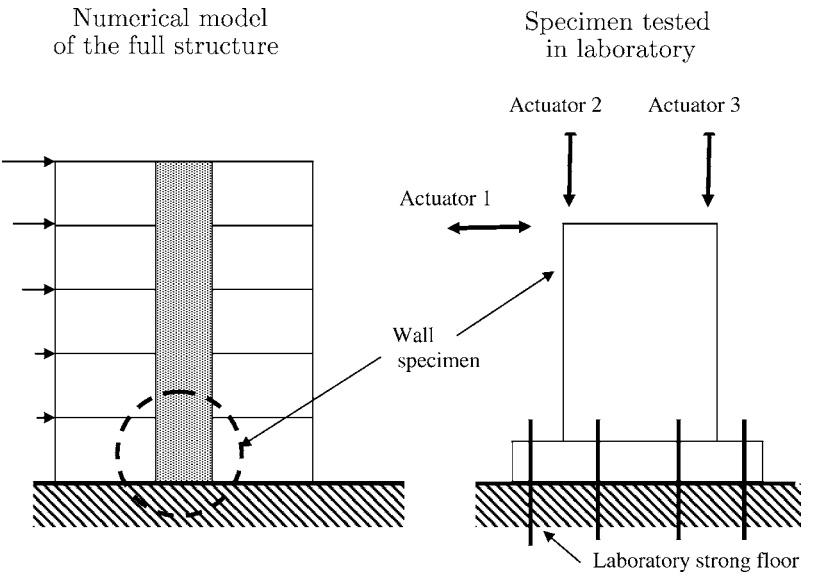

Figure 6.12 Testing of shear wall using the PsD method with substructuring

Two sample applications with substructuring features are illustrated in Figures 6.12 and 6.13. The three actuators shown in these figures can be configured in a number of ways to test full-size, storey-high shear walls and columns, scaled models of large bridge columns, storey-high braced frames, beam column subassemblies, base isolation pads, and passive or semiactive control devices.

There are several other applications where the PsD substructuring concept can be applied efficiently and economically. For civil buildings with base isolation, for which the behaviour of the superstructure itself is known (base isolation preventing non-linearity from taking place in the upper structure), the test set-up can be limited to two bearing units, the rest being modelled numerically. Moreover, most structural specimens that have been tested in the

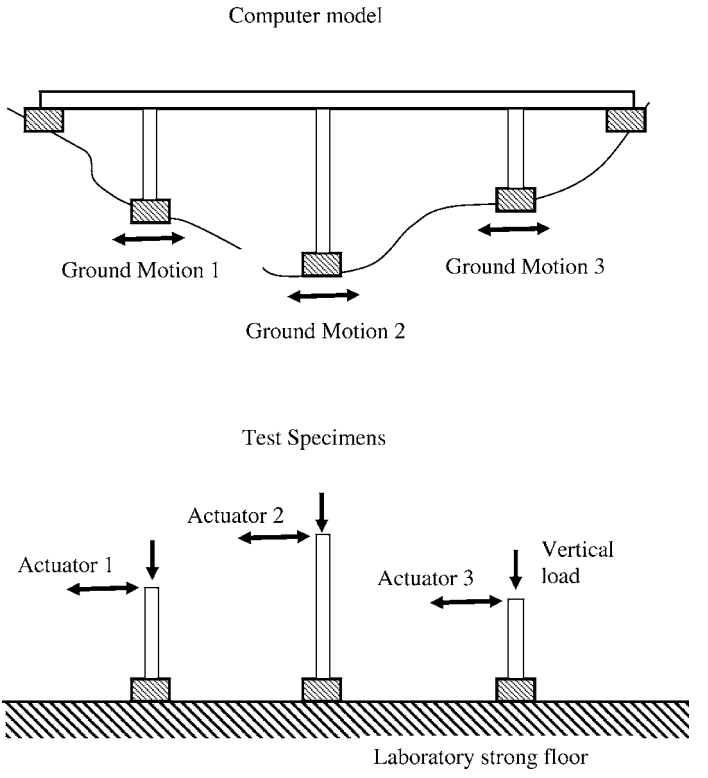

Figure 6.13 Testing of bridge columns using the PsD method with substructuring

past did not include the flexibility effects of the supporting soil and foundations. Substructuring would be useful to account for such flexible boundary conditions.

It is evident that substructuring brings substantial versatility to the PsD test method. However, its applications are not without limitations. It should be understood that the reliability of the PsD test results directly depends on the realism of the analytical substructure. Furthermore, care must be taken to apply realistic boundary conditions at the interface DOF. In some cases, control of the boundary may

render an experiment impractical to perform. The substructure PsD method has become particularly appealing for the experimental evaluation of structures incorporating additional dampers or equipped with base isolation (Molina 2002), and certainly presents a high potential for the experimental evaluation of modern protective systems involving passive and semiactive energy dissipation devices.

To extend the applicability of the continuous PsD method to fast on-line substructuring tests, the integration schemes, control algorithm and hardware architecture need to be upgraded as explained in the next section.

6.5.2.4 High-speed Continuous PsD Testing on Components

Many laboratories are currently developing systems capable of performing high-speed continuous PsD tests, aiming to measure accurately the response of structures containing velocity-dependent devices. The general proposal is for an advanced dynamic testing facility in which the critical section or component of a structure is tested at full or large scale (and possibly in real time) by reproducing the forces and displacements imposed on it by the surrounding structure modelled numerically. Usually such a development implies a very significant upgrading of the control systems of our experimental facility and includes:

- The implementation of a system coupling the substructuring technique and the continuous PsD technique performed at high speed.
- The implementation of a servo-controller algorithm which retains an extremely low tracking error when the structure is loaded at high rate.

In PsD tests, accurate displacement control has been found to be of prime importance to ensure reliable response; otherwise, displacement error propagation and eventual severe distortion in response will prevail in the test. Moreover, in a test applied to a structure with a highly velocity-dependent restoring force, accurate velocity control is also a necessity to measure the restoring force accurately. Unfortunately, the parameters of the tested object are poorly known and the controllers operate in environments where unpredictable large-system-parameter variations and unexpected disturbances are possible. In such situations, the usual fixed-gain PID control must be improved to achieve the requested performance in the entire range over which the characteristics of the system may vary. Very often, full-state feedback or adaptive control algorithms are suggested to achieve the necessary accuracy in both displacement and velocity of the servo-hydraulic actuators and guarantee an accurate PsD simulation.

Moreover, when multiple actuators are used to test components, synchronization between individual actuators needs to be accomplished. This requires additional refinement in the architecture of the control system. Because of the very high speed needed for computing and communicating, the computational capacity of the controllers must be increased and an advanced communication system must be designed, assuring the "strong coupling" of all the controllers. Specific hardware is currently in development in many laboratories to tackle this problem.

Such new experimental facilities enable dynamic tests of critical components to be coupled with a numerical model of the superstructure. Because of the very high computing speed needed, it is not yet possible to calculate the required displacement increment directly from a non-linear analysis except in the simplest cases. Instead, an equivalent linearized model is created, which takes as input any

applied forces or displacements together with measured forces from the test specimen and generates the required displacements to be imposed on the specimen.

System robustness as well as hardware and software reliability are assessed in several laboratories where multi-DOF substructuring tests were initially executed on simple mechanical set-ups (see, for example, Figure 6.14) in preparation to more complex tests on structures including rate-sensitive devices and components such as passive or semiactive isolators or energy dissipation systems.

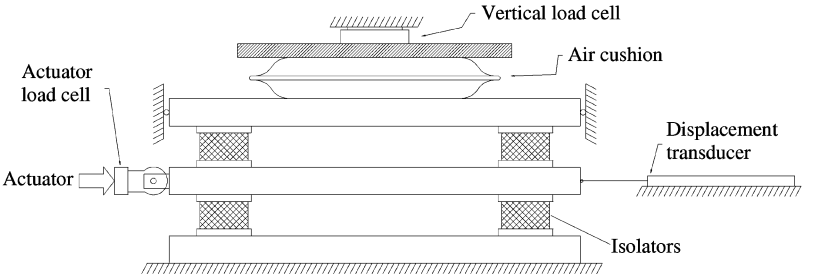

(a)

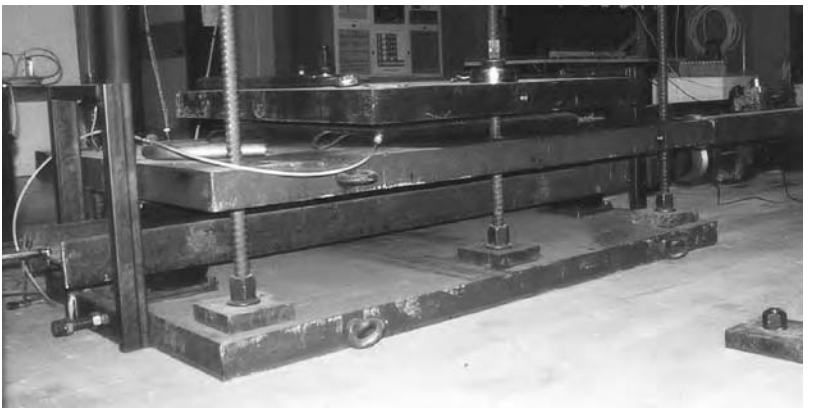

(b)

Figure 6.14 Experimental set-up for rubber bearing characterization and PsD test with substructuring

Most often, prototype testing systems are constructed by modifying existing experimental set-ups with particular attention being paid to the actuator dynamics and actuator response delay compensation. This is because the dynamic characteristics of hydraulic actuators inevitably include a response delay which is equivalent to negative damping in a fast hybrid experiment. In order to compensate for this delay (Horiuchi and Nakagawa 1996) proposed that the desired position of the actuator be predicted using a polynomial fit of previous displacements. Typically a third-order polynomial is used since it has good stability properties whilst maintaining a low computing overhead. The system was applied successfully to real-time on-line tests of a few model structures treated as up to four DOF systems, with one DOF tested and the others treated numerically using the substructuring technique. The system designed at the University of Oxford (Williams 2001) has some features in common with that reported by Horiuchi and Nakagawa, but is ultimately more powerful since it includes non-linear behaviour both within the test specimen itself and in the computer model of the surrounding structure.

The testing systems developed in these interesting exploratory researches have the following features in common: they pertain to the class of apparatus referred to as "real-time hybrid testing systems", and they are designed to perform real-time tests on single devices, with the rest of the structure modelled numerically. The actuator delay compensation is based on prediction techniques and remains strongly dependent on the characteristics of the installation and of the structure under test.

In general the standard substructuring technique, as shown in Figure 6.15, is readily applicable to fast hybrid testing and most of the applications share a common substructuring strategy, but the numerical schemes may differ from one installation to another depending mainly on the

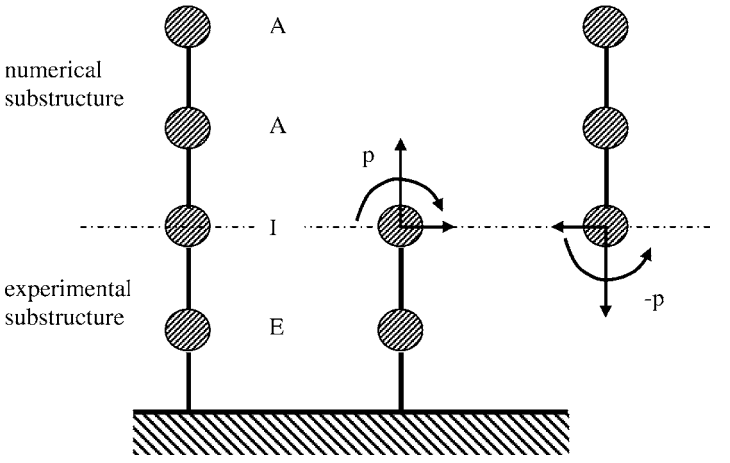

Figure 6.15 Standard substructuring technique

servo-control performances and the sophistication of the numerical model. The basic procedure is described below.

The equations of motion for the experimental and numerical substructures shown in Figure 6.15 can be expressed as

$$\begin{bmatrix} \mathbf{M}_{EE} & \mathbf{M}_{EI} \\ \mathbf{M}_{IE} & \mathbf{M}_{II}^{E} \end{bmatrix} \begin{bmatrix} \mathbf{a}_E \\ \mathbf{a}_I \end{bmatrix} + \begin{bmatrix} \mathbf{C}_{EE} & \mathbf{C}_{EI} \\ \mathbf{C}_{IE} & \mathbf{C}_{II}^{E} \end{bmatrix} \begin{bmatrix} \mathbf{v}_E \\ \mathbf{v}_I \end{bmatrix} + \begin{bmatrix} \mathbf{r}_E \\ \mathbf{r}_I^{E} \end{bmatrix} = \begin{bmatrix} \mathbf{f}_E \\ \mathbf{f}_I \end{bmatrix} + \begin{bmatrix} \mathbf{0} \\ \mathbf{p} \end{bmatrix} \tag{6.6}$$

and

$$\begin{bmatrix} \mathbf{M}_{II}^{A} & \mathbf{M}_{IA} \\ \mathbf{M}_{AI} & \mathbf{M}_{AA} \end{bmatrix} \begin{bmatrix} \mathbf{a}_I \\ \mathbf{a}_A \end{bmatrix} + \begin{bmatrix} \mathbf{C}_{II}^{A} & \mathbf{C}_{IA} \\ \mathbf{C}_{AI} & \mathbf{C}_{AA} \end{bmatrix} \begin{bmatrix} \mathbf{v}_I \\ \mathbf{v}_A \end{bmatrix} + \begin{bmatrix} \mathbf{r}_I^{A} \\ \mathbf{r}_A \end{bmatrix} = \begin{bmatrix} \mathbf{0} \\ \mathbf{f}_A \end{bmatrix} + \begin{bmatrix} -\mathbf{p} \\ \mathbf{0} \end{bmatrix} \tag{6.7}$$

in which the subscripts E and A denote the DOF internal to the experimental and numerical substructures, respectively, and I denotes those at the interface nodes. The equations of motion for the complete structure can be recovered by combining these two equations with the elimination of the interface force $\mathbf{p}$.

As explained before, in a fast on-line test it is essential to solve the equations of motion within the sampling interval of the servo-control system so that the computation of the displacements can make use of the most recent measure of the reaction forces of the experimental substructure. This may not be possible when the number of DOF of the numerical substructure is large or if non-linearities are modelled. It is often advantageous to condense out the internal DOF in the analytical structure and to avoid the insertion of strong non-linearities on the analytical substructure. Currently many studies are on course to avoid such drawbacks. In (Pegon and Magonette 2002; Pegon and Magonette 2005) it is highlighted how the speed of the numerical computation can be significantly enhanced by implementing the substructuring method in a parallel computing environment. This literature also proposes formulations that can be easily expanded to accommodate multiple experimental and analytical substructures for multi-site distributed tests.

Before proceeding further it must be noted that, because of dynamic loading, the fast PsD test is expected to lose two of the most significant benefits that we enjoy from the PsD test based on quasi-static loading, namely the opportunity of careful observation and testing on a large size. In this sense, the fast (real-time) PsD test must not be regarded as a means of superseding the quasi-static PsD test, but rather as one promising extension to the variety of PsD testing methods (Nakashima 1999).

6.6 ASSESSMENT OF STRUCTURAL CONTROL DEVICES

The development of reliable and economic structural protection systems is in continuous expansion and the

demands for their experimental verification are increasing consequently. The protection devices may be passive, semi-active or active, and respond to displacement, velocity or a combination of both to mitigate the vibrations of structures caused by dynamic loads, such as wind, earthquake, traffic, pedestrians, etc. Cyclic tests are commonly performed initially to characterize the device behaviour but a full validation requires the simulation of realistic dynamic loads and the accurate reproduction of the real boundary conditions. Tests satisfying such requirements can be successfully achieved by applying the on-line testing method with substructuring described previously.

Figure 6.16 illustrates an example where a component (circled in the figure) is tested in laboratory to assess its functionality and performance. In the top left of the figure the complete structure is shown. In the analysis the complete structure is split into two substructures, a structural subassemblage (physical specimen) of one element tested in the laboratory and a numerical model simulating on a computer the dynamic behaviour of the remaining part of the structure. The interface nodes are the linking points where the forces and displacements are common to both substructures. The interaction between the two substructures is achieved in the numerical scheme solving the equations of motion for the experimental and analytical substructures.

It is emphasized that the success of this testing method depends mainly on the following factors:

1. The ability to represent adequately the structural response of the numerical part of the structure, especially when considering non-linear behaviour.
2. The ability to design a testing rig capable of simulating the boundary conditions between the tested component and the part of the structure simulated numerically.

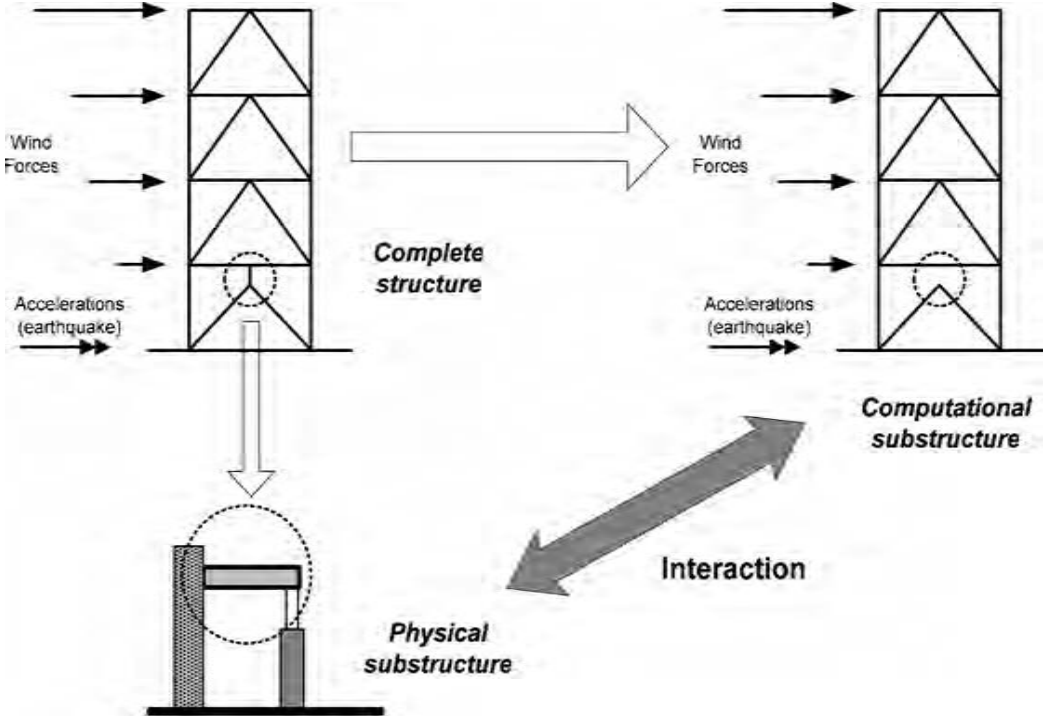

Figure 6.16 Schematic diagram of an on-line test with substructuring to assess the behaviour of a protection device

3. The ability to control accurately the performance of tests carried out at high speed (possibly in real time) on velocity-dependent devices.

Recently, many on-line tests with substructuring have been successfully performed on passive devices, in particular for base isolation of building structures equipped with high-damping rubber bearings or steel yielding devices. This methodology, initially developed for passive devices, was extended to include its application to semiactive device assessment. It is now a valid and cost-effective approach to validate the effectiveness of full-scale semiactive devices and related control strategies without having to test the whole protected structure.

Figure 6.17(a) represents the cross-section of a 150 m long, three-span bridge protected with controllable friction devices (CFDs) installed in parallel with elastomeric bearings mounted at the top of the piles. This design was studied and tested under the EC-ECOLEADER-TASCB Project: "Testing of Algorithms for Semiactive Control of Bridges" (Dorka 2003; Rodellar et al. 2004; Taucer 2005). The control objective was to mitigate transversal vibrations of the structure by means of these protection devices. The CFD analysed during the experimental testing campaign consists of two steel plates, a set of bronze inserts and a pressure chamber acting on the bronze inserts. One of the steel plates serves as a guide for the bronze inserts, while the other plate interfaces the sliding surface with the head of the bronze inserts. The amount of friction can be modulated by varying the normal force acting on the bronze inserts by means of the pressurized gas chamber.

Quite different force–displacement characteristics can be achieved. The gas pressure can be manipulated by a control algorithm. Since no external energy is needed for controlling the dynamic behaviour of the structure, other than for

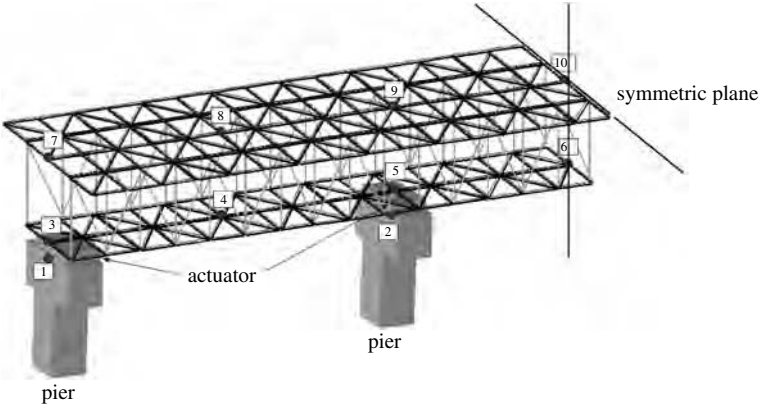

(a) Finite element scheme of the bridge with CFDs and elastomeric bearings

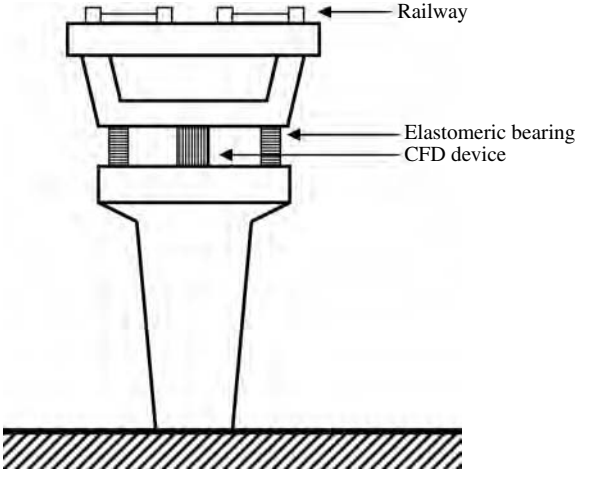

(b) Schematic view of the protected bridge

Figure 6.17 Railway bridge protected by CFD devices

the adjustment of the gas pressure, this concept belongs to the family of semiactive control devices.

Another important aim of the project was to assess and compare semiactive control strategies applied to a realistic bridge structure subjected to severe earthquake ground

motions. For this purpose, the on-line test method with substructuring was used, allowing a realistic nearly full-scale test without having to build a physical model of the bridge.

The bridge structure was modelled analytically, as shown in Figure 6.17(b), while the CFD[1] and the associated control system, shown in Figure 6.18, were tested experimentally.

In the example considered here the elastic analytical part was modelled by small-size mass, damping and stiffness matrices. The initial, complex, finite element model was condensed to a few DOF to obtain small-size matrices with the aim of solving the equations of motion in a very short time. Under these conditions it was possible to perform the test in real time and to characterize the isolation system fully by imposing its predefined loading histories and testing it in realistic seismic conditions taking into account the actions of the protected substructure.

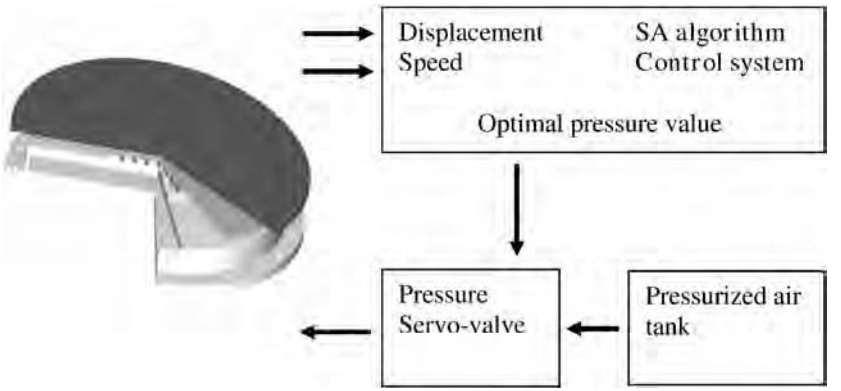

Figure 6.18 Controllable friction device (UHYDE-f-Br)

[1] These CFDs (referred to as UHYDE-f-Br) were designed and developed by Professor Uwe Dorka (coordinator of the TASCB Project) who reserves all the rights protected by a patent.

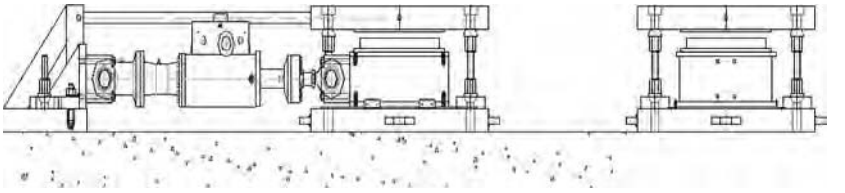

Figure 6.19 The testing set-up used for CFD characterization and on-line testing

The experimental test set-up is shown in Figure 6.19. The CFD is placed between two fixed steel plates with the lower part of the device free to slide on a Teflon plate and with the upper part rigidly connected to the upper steel plate.

The results of the characterization of the devices are shown in Figure 6.20 (Bosi 2003) in which cyclic loading has been imposed with an internal pressure of respectively

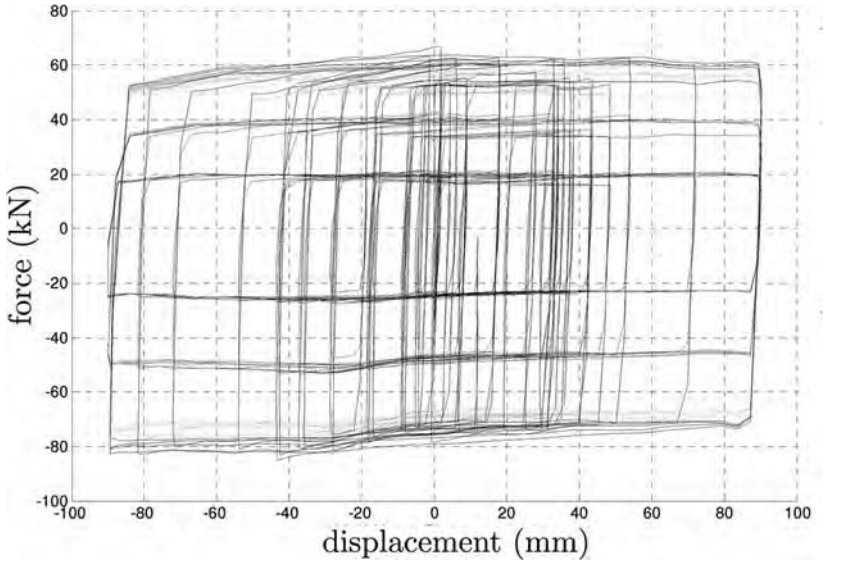

Figure 6.20 Adaptive friction device characterization results

20, 40, 60 and 70 MPa. This almost elastoplastic behaviour is practically not altered by the loading velocity.

The device is used to isolate a structure which, in this case, is the bridge shown in Figure 6.21. Since the structure (and location of isolators) is symmetrical, only half of its construction was considered in the test. Anticipating the use of isolators working at the top of the piers mainly in shear, elastomeric supports were used to support the weight of the deck under static conditions and to realign the deck following a seismic event. The structure (and the elastomeric supports) was modelled using finite element beams and plates, statically condensed on 20 appropriately selected DOF (Rodellar et al. 2004; Taucer 2005). Thus, the analytical substructure is characterized by its stiffness K, damping C and mass M matrices. For the first time, only the configuration in which a CFD was mounted at the top of the external piers was considered.

Assuming that the value of the actuator force is measured by the load cell at the level of the CFD and that the isolator connects the fourth and the sixth DOF, the central difference algorithm is implemented as illustrated in Figure 6.22 (Bosi 2003).

The CFD was first tested with a constant pressure of 60 MPa. Under these conditions it behaves as a passive friction device. Figure 6.23 shows the seismic response of the

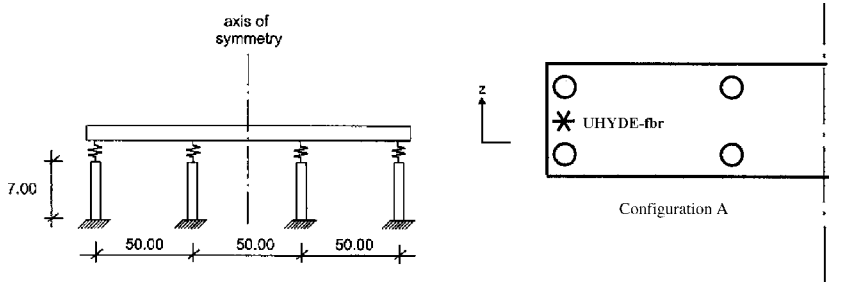

Figure 6.21 The bridge to be isolated

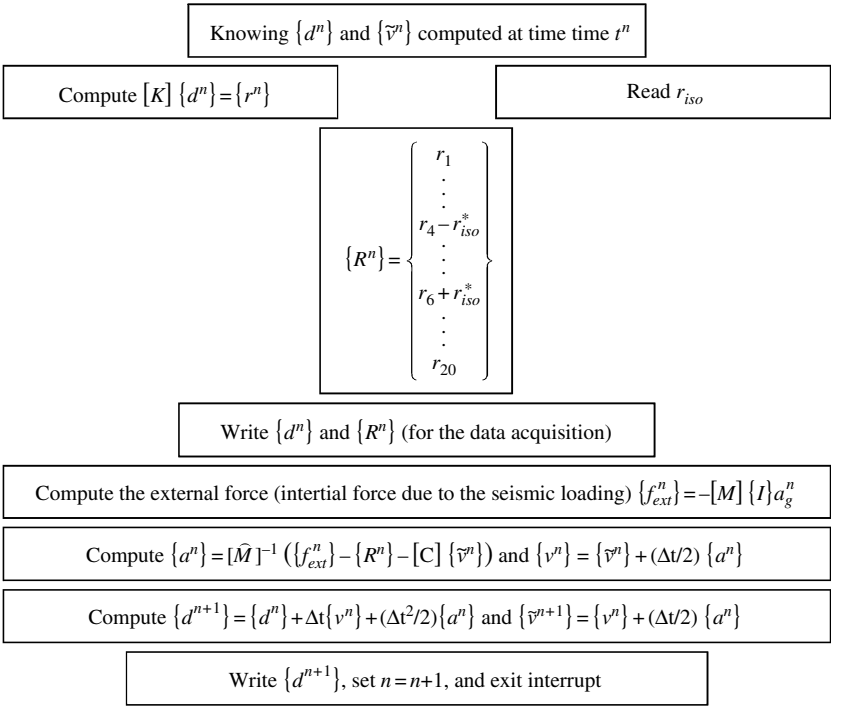

Figure 6.22 On-line testing algorithm with substructuring

specimen (for 30% of the seismic input) in terms of displacements, for different values of the time scale expansion parameter, λ ($\lambda = 5$, $\lambda = 3$, $\lambda = 2$ and $\lambda = 1$). The maximum stroke of the actuator during the test was approximately 10 cm. Figure 6.24, which plots the logarithm of the error with respect to the logarithm of λ (with a slope close to 2), shows that the displacement error increases with increasing speed of test execution.

From this test two important conclusions can be stated:

1. Accurate real-time subcomponent tests with a substructure are feasible.
2. The error tends to increase quadratically with the velocity of the test.

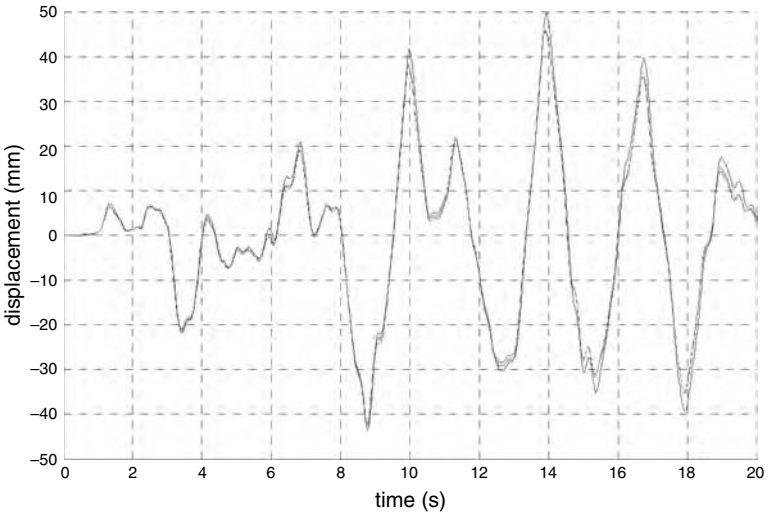

Figure 6.23 Displacement time history

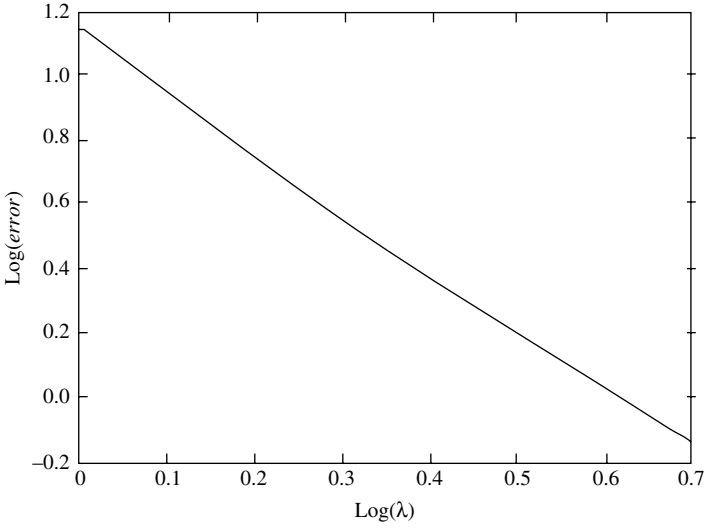

Figure 6.24 Logarithm of the error versus the logarithm of λ

While the previous analysis refers to the passive behaviour of the CFD, it is quite interesting to note that the experimental set-up and on-line testing procedure can be immediately employed to assess its semiactive properties as well as to verify the robustness and reliability of the control algorithm implementation. In fact the semiactive control algorithm can be inserted in sequence with the on-line procedure described in Figure 6.25. At each step of the integration of the motion equations, the current values of the relative displacement, speed and acceleration are available as input variables for the control algorithm. At this point an optimal value of the device control variable can be computed and applied to the command hardware

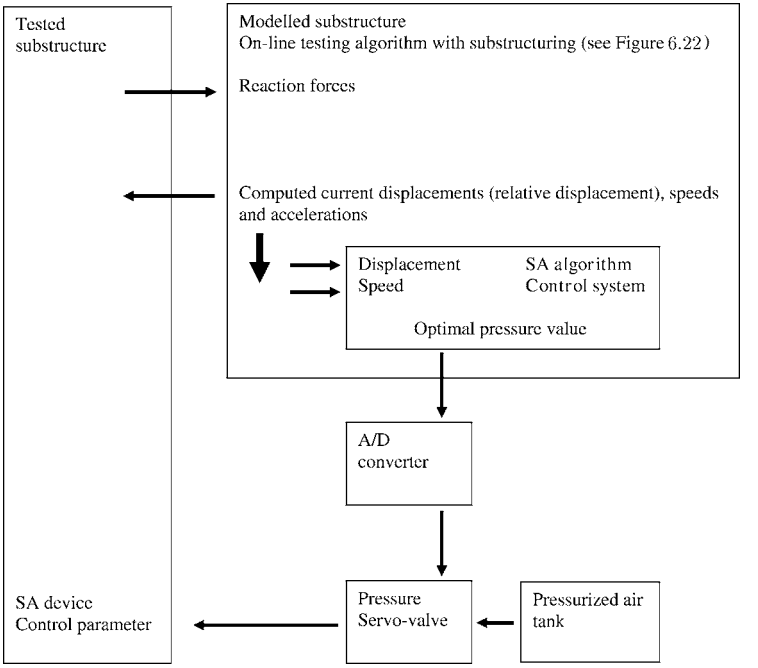

Figure 6.25 Fast on-line testing with substructuring for semiactive (SA) devices and control system assessment

after conversion in electrical value by a digital-to-analogue converter. This implementation is extremely flexible for performing a complete verification of the semiactive control system as well as for testing the physical device over a very large range of operational conditions.

7
Stability and Foreseen Developments

7.1 PRELIMINARY CONCEPTS

In structural control systems where no external energy is introduced in the system no instability can appear owing to the damping in the system. Nevertheless time delays, which influence the performance of the system, can be present. This leads in general, with an increasing delay, to unstable systems or systems which damp excitations very slowly. Of course, systems which are very slow to return to the equilibrium are less desirable than others which return quickly. Therefore it might be interesting to have not only the qualitative statement that the control system is stable, but also some quantitative results about the velocity with which the system returns to the initial position after excitation.

For linear control systems there exists an extended mathematical theory, whereas for non-linear systems the theory is far from being complete. A newer development which tries to use the results from linear systems to approximate non-linear systems is the method of piecewise linear systems. In this method the state space is divided into a

Technology of Semiactive Devices and Applications in Vibration Mitigation Fabio Casciati, Georges Magonette and Francesco Marazzi

number of subsets, where the dynamics of the system is linear.

7.1.1 Stability of Linear Differential Systems

Consider an n-dimensional linear differential system in the form

$$\dot{\mathbf{x}}(t) = \boldsymbol{\mathcal{A}}\mathbf{x}(t) \tag{7.1}$$

with $\boldsymbol{\mathcal{A}}$ an $n \times n$ matrix.

In the case of controlled systems, this matrix also accounts for the control in the form $\mathbf{u}(t) = \boldsymbol{\mathcal{B}}\mathbf{x}(t)$. The problem of stability of the system is related to the location of the zeros of the characteristic function $p(\mu)$ of the matrix $\boldsymbol{\mathcal{A}}$ given by

$$p(\mu) = \det(\mu \boldsymbol{I}_n - \boldsymbol{\mathcal{A}}) = \mu^n + \mathtt{trace}(\boldsymbol{\mathcal{A}})\mu^{n-1} + \cdots + \det \boldsymbol{\mathcal{A}} \tag{7.2}$$

Here $\boldsymbol{I}_n$ denotes the n-dimensional unity matrix. The zeros $\mu_1, \ldots, \mu_n$ of this polynomial which are also the eigenvalues of the matrix $\boldsymbol{\mathcal{A}}$ determine the solutions of the differential system in Equation (7.1). All solutions $\mathbf{x}(t)$ of the homogeneous system have in the case of simple zeros the form

$$\mathbf{x}(t) = \sum_{i=1}^{n} a_i e^{\mu_i t} \tag{7.3}$$

If all eigenvalues $\mu_1, \ldots, \mu_n$ of the matrix $\boldsymbol{\mathcal{A}}$ have negative real parts, the system is asymptotically stable. If at least one of the eigenvalues has a positive real part, the system is unstable. The case when the maximal values of the real parts of the eigenvalues are equal to zero needs special consideration.

7.1.2 Stability of Linear Delay Systems

In the case of a linear differential equation system with one time delay τ, the system has the form

$$\dot{\mathbf{x}}(t) = \boldsymbol{\mathcal{A}}\mathbf{x}(t) + \boldsymbol{\mathcal{B}}\mathbf{x}(t-\tau) \tag{7.4}$$

with $\boldsymbol{\mathcal{A}}$ and $\boldsymbol{\mathcal{B}}$ $n \times n$ matrices. In the case of control systems usually $\boldsymbol{\mathcal{B}}$ is the control, that is the control has the form $\mathbf{u}(t) = \boldsymbol{\mathcal{B}}\mathbf{x}(t-\tau)$. The characteristic function $f(z)$ of such a system is then given by

$$f(z) = \det(z\boldsymbol{I}_n - \boldsymbol{\mathcal{A}} - e^{-z\tau}\boldsymbol{\mathcal{B}}) \tag{7.5}$$

This function is a sum of a polynomial $P(z)$ and a polynomial $Q(z)$ multiplied by powers of $\exp(-z\tau)$. Such a function is called a quasi-polynomial. It can be shown that under some regularity conditions and if all zeros are simple, all solutions of the differential equation system (7.4) have the form

$$\mathbf{x}(t) = \sum_{j\in\Lambda} a_j e^{\lambda_j t} \tag{7.6}$$

with $\Lambda = \{z;\, f(z) = 0\}$, the set of zeros of $f(z)$, and the a_j complex constants.

In the case of multiple zeros, the solutions for these zeros μ_i are of the form $P(t)\exp(\mu_i t)$ with $P(t)$ a polynomial in t whose minimal order is the multiplicity of the zero μ_i minus one. So also in this case the stability of the system can be established if one can show that there are no zeros with non-negative real parts.

7.1.3 Piecewise Linear Systems

Piecewise linear systems are a way to model approximately non-linear systems by dividing the state space into a number of regions where the system has a linear behaviour.

Such systems were introduced by (Sontag 1981). A monograph treating them is (Pettit 1995). Further results on them can be found in (Pettit and Miur 1997), (Yfoulis et al. 1998) and (Manavis et al. 1998). The basic idea is to divide the state space into a number of disjoint sets $S_0, S_1, \ldots, S_n$ in which the system shows a linear behaviour. For each region S_i there is the corresponding affine linear dynamics:

$$\dot{\mathbf{x}}(t) = \boldsymbol{\mathcal{A}}_i \mathbf{x}(t) + \boldsymbol{\mathcal{B}}_i \mathbf{u}(t) + \boldsymbol{c}_i \quad \mathbf{x}(t) \in S_i \tag{7.7}$$

where $\mathbf{x}, \mathbf{u}, \boldsymbol{c}_i \in \mathcal{R}^n$ and $\boldsymbol{\mathcal{A}}_i, \boldsymbol{\mathcal{B}}_i \in \mathcal{R}^{n\times n}$ and $S_i \in S$. The control input $\mathbf{u}(t)$ is assumed to be linear in the form

$$\mathbf{u}_i(t) = \boldsymbol{F}_i \mathbf{x}(t) + \boldsymbol{g}_i(t) \quad \mathbf{x}(t) \in S_i \tag{7.8}$$

where $\boldsymbol{F}_i \in \mathcal{R}^{n\times n}$ and $\boldsymbol{g}_i \in \mathcal{R}^n$. Then the closed-loop system has the form

$$\dot{\mathbf{x}}(t) = (\boldsymbol{\mathcal{A}}_i + \boldsymbol{\mathcal{B}}_i \boldsymbol{F}_i)\mathbf{x}(t) + (\boldsymbol{\mathcal{B}}_i \boldsymbol{g}_i + \boldsymbol{c}_i) \quad \mathbf{x}(t) \in S_i \tag{7.9}$$

In the following, to outline these concepts a simplified form is considered where $\boldsymbol{\mathcal{A}}_i \equiv \boldsymbol{\mathcal{A}}, \boldsymbol{c}_i, \boldsymbol{g}_i \equiv 0$ and $\boldsymbol{F}_i \equiv \boldsymbol{I}$ with $\boldsymbol{I}_n$ the n-dimensional unity matrix. In this form the closed-loop system has the form

$$\dot{\mathbf{x}}(t) = (\boldsymbol{\mathcal{A}} + \boldsymbol{\mathcal{B}}_i)\mathbf{x}(t) \tag{7.10}$$

7.1.4 Stabilization of Piecewise Linear Systems

The stabilization of piecewise linear systems can be related to the decay of suitably chosen Lyapunov functions[1]. As

[1] This section, as the previous one, summarizes some findings by the third author and Dr. Karl Breitung. They were published during the time the latter author spent at the University of Pavia (1999–2003).

an example a simple two-dimensional system is studied. Details of the methods and the obvious generalizations can be found in the references cited above. Consider now a central rectangular region S_0 surrounded by a ring R (Figure 7.1). The rectangle S_0 is defined by

$$S_0 = \{-c_{1,1} \le x_1 \le c_{1,1}; -c_{2,1} \le x_1 < c_{2,1}\} \tag{7.11}$$

with $c_{1,1}, c_{2,1} > 0$. The surrounding ring of the four regions is defined by

$$\begin{aligned}
S_1 &= \{c_{1,1} \le x_1 \le c_{1,2}; -c_{2,1} - \gamma(x_1 - c_{1,1}) \\
&\quad \le x_2 < c_{2,1} + \gamma(x_1 - c_{1,1})\} \\
S_2 &= \{c_{2,1} \le x_2 \le c_{2,2}; -c_{1,1} - \gamma^{-1}(x_2 + c_{2,1}) \\
&\quad \le x_1 < c_{1,1} + \gamma^{-1}(x_2 - c_{2,1})\} \\
S_3 &= \{-c_{1,2} \le x_1 \le -c_{1,1}; -c_{2,1} + \gamma(x_1 + c_{1,1}) \\
&\quad \le x_2 < c_{2,1} - \gamma(x_1 + c_{1,1})\} \\
S_4 &= \{c_{2,1} \le x_2 \le c_{2,2}; -c_{1,1} + \gamma^{-1}(x_2 + c_{2,1}) \\
&\quad \le x_1 < c_{1,1} - \gamma^{-1}(x_2 + c_{2,1})\}
\end{aligned} \tag{7.12}$$

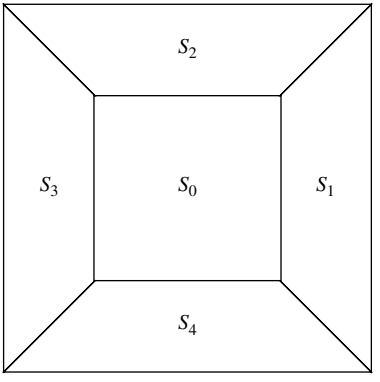

Figure 7.1 A ring domain

Here $c_{1,2} > c_{1,1} > 0$ and $c_{2,2} > c_{2,1} > 0$ and $\gamma = (c_{2,2} - c_{2,1})/(c_{1,2} - c_{1,1})$. On the ring R one now defines a scalar function $V(x)$ by

$$V(\mathbf{x}) = \max_{j=1,2} \left[\max \left(\frac{x_j - c_{j,1}}{c_{j,2} - c_{j,1}}, -\frac{x_j + c_{j,1}}{c_{j,2} - c_{j,1}} \right) \right] \tag{7.13}$$

This is called a RP-Lyapunov function (Ring Polyhedral) (Figure 7.2).

In each of the sectors $S_1, \ldots, S_4$ one has for the function: $V(\mathbf{x}) = \frac{x_1 - c_{1,1}}{c_{1,2} - c_{1,1}}$ for $\mathbf{x} \in S_1$, $V(\mathbf{x}) = \frac{x_2 - c_{2,1}}{c_{2,2} - c_{2,1}}$ for $\mathbf{x} \in S_2$, $V(\mathbf{x}) = -\frac{x_1 + c_{2,1}}{c_{2,2} - c_{2,1}}$ for $\mathbf{x} \in S_3$, $V(\mathbf{x}) = -\frac{x_2 + c_{2,1}}{c_{2,2} - c_{2,1}}$ for $\mathbf{x} \in S_4$.

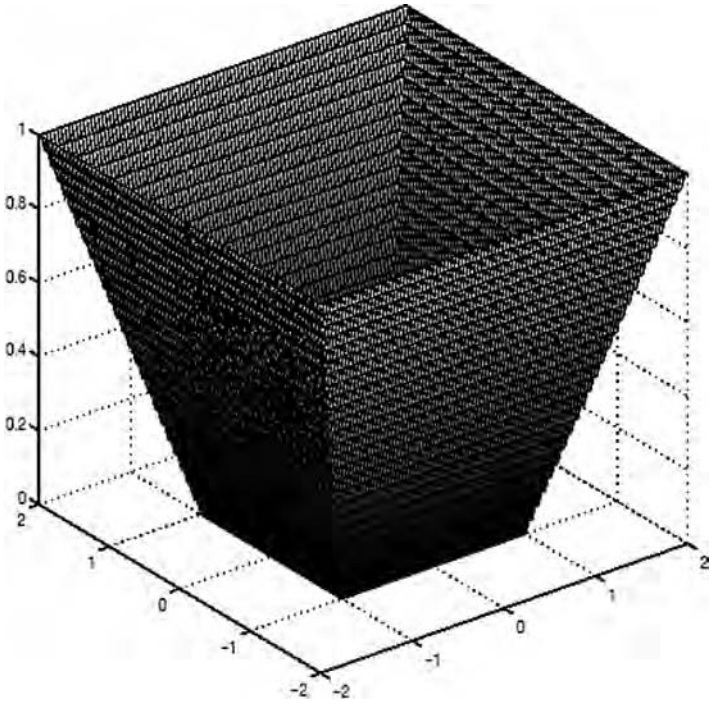

Figure 7.2 A simple example the RP-Lyapunov function

One can see that:

- $0 \leq V(\mathbf{x}) \leq 1 \quad \forall \mathbf{x} \in R$,
- $\mathbf{x}$ is on the outer boundary of R if and only if $V(\mathbf{x}) = 1$,
- $\mathbf{x}$ is on the inner boundary of R if and only if $V(\mathbf{x}) = 0$.

As one can see, this function is linear in each of the four regions $S_1, \ldots, S_4$. If one can choose the control forces in such a way that $\dot{V}(\dot{\mathbf{x}}) < 0$ always for all points in the ring R, then the path will lead down from a point in the ring to the inner boundary of the ring. This function is now taken as a Lyapunov-like function. With $\boldsymbol{b}_i$ denoting the i^{th} row of the control matrix $\boldsymbol{\mathcal{B}}(t)$ the stability conditions take the form:

- $\dot{x}_1 < 0 \Leftrightarrow (\boldsymbol{a}_1 + \boldsymbol{b}_1(\mathbf{x}(t)))^T \cdot \mathbf{x}(t)$ in S_1
- $\dot{x}_2 < 0 \Leftrightarrow (\boldsymbol{a}_2 + \boldsymbol{b}_2(\mathbf{x}(t)))^T \cdot \mathbf{x}(t)$ in S_2
- $\dot{x}_1 > 0 \Leftrightarrow (\boldsymbol{a}_1 + \boldsymbol{b}_1(\mathbf{x}(t)))^T \cdot \mathbf{x}(t)$ in S_3
- $\dot{x}_2 > 0 \Leftrightarrow (\boldsymbol{a}_2 + \boldsymbol{b}_2(\mathbf{x}(t)))^T \cdot \mathbf{x}(t)$ in S_4

Further one can consider also the velocity of the decrease of the RP-Lyapunov function. To an exponential decrease, one has the condition $\dot{V}(\mathbf{x}) < -\varepsilon V(\mathbf{x}) \Leftrightarrow V(\mathbf{x}(t)) < V(\mathbf{x}(0)) \exp(-\varepsilon t)$. To get this decrease of the function, one has to find control forces which fulfil the following equations (for appropriately chosen p and $\gamma_p = \pm 1$):

$$\gamma_p \dot{x}_p < -\varepsilon x_p \Leftrightarrow (\boldsymbol{a}_p + \boldsymbol{b}_p + \varepsilon \boldsymbol{e}_p)^T \cdot \mathbf{x} < 0 \qquad (7.14)$$

where $\boldsymbol{e}_p = (0, 0, \ldots, 0, 1, 0, \ldots, 0) \in \mathcal{R}^n$ is the p^{th} unity vector. Since the functions in the stability conditions are linear and the domains are polygons, one has to check the function values only at the corner points of the domains to see if some chosen control force guarantees stability.

Finding the minimal control values for stability is a simple problem of linear programming.

7.2 SEMIACTIVE FEATURES

In Chapter 4, methods of semiactive structural control have been discussed. In comparison with active control these do need not much external energy. Compared with passive control one can get a better performance of the system, since one can tune its behaviour directly.

The basic idea of semiactive control is to change some parameters of the structural system to optimize the behaviour of the system with respect to a control criterion. The only energy necessary here is the energy for regulating the devices which modify the parameters of the system.

In general for a single degree-of-freedom (SDOF) system there are two parameters which one can vary in this context: the stiffness and the damping. The first method is called AVS (Active Variable Stiffness) and the second AVD (Active Variable Damping). A third possibility is a combination of both methods.

Let the SDOF system be driven by the classical equation

$$m\ddot{x}(t) + c\dot{x}(t) + kx(t) = f(t) \tag{7.15}$$

Here m is the mass, c and k are values of damping and stiffness without control, and $f(t)$ is the external force acting on the system. Using the notation that ξ is the nominal damping factor and ω_0 the natural circular frequency, this is written as

$$\ddot{x}(t) + 2\xi\omega_0\dot{x}(t) + \omega_0^2 x(t) = f(t)/m \tag{7.16}$$

A semiactive control system varies the values of the stiffness and/or the damping. This can be written as follows:

$$\ddot{x}(t) + 2\xi\omega_0[1 + \alpha_c(t)]\dot{x}(t) + \omega_0^2[1 + \alpha_k(t)]x(t) = f(t)/m \tag{7.17}$$

where $\alpha_c(t)$ and $\alpha_k(t)$ are now functions of time. The control action $f_c(t)$ on the system can be written in the form

$$f_c(t) = -[2\xi\omega_0\alpha_c(t)\dot{x}(t) + \omega_0^2\alpha_k(t)x(t)] \tag{7.18}$$

Such control systems where parameters of the system can be varied are called variable structure systems. Here one has the special case of a bilinear system, that is a system in the form

$$\dot{\mathbf{x}}(t) = \boldsymbol{\mathcal{A}}\mathbf{x}(t) + v\boldsymbol{\mathcal{B}}\mathbf{x}(t) \tag{7.19}$$

with v a scalar function of t and the state $\mathbf{x}(t)$ of the system (see (Mohler 1973)). For the case of bilinear systems the literature on stability is sparse. In (Longchamp 1980), (Ryan and Buckingham 1983) and (Chen et al. 2002) the stability of such systems is examined but without taking time delays into account. The only article known to the authors which treats bilinear systems with time delay is about systems where the switching occurs only in the non-delayed part (Niculescu et al. 1996). But in semiactive control the switching of the control parameter usually depends on the observed delayed system states.

7.2.1 Delay Differential Equations

In a realistic setting the reaction of the control system comes with a certain delay; that is, the variables which enter in the control mechanism for switching the system parameters are not $x(t)$, $u(t)$ and $\dot{x}(t)$, but $x(t-\tau)$, $u(t-\tau)$ and $\dot{x}(t-\tau)$, where τ is the delay time. This delay time is in the region

of milliseconds for modern semiactive control systems, but its influence on the performance and stability of the system cannot be neglected.

Systems without delays can be described by ordinary differential equations (ODEs) which give in case of Equation (7.20) an equation in the form

$$\begin{aligned}\ddot{x}(t) &= -2\xi\omega_0\dot{x}(t) - \omega_0^2 x(t) + f(t)/m \\ \ddot{x}(t) &= F(x(t), \dot{x}(t), f(t)/m)\end{aligned} \tag{7.20}$$

Mathematical modelling of the delays leads to delay differential equations (DDEs) which contain not only the values of the function and its derivatives at time t, but also the values of the function and its derivatives in the past. A differential equation in the form

$$\ddot{x}(t) = F(x(t), \dot{x}(t), x(t-\tau), \dot{x}(t-\tau)) \tag{7.21}$$

is a special case of a delay differential equation (for simplicity here only an equation involving $x(t)$ and its derivatives and delays is considered). The mathematical theory of such equations has been developed in the last few decades ((El'sgol'ts and Norkin 1973; Kolmanovskii and Nosov 1986)). Unfortunately, not many analytical solutions are available for such mathematical models, and many results are more of a qualitative type, that is giving conditions for stability and non-oscillatory behaviour.

A further problem in the study of such equations is that it has been shown that heuristic approximations may lead to erroneous results. For example, in (El'sgol'ts 1964), p. 191 it is shown that for the delay differential equation

$$\dot{x}(t) + ax(t) + bx(t-\tau) = 0 \tag{7.22}$$

the region of stability as a function of the parameters a and b is different from the stability domain of the approximating ordinary differential equation

$$\dot{x}(t) + ax(t) + b[x(t) - \tau\dot{x}(t)] = 0 \tag{7.23}$$

If one now tries to use Simulink® for studying the stability of the equation, the results are not always in agreement with the theory. Figure 7.3 compares the solutions for the time delay $\tau = 0.2$, $b = 5$ and $a = 4.8$ (with initial condition $x(-\tau) = 1$) given by Simulink© and the special delay differential equation solver. Taking higher order Taylor expansions does not necessarily improve the situation, but

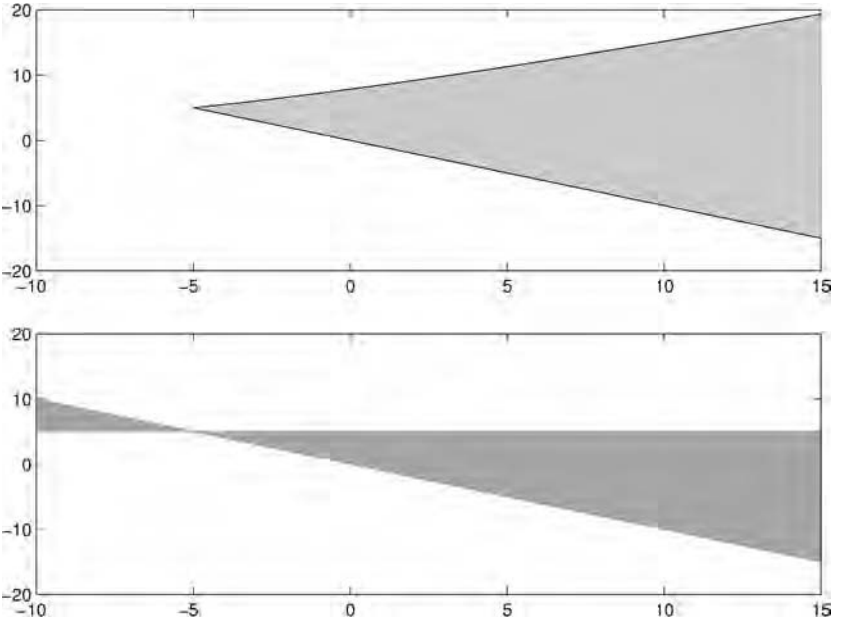

Figure 7.3 The stability regions for $\tau = 0.2$: upper figure, Equation (7.22), lower figure; Equation (7.23)

it can make it worse. If one considers the delay differential equation

$$\dot{x}(t) = -ax(t-\tau) \tag{7.24}$$

with $a > 0$, the first-order Taylor expansion gives an approximating ordinary differential equation

$$\begin{aligned} \ddot{x}(t) &= -a(x(t) - \tau\dot{x}(t)) \\ (1 - a\tau)\ddot{x}(t) &= -ax(t) \end{aligned} \tag{7.25}$$

which for $|a\tau| < 1$ has the solution

$$x(t) = \exp\left(-\frac{a}{1-a\tau}t\right) \tag{7.26}$$

Taking a second-order Taylor expansion for the delay term gives

$$\begin{aligned} \ddot{x}(t) &= -a[(x(t) - \tau\dot{x}(t) + \tau^2/2\ddot{x}(t))] \\ \ddot{x} + \frac{2(1-a\tau)}{\tau^2}\dot{x}(t) &+ \frac{2}{a\tau^2}x(t) = 0 \end{aligned} \tag{7.27}$$

This is now an ordinary differential equation of second degree and the solution will show an oscillatory behaviour which is not present in the exact solution and in the first-order approximation. Indeed, by trying to get a better estimate for the delayed argument, the order of the differential equation system has been increased. Similar problems can appear if higher order extrapolation formulae are used to approximate the process values in the future, since in the limit these are Taylor expansions.

These examples show that in dealing with delay differential equations, heuristic approaches which work well in other contexts might lead to wrong conclusions. Therefore a careful study of the properties of systems modelled by such equations is necessary.

The influence of delay on a system is not monotonous in the sense that if a system is stable for a given delay τ_0 it will be stable for shorter delays $0 < \tau < \tau_0$. A counterexample is given in (Kolmanovskii and Nosov 1986), p. 61. If one considers the delay differential equation

$$\ddot{x}(t) + 0.25\dot{x}(t) + x(t) + 0.5x(t-\tau) = 0 \qquad (7.28)$$

this equation is stable for $\tau = 5$, but unstable for $\tau = 1$ (see Figure 7.4).

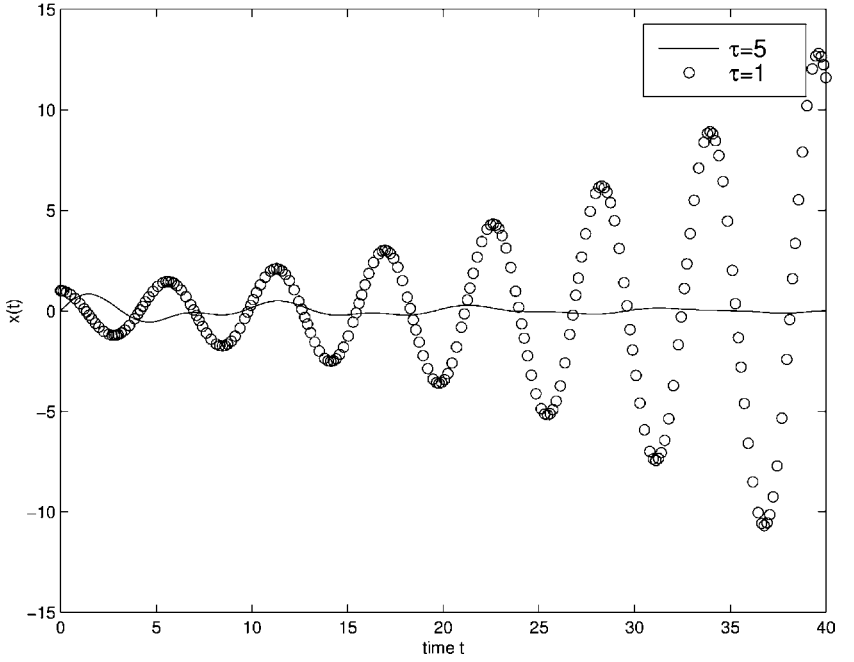

Figure 7.4 Solutions of Equation (7.28) for $\tau = 5$ and $\tau = 1$

7.2.2 Delay in Structural Control

Delay in active control systems has been studied in a number of papers, see for example the overview in (Agrawal and Yang 2000).

Let the system be put in the form

$$\ddot{x}(t) + 2\xi\omega_0[1 + \alpha_c(t)]\dot{x}(t) + \omega_0^2[1 + \alpha_k(t)]x(t) = u(t) \quad (7.29)$$

In (Palazzo et al. 2001) criteria were derived on how to choose the values of α_c and α_k in dependence on the dynamic behaviour of the system and its structural parameters.

Three criteria were considered:

1. Maximization of energy absorbed by the extrastructural control system.
2. Kinetic energy minimization.
3. Main structure input energy minimization.

The values of $\alpha_c(t)$ and $\alpha_k(t)$ in Equation (7.29) now have to be chosen such that they are optimal under the chosen criterion. From these criteria one can derive two different control laws, since the second and the third criteria lead to the same result. This influence on semiactive control will be studied here. Since the control law is non-linear, it is not possible to evaluate the effects of delays by studying the transfer function multiplied by the time delay transfer. Therefore the behaviour in the time domain is studied here.

To find the numerical solutions of the equations of motion of the controllers efficient algorithms for integrating delay differential equations are needed. Such an algorithm

is the MATLAB program `dde23` by (Shampine and Thompson 2000). In the following this program is used for the numerical study of the controllers and the only case is treated where the time delay is equal for all variables. However, the MATLAB software used (Shampine and Thompson 2000) can also handle the case of a set of different constant time delays for the variables of the equation system.

The two control laws derived in (Palazzo et al. 2001) are modified to take the delay into account. The controller does not use the values of $x(t), \dot{x}(t)$ and $\dot{u}(t)$ but the values of these function at a time point $t-\tau$ where τ denotes the time lag. So the actual control law in the first case is

$$\begin{aligned} \alpha_c(t) &= \alpha_{c,\max} \\ \alpha_k(t) &= \begin{cases} \alpha_{k,\max} & \text{if} \quad x(t-\tau)\dot{x}(t-\tau) > 0 \\ \alpha_{k,\min} & \text{if} \quad x(t-\tau)\dot{x}(t-\tau) < 0 \end{cases} \end{aligned} \tag{7.30}$$

and for the second controller is

$$\begin{aligned} \alpha_c(t) &= \begin{cases} \alpha_{c,\max} & \text{if} \quad \dot{x}(t-\tau)\dot{u}(t-\tau) > 0 \\ \alpha_{c,\min} & \text{if} \quad \dot{x}(t-\tau)\dot{u}(t-\tau) < 0 \end{cases} \\ \alpha_k(t) &= \begin{cases} \alpha_{k,\max} & \text{if} \quad x(t-\tau)\dot{u}(t-\tau) > 0 \\ \alpha_{k,\min} & \text{if} \quad x(t-\tau)\dot{u}(t-\tau) < 0 \end{cases} \end{aligned} \tag{7.31}$$

The value of $\alpha_{c,\min}$ is usually taken as zero and $\alpha_{c,\max} \leq 50$. For the stiffness the minimal value is again $\alpha_{k,\min} = 0$ and $\alpha_{k,\max} \leq 2$. In the following the SDOF system with the semiactive controllers described in Equations (7.30) is studied. The values are $\alpha_{k,\min} = 0$ and $\alpha_{k,\max} = 1$. For the parameters of the system it is assumed that $\omega_0 =$

10 and $\xi = 0.02$. For a stationary sinusoidal excitation function with frequency $\omega = 5$, the responses for delay times $\tau = 0.05,\ 0.01,\ 0.005,\ 0$ are shown in Figure 7.5. In the case of an excitation during a limited time the responses are different. Applying the same excitation function as before, but only during the time interval $[0, 2]$ and with no external excitation after time $t = 2$, gives the responses shown in Figure 7.6. Here the influence of a relatively large time delay $\tau = 0.05$ in slowing down the return to zero position can be seen. In Figure 7.7, after time $t = 2$ a sinusoidal excitation is added with amplitude 0.1.

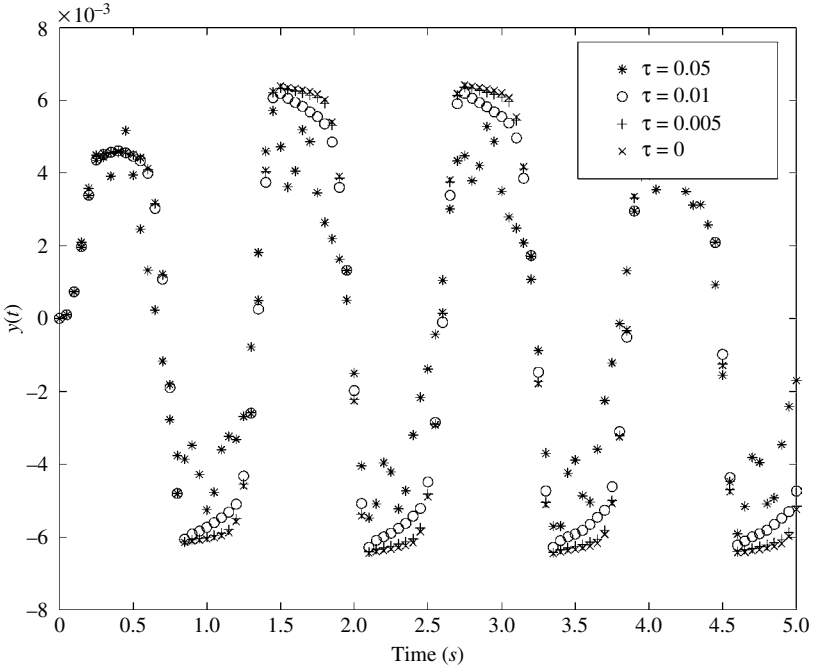

Figure 7.5 Response to sinusoidal excitation $\sin(5t)$ in $[0, 2]$ and afterwards $0.1\sin(5t)$

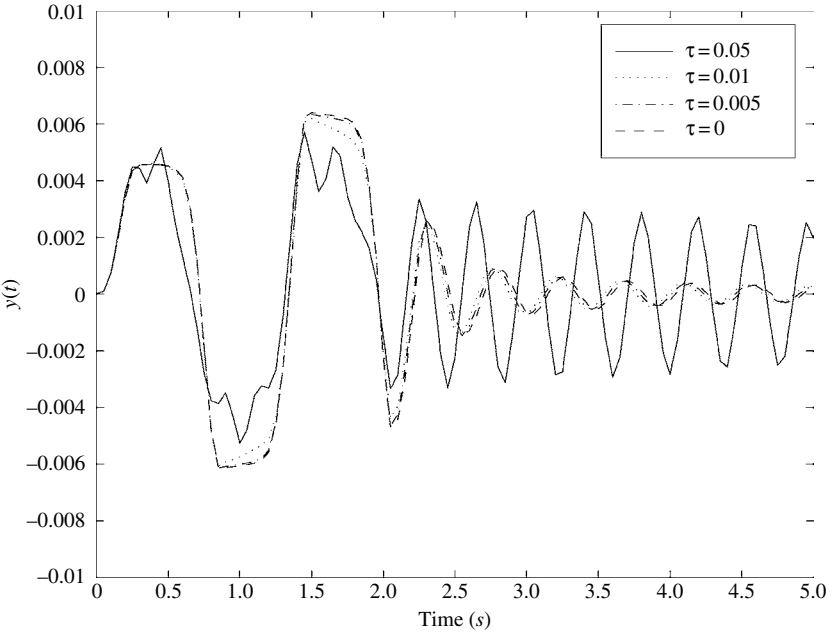

Figure 7.6 Response to sinusoidal excitation in [0,2]

7.3 CONCLUSIONS

A manuscript covering a topic without omissions results in a handbook rather than a monograph!

The authors are aware that the six main chapters of this book are not exhaustive on the topic of semiactive devices. They covered the topics with which they became more familiar and provide a rich bibliography allowing the reader to follow the specific point of view of his/her interest. Nevertheless, one aspect which is absent in the book requires to be mentioned: the one related to optimization of the device placement.

As always optimization is an attractive area to the academic world. Give scientists an objective function and the

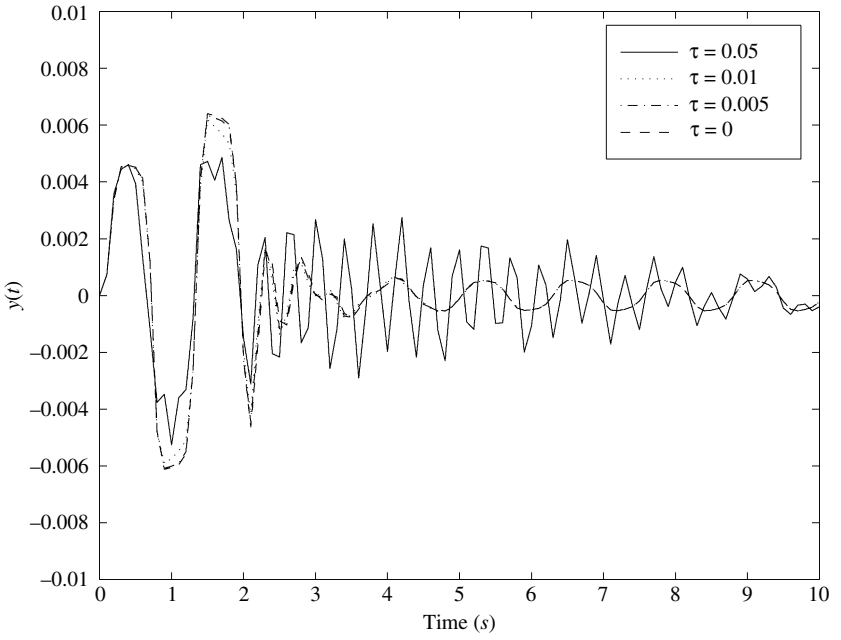

Figure 7.7 Response to sinusoidal excitation $\sin(5t)$ on [0,2] and afterwards $0.1\sin(5t)$

relevant constraints, and they will discuss whether or not the problem is well posed, the existence and uniqueness of the solution, the properties of the searching mathematical algorithm, the convergence process and the robustness of the solution. Several references along these lines can be found in the scientific literature.

Although such papers may be worth mentioning, the authors of this book are not convinced that a chapter can be devoted to these approaches at present. The main reason is that optimal placement requires the construction of a mathematical model which covers most of the structural needs but often forgets (or covers by a fictitious noise) the interaction between the structural systems, the monitoring apparatus and the control devices. In laboratory

applications, a trial and error process replaces such mathematical procedures and provides the designer with the necessary expertise to operate on real structures. Therefore, the authors prefer that the reader arrives at the end of the book convinced that to build up his/her own expertise in the field is a major feature in the design of a semiactive control system, much more so than relying on complex mathematical formulations.

Appendix A
Damping

The phenomenon by which the mechanical energy is dissipated in dynamic systems is called damping. For this reason this book sometimes uses the term *damping* as synonymous to *energy dissipation*. The damping always generates hysteretic loops in the force vs. displacement plane. The loops dissipate energy, either as internal thermal energy or as structural damage.

It is very important to characterize the damping of a dynamical system because it allows one to understand the major mechanisms associated with the mechanical energy dissipation in the system. A suitable damping model should be chosen to represent the associated energy dissipation. Damping values (model parameters) are determined, for example, by testing the system or a representative physical model, by monitoring the system response under transient conditions during its normal operation, or by analysing the data already available.

A.1 TYPES OF DAMPING

The damping types can be classified as follows:

- **Internal damping:** this refers to a damping that is internal to the structure; that is, it is not related to the

Technology of Semiactive Devices and Applications in Vibration Mitigation Fabio Casciati, Georges Magonette and Francesco Marazzi

particular ambient where the structure is placed nor on the boundary conditions. Its origin can be found in the material properties of the structural members: it originates from the energy dissipation associated with microstructural defects, such as grain boundaries and impurities, thermoelastic effects caused by local temperature gradients resulting from non-uniform stresses, dislocation motion in metals and chain motion in polymers.

Several models have been employed to represent the energy dissipation caused by internal damping. This variability is primarily the result of the vast range of engineering materials; no single model can satisfactorily represent the internal damping characteristics of all materials. Nevertheless, two general types of internal damping can be identified: *viscoelastic damping* and *hysteretic damping*.

The first type of internal damping is usually not related to damage, at least in a first stage. On a "Displacement vs. Force" (or "Stress vs. Strain") graph, this type of damping generates ellipses that are followed clockwise around the origin (Figure A.1).

For a linear viscoelastic material, the stress–strain relationship is given by a linear differential equation, with respect to time. Its coefficients are usually assumed to be constant. A commonly employed relationship is

$$\sigma = E\varepsilon + E^* \frac{d\varepsilon}{dt} \tag{A.1}$$

which is known as the Kelvin–Voigt model. In Equation (A.1), E is Young's modulus and E^* is a viscoelastic parameter that is assumed to be time independent. The elastic term $E\varepsilon$ does not contribute to damping, and its cyclic integral vanishes. According to (De Silva 2000),

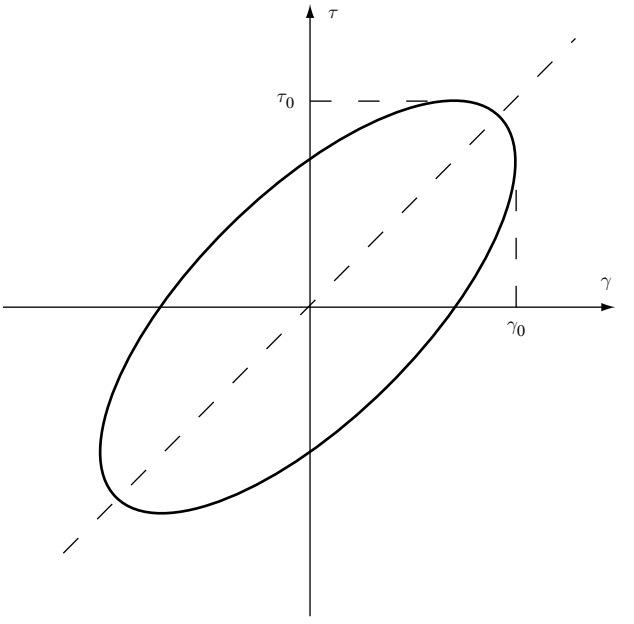

Figure A.1 "Stress vs. Strain" plot for a viscoelastic material

the damping capacity per unit volume under a harmonic load of given frequency Ω is

$$\Phi = \frac{\pi \Omega E^* \sigma_{max}^2}{E^2} \tag{A.2}$$

where σ_{max} is the maximum stress caused by the harmonic load. For modelling purposes, this damping is usually taken into account in the equations of motion by adding the term $c\dot{x}$. The term c is a constant quantity which is derived from the energy dissipated by the material for each cycle.

The *hysteretic damping* is usually related to yielding[1] and relative displacements among elements.[2] In this case it is no longer possible simply to add a term in the force balance of the equation of motion: this type of damping clearly shows non-linear characteristics. In order to reduce computation difficulties to an acceptable level, an equivalent c_{eq} value of the damping coefficient is often estimated for a given level of excitation and added to the value c of the viscous damping in order to allow linear analysis.

- **Structural damping:** this is a result of the mechanical energy dissipation. This dissipation is caused by the rubbing friction resulting from the relative motion between components and by the impacting or the intermittent contact at joints in a mechanical system or structure. The energy dissipation behaviour depends on the details of the particular mechanical system. It is extremely difficult to develop a generalized analytical model describing the structural damping. The energy dissipation caused by rubbing is usually represented by a Coulomb-friction model: the energy dissipation caused by impacting should be determined from the coefficient of restitution of the two members which are in contact.

  The common method for estimating the structural damping is by measurement. The measured values, however, represent the overall damping in the mechanical

---

[1] Especially for metallic elements, but also for composite elements such as reinforced concrete structural components. This damping is usually strictly connected with irreversible damage.

[2] This damping can be found in structures made up of several assembled elements, for example composite structures.

system. The structural damping component is obtained by subtracting, from the overall damping value, the values corresponding to other types of damping (such as the material damping present in the system which should be previously estimated by environmentally controlled experiments, previous data, etc.).

This damping originates at the interface between the structure and its boundaries. It can be found at the bridge bearings or in the expansion joints, for example.

- **Fluid damping:** this refers to a damping that is external to the structure; that is, it is related to the ambient where the structure is. Some examples are dissipative effects due to flow–structure interaction (both with air and water), soil–structure interaction at the foundation level and dissipating links between the structure and the surroundings.

A.2 WHY HAVE A DAMPING MATRIX?

In modal analysis, there is generally no need to express the damping of a typical viscously damped system by means of the damping matrix. The damping is more conveniently represented in terms of the modal damping ratios ξ_n (where n is the mode index). When the response of the structure cannot be obtained by superposition of the uncoupled modal response, however, an explicit damping matrix is required. This is true if the structure itself is non-linear (for example, in seismic analysis, where the structure can be damaged, so the stiffness and the damping are not constant in time) or because there is a need for simulations in the time domain (for example, when a non-linear model for the actuators leads one to conduct a non-linear analysis even for a linear structure).

A.3 RAYLEIGH DAMPING

The simplest way to formulate a proportional damping matrix is to make it proportional to both the stiffness and the mass of the structure. More details about this technique can be found in (Clough and Penzien 1993).

Bibliography

Abe, M. and Y. Fujino (1994). Dynamic Characterization of Multiple Tuned Mass Dampers and Some Design Formulas. *Earthquake Engineering and Structural Dynamics 23*, 813–835.

Ackermann, J. (1984). Robustness Against Sensor Failures. *Automatica 20*(2), 211–215.

Agrawal, A. and J. Yang (2000). Compensation of Time-Delay for Control of Civil Engineering Structures. *Earthquake Engineering and Structural Dynamics 29*, 37–62.

Akbay, Z. and H. Aktan (1991). Actively Regulated Friction Slip Devices. In *6th Canadian Conference on Earthquake Engineering*, pp. 367–374.

Anton, M. and F. Casciati (1998). Structural Control Against Failure Interaction. *Journal of Structural Control 5*(1), 63–73.

Auricchio, F., L. Faravelli, G. Magonette, and V. Torra (2001). *Shape Memory Alloys: Advances in Modelling and Applications*. Barcelona: CIMNE.

Balas, M. J. (1978). Feedback Control of Flexible Structures. *IEEE Transactions on Automatic Control AC-23*, 673–679.

Baratta, A., C. Cenammo, and G. Voiello (1998). Design of Linear Active Control Algorithms for Non-Stationary Unknown Forcing. *Journal of Structural Control 5*(2), 7–31.

Barroso, L. (1999). Performance Evaluation of Vibration Controlled Steel Structures Under Seismic Loading. PhD thesis, Stanford University, Department of Civil and Environmental Engineering.

Barroso, L., J. Chase, and S. Hunt (2003). Resettable Smart Dampers for Multi-Level Seismic Hazard Mitigation of Steel Moment Frames. *Journal of Structure Control 10*(1), 41–58.

Technology of Semiactive Devices and Applications in Vibration Mitigation Fabio Casciati, Georges Magonette and Francesco Marazzi

Barroso, L. R., S. Hunt, and J. G. Chase (2002). Smart-Dampers for Multi-Level Seismic Hazard Mitigation of Steel Moment Frames. In F. Casciati (Ed.), *Third World Conference on Structural Control (3WCSC)*, Volume 3, Como, Italy, pp. 495–500. ASC. Chichester: John Wiley & Sons, Ltd.

Battaini, M., F. Casciati, and M. Domaneschi (2003). Electro-Inductive Passive and Semi-Active Control Devices. In F. Bontempi (Ed.), *System-Based Vision for Strategic and Creative Design*, Volume ISEC-02, Rome, pp. 2085–2090. Leiden: Balkema.

Battaini, M., F. Casciati, A. Silvestri, and M. Ubaldini (1998). Semi-Active Control by Electro-Inductive Energy Dissipator. In *Second World Conference on Structural Control (2WCSC)*, Kyoto, Japan. ACS.

Battaini, M. and S. Dyke (2000). Experimental Investigation of Sensor Failure in Structural Control. In L. Jezequel (Ed.), *Active Control in Mechanical Engineering*, Lyons, France, pp. 273–284.

Battaini, M. and A. Marioni (2001). Design and Experimental Tests on Electro-Inductive Dissipators. In *Fifth world Congress on Joints, Bearings and Seismic Systems for Concrete Structures*, Rome, Italy. ACEDIS.

Battaini, M., A. Marioni, F. Casciati, A. D. Gerlando, R. Perini, A. Silvestri, and M. Ubaldini (2002). Semi-Active Electro-Inductive Dissipator: Design and Experimental Tests. In F. Casciati (Ed.), *Third World Conference on Structural Control (3WCSC)*, Volume 2, Como, Italy, pp. 51–58. ASC. Chichester: John Wiley & Sons, Ltd.

Bechmann, H. and B. Weber (1996). Tuned Vibration Absorbers for "Lively" Structures. *Structural Engineering International 1*, 31–36.

Beolchini, G. C. and F. Vestroni (1997). Experimental and Analytical Study of the Dynamic Behaviour of a Bridge – A Case of Close Frequencies. *Journal of Structural Engineering 2*(11), 1506.

Bergamo, G. (2002). Evaluation Testing of MR-Fluid Based Dampers. In F. Casciati (Ed.), *Third World Conference on Structural Control (3WCSC)*, Volume 2, Como, Italy, pp. 1103–1112. ASC. Chichester: John Wiley & Sons, Ltd.

Bertero, V. V. (2000). Performance-Based Seismic Engineering: Conventional vs. Innovative Approaches. In *12th World Conference on Earthquake Engineering (12WCEE)*, paper no. 2074, Auckland, New Zealand.

Bosi, A. (2003). Isolamento Sismico: Prove di Dispositivi Dissipativi con il Metodo Pseudodynamico Continuo con Sottostrutturazione. Laura thesis, University of Perugia, Facoltà di Ingegneria (in Italian).

Bouygues (2000). Active Control in Civil Engineering. Final technical Report BE96–3334, Bouygues SA, St Quentin en Yvelines, France,

together with Newland Technology, Johs.Holt, Joint Research Centre of EC, Mannessmann Rexroth, Technisce Universität Dresden, Université Libre de Bruxelles, VSL.

Brambilla, M. (1999). Design and Implementation of a Jet Actuator for Active Structural Control. *Journal of Structural Control 6*(1), 117–127.

Brambilla, M., F. Casciati, and S. F. Masri (1998). Testing Air Jet Actuator. In *Second World Conference on Structural Control (2WCSC)*, Kyoto, Japan. ACS.

Breitung, K. and F. Casciati (2000). The Influence of Time Delay in Semi-Active Control Systems. In *Second European Conference on Structural Control (2ECSC)*, Champs-sur-Marne, France. ENPC.

Carlson, J. D. (2002). Innovative Devices That Enable Semi-Active Control. In F. Casciati (Ed.), *Third World Conference on Structural Control (3WCSC),* Volume 1, Como, Italy, pp. 227–236. ASC. Chichester: John Wiley & Sons, Ltd.

Carter, A. K. (1998). Transient Motion Control of Passive and Semiactive Damping for Vehicle Suspensions. Master of science thesis in electrical engineering, University of Virginia.

Casciati, F. (1997). Checking the Stability of a Fuzzy Controller for Nonlinear Structures. *Microcomputers in Civil Engineering 12*, 205–215.

Casciati, F. (1998). Scale Laboratory Testing Towards Actual Actively Controlled Structural System. In *Second World Conference on Structural Control (2WCSC),* Kyoto, Japan. ACS.

Casciati, F. (2004). *CISM Course: Advanced Dynamics and Control of Structures and Machines*, pp. 217–248. Vienna: Springer-Verlag. Ed. H. Irshik and K. Shlacher.

Casciati, F., E. De Petra, and L. Faravelli (1993). Neural Networks is Structural Control. In *Structural Engineering in Natural Hazard Mitigation*, Irvine, California, USA, pp. 790–795. ASCE.

Casciati, F. and L. Faravelli (1995a). Application of Adaptive Fuzzy Controllers to Structural Engineering Systems. In *Sixth International Conference on Adaptive Structures*, Key West, Florida, USA, pp. 393–403.

Casciati, F. and L. Faravelli (1995b). Fuzzy Control of Nonlinear Systems in the Presence of Noise. In *Vibration of Nonlinear, Random and Time-Varying Systems*, Boston, Massachusetts, USA, pp. 863–868.

Casciati, F., L. Faravelli, and F. Borghetti (2003a). Wireless Link Between Sensor/Device Control Stations in Long Span Bridges. In *Proceedings of the SPIE*, San Diego, USA.

Casciati, F., L. Faravelli, R. Rossi, and G. Torelli (1999). Controlling Non-linear Systems by Fuzzy Chip. In *International conference on Monitoring and Control of Marine and Harbour Structures*, Genoa, Italy.

Casciati, F., L. Faravelli, and T. Yao (1995a). Active Structural Control toward Intelligent Infrastructures. In *Fourth US Conference on Lifeline Earthquake Engineering*, San Francisco, USA, pp. 620–627 ASCE.

Casciati, F., L. Faravelli, and T. Yao (1995b). The Tuning of Fuzzy Controllers for Active Structural Control. In *Civil Engineering Reliability and Risk Analysis*, Paris, France, pp. 741–745.

Casciati, F., L. Faravelli, and T. Yao (1996). Control of Nonlinear Structures Using the Fuzzy Control Approach. *Nonlinear Dynamics 11*, 171–187.

Casciati, F., F. Maceri, M. P. Sing, and P. Spanos (1999). *Civil Infrastructure Systems: Intelligent Renewal*. Singapore: World Scientific.

Casciati, F. and R. Rossi (2004). Fuzzy Chip Controllers and Wireless Link in Smart Structures. *Advances in Smart Technologies in Structural Engineering*, In J. Holnicki-Szulc and C. Muta-Suares (Eds), Berlin: Springer-Verlag.

Casciati, F., A. D. Stefano, and E. Matta (2003b). Simulating a Conical Tuned Liquid Damper. *Earthquake Engineering and Structural Dynamics 11*, 353–370.

Casciati, F. and T. Yao (1994). Comparison of Strategies for the Active Control of Civil Structures. In *First World Conference on Structural Control (1WCSC)*, Pasadena, California, USA. ACS.

Chen, G. and C. Chen (2004). Semiactive Control of the 20-Story Benchmark Building with Piezoelectric Friction Dampers. *Journal of Engineering Mechanics 130*.

Chen, G., W. Wang, M. Lou, and F. Y. Cheng (2002). Soils-Structure Interaction Effects on Seismic Performance of Various Control Devices and Systems. In *Third World Conference on Structural Control (3WCSC)*, Volume 2, Como, Italy, pp. 127–136. ASC. Chichester: John Wiley & Sons, Ltd.

Chen, L., X. Yang, and R. Mohler (1991). Stability Analysis of Bilinear Systems. *IEEE Transactions on Automatic Control 36*(11), 1310–1315.

Ciampi, V. and M. De Angelis (1996). Optimal Design of Passive Control System Based on Energy Dissipation for Earthquake Protection of Structures. In *European Conference on Structural Dynamics (EURODYN96)*, Florence, Italy.

Ciampi, V., M. De Angelis, and E. Renzi (1996). Optimal Selection of Special Connections Between Adjacent Structures in Passive and

Semi-Active Vibration Control Strategies. In *European conference on Structural Dynamics (EURODYN96)*, Florence, Italy.

Clough, R. and J. Penzien (1993). *Dynamics of Structures*. New York: McGraw-Hill International.

Curtain, R. and H. Zwart (1995). *An Introduction to Infinite-Dimensional Linear Systems Theory*. New York: Springer-Verlag.

De Angelis, M. and E. Renzi (1998). Energy Aspects in Control of Variable Structure Systems. In *Second World Conference on Structural Control (2WCSC)*, Kyoto, Japan. ACS.

De Silva, C. W. (2000). *Vibration: Fundamentals and Practice*. Boca Raton, Florida: CRC Press.

Degryse, E. and S. Mottelet (2000). A Novel Approach for Placing/Shaping Sensors and Actuators for the Feedback Control of Flexible Structures. In *Second European Conference on Structural Control (2ECSC)*, Champs-sur-Marne, France. ENPC.

Dorka, U. (2003). Hybrid Experimental-Numerical Simulation of Vibrating Structures. In N. Chouw and G. Schmid (Eds), *Proceedings of the International Workshop WAVE2002*, Okayama, Japan. Lisse: Swets & Zeitlinger.

Dorka, U., E. Flygare, and A. Ji (1998). Passive Seismic Control of Bridges by Hysteretic Device Systems. In *Second World Conference on Structural Control (2WCSC)*, Kyoto, Japan. ACS.

Dorka, U. and K. Schmidt (2000). Cost Efficient Retrofitting with Passive Control Systems. In *Workshop on Mitigation of Seismic Risk Support to Recent Affected European Countries*, Belgirate, Verbania, Italy.

Dowdell, D. and S. Cherry (1994). Semiactive Friction Dampers for Seismic Response Control of Structures. In *Proceedings of 5th US Conference on Earthquake Engineering*, Volume 1, pp. 819–828.

Dusi, A., M. Forni, and F. Bettinali (2002). Numerical Modelling of Semi-Active Devices within General Purpose FE Codes. In F. Casciati (Ed.), *Third World Conference on Structural Control (3WCSC)*, Volume 2, Como, Italy, pp. 1095–1102. ASC. Chichester: John Wiley & Sons, Ltd.

Dyke, S. J. and B. F. Spencer (1997). A Comparison of Semi-Active Control Strategies for the MR Damper. In *Intelligent Information Systems*, The Bahamas, USA. IASTED.

Dyke, S. J., B. F. Spencer, M. K. Sain, and J. D. Carlson (1996). Modeling and Control of Magnetorheological Dampers for Seismic Response Reduction. *Smart Materials and Structures 5*, 565–575.

El-Borgi, S., F. Sadek, B. Jemai, M. A. Walha, and M. A. Riley (2002). Semi-Active Control of Seismically Excited Hysteretic Structures Using Variable Viscous Dampers. In F. Casciati (Ed.), *Tird World Conference on Structural Control (3WCSC)*, Volume 3, Como, Italy, pp. 477–482. ASC. Chichester: John Wiley & Sons, Ltd.

El'sgol'ts, L. (1964). *Qualitative Methods in Mathematical Analysis*. London: American Mathematical Society.

El'sgol'ts, L. and S. Norkin (1973). *Introduction to the Theory and Applications of Differential Equations with Deviating Arguments*. New York: Academic Press.

Faravelli, L. and R. Rossi (2002). Adaptive Fuzzy Control: Theory versus Implementation. *Journal of Structural Control 9*(1), 59–73.

Faravelli, L. and R. Rossi (2003). Wireless Communication Between Sensor/Device Stations. In F. Bontempi (Ed.), *System-Based Vision for Strategic and Creative Design*, Volume ISEC-02, Rome, pp. 2091–2095. Leiden: Balkema.

Faravelli, L. and J. Spencer (2003). *US-Europe Workshop on Sensors and Smart Technology*. Chichester: John Wiley & Sons, Ltd. Ed. J. Holnicki-Szulc and C. Muta-Suares.

Faravelli, L. and T. Yao (1995). Self-Learning Fuzzy Control of Civil Structures. In *Third International Symposium on Uncertainty Modeling and Analysis*, College Park, Maryland, USA, pp. 52–57.

Faravelli, L. and T. Yao (1996). Use of Adaptive Networks in Fuzzy Control of Civil Structures. *Microcomputers in Civil Engineering 11*, 67–76.

Feng, M. Q., M. Shinozuka, and S. Fujii (1993). Friction-Controllable Sliding Isolation System. *Journal of Engineering Mechanics 119*(9), 1845–1864.

Foliente, G. (2000). Developments in Performance-Based Building Codes and Standards. *Forest Products Journal 50*(7/8).

François, A., P. D. Man, F. Bossens, and A. Preumont (2000). State of the Art of MR Fluids Technology and Semi-Active Control. Workpackage No. 1, Université Libre de Bruxelles, Brussels, Belgium. CaSCo - Consistent Semiactive System Control.

Gattulli, V. and F. Romeo (1999). An Adaptive Mass Damper for Self-Excited Oscillation. *Journal of Structural Control 6*(2), 187–203.

Gaul, L. and J. Lenz (1998). Active Damping of Space Structures by Contact Pressure Control in Joints. *Mechanical Structures and Mechatronics 26*(1), 80–100.

Gaul, L. and R. Nitsche (2001). The Role of Friction in Mechanical Joints. *Applied Mechanics Reviews 54*(2), 93–105.

Gavin, H. P., P. P. Phulé, and A. J. Jones (2002). Design Optimisation of MR Devices and Materials. In F. Casciati (Ed.), *Third World Conference on Structural Control (3WCSC)*, Volume 2, Como, Italy, pp. 309–314. ASC. Chichester: John Wiley & Sons, Ltd.

Harrigan, G., J.-P. Pinelli, and H. Gutierrez (2004). Controlling Seismic Vibrations with Magneto-Rheological Tuned Mass Dampers. In H. I. R. Flesch and M. Krommer (Eds.), *Third European Conference on Structural Control (3ECSC)*, Volume 2, Vienna, Austria, pp. S2-30–S2-33. EASC: TU-Wien.

He, W. L., A. K. Agrawal, and J. N. Yang (2003). Novel Semiactive Friction Controller for Linear Structures against Earthquakes. *Journal of Engineering Mechanics 129*.

Helgeson, R. J., M. Reed, R. McDaniel, and S. Priddy (2002). Semi-Active Frame Energy (SAFE) Earthquake System. In F. Casciati (Ed.), *Third World Conference on Structural Control (3WCSC)*, Volume 4, Como, Italy, pp. 489–494. ASC. Chichester: John Wiley & Sons, Ltd.

Hitchcock, G. H., F. Gordaninejad, and X. Wang (2002). Study of a New By-Pass Magneto-Rheological Fluid Damper. In F. Casciati (Ed.), *Third World Conference on Structural Control (3WCSC)*, Volume 2, Como, Italy, pp. 121–126. ASC. Chichester: John Wiley & Sons, Ltd.

Hiwatashi, T., Y. Shiozaki, H. Fujitani, M. Iiba, T. Tomura, H. Sodeyama, and S. Soda (2002). Semi-Active Control of Large-Scale Frame by Magneto-Rheological Damper. In F. Casciati (Ed.), *Third World Conference on Structural Control (3WCSC)*, Volume 2, Como, Italy, pp. 355–360. ASC. Chichester: John Wiley & Sons, Ltd.

Horiuchi, T. and M. Nakagawa (1996). Development of a Real-Time Hybrid Experimental System with Actuator Delay Compensation. In *Proceedings of the Eleventh World Conference on Earthquake Engineering*, Paper No. 660.

Housner, G. W., L. A. Bergman, T. K. Caughey, A. G. Chassiakos, R. O. Claus, S. F. Masri, R. E. Skelton, T. T. Soong, B. F. Spencer, and J. T. P. Yao (1997). Structural Control: Past, Present and Future. *Engineering Mechanics ASCE 123*(9), 897–971. Special Issue.

Housner, G. W., T. T. Soong, and G. F. Dargush (1994). Second Generation of Active Structural Control in Civil Engineering. In *First World Conference on Structural Control (1WCSC),* Pasadena, California, USA. ACS.

Hrovat, D., P. Barak, and M. Rabins (1993). Semi-Active versus Passive or Active Tuned Mass Dampers for Structural Control. *Journal of Engineering Mechanics ASCE 109*(3), 691–705.

Hughe, T., K. Pister, and R. Taylor (1979). Implicit-Explicit Finite Elements in Nonlinear Transient Analysis. *Computer Methods in Applied Mechanics and Engineering 17/18*, 159–182.

Iemura, H., A. Igarashi, and N. Nakata (2002). Full-Scale Verification Tests of Semi-Active Control Structures Using Variable Joint Damper System. In F. Casciati (Ed.), *Third World Conference on Structural Control (3WCSC)*, Volume 1, Como, Italy, pp. 175–180. ASC. Chichester: John Wiley & Sons, Ltd.

Jansen, L. M. and S. J. Dyke (2000). Semiactive Control Strategies for MR Dampers: Comparative Study. *Journal of Engineering Mechanics 126*.

Johnson, E., J. Ramallo, B. Spencer, and M. Sain (1998). Intelligent Base Isolation Systems. In *Proceedings of the Second World Conference on Structural Control*, Kyoto, Japan.

Kannan, S., M. Uras, and H. M. Aktan (1995). Active Control of Building Seismic Response by Energy Dissipation. *Earthquake Engineering and Structural Dynamics 24*, 747–759.

Karnopp, D. (1990). Design Principles for Vibration Control System Using Semiactive Dampers. *ASME Journal of Dynamics, Measurement and Control 112*(9), 448–455.

Karnopp, D., M. Crosby, and R. Harwood (1974). Vibration Control Using Semi-Active Force Generation. *Journal of Engineering for Industry 96*(2), 619–626.

Kobori, T. (1994). Future Direction on Research and Development of Seismic-Controlled Structure. In *First World Conference on Structural Control (1WCSC)*, Pasadena, California, USA. ACS.

Kobori, T. (1998). Mission and Prospective Towards Future Structural Control Research. In *Second World Conference on Structural Control (2WCSC)*, Kyoto, Japan. ACS.

Kobori, T. (2002). Past, Present and Future in Seismic Response Control of Civil Engineering Structures. In *Third World Conference on Structural Control (3WCSC)*, Volume 1, Como, Italy, pp. 9–14. ASC. Chichester: John Wiley & Sons, Ltd.

Kohl, M. (2004). *Shape Memory Microactuators*. Berlin: Springer-Verlag.

Kolmanovskii, V. and V. Nosov (1986). *Stability of Functional Differential Equations*. Providence, Rhode Island: American Mathematical Society and Academic Press.

Kurino, H. and T. Kobori (1998). Semi-Active Structural Response Control by Optimizing the Force-Deformation Loop of Variable Damper. In *Second World Conference on Structural Control (2WCSC)*, Kyoto, Japan. ACS.

Kurino, H. T. Yamada, J. Tagami, and K. Shimizu (2002). Semi-Active Structural Control by Switching Oil Damper with Built-In Controller. In F. Casciati (Ed.), *Third World Conference on Structural Control (3WCSC)*, Volume 1, Como, Italy, pp. 211–216. ASC. Chichester: John Wiley & Sons, Ltd.

Longchamp, R. (1980). Stable Feedback Control of Bilinear Systems. *IEEE Transactions on Automatic Control 25*(2), 302–306.

Lu, L. -Y. and G. -L. Lin (2002). Predictive Control of Seismic Structures with Semi-Active Friction Dampers. In F. Casciati (Ed.), *Third World Conference on Structural Control (3WCSC)*, Volume 3, Como, Italy, pp. 507–512. ASC. Chichester: John Wiley & Sons, Ltd.

Lynn, P. A. (1982). *An Introduction to the Analysis and Processing of Signals*. Hong Kong: Macmillan.

Magonette, G. (1991). Digital Control of Pseudodynamic Tests. *Experimental and Numerical Methods in Earthquake Engineering*, In J. Donea and P. M. Jones (Eds), Dordrecht: Kluwer Academic.

Magonette, G., F. Marazzi, and J. Molina (2001). Contributions of the ELSA Laboratory for the Development of Testing Methodologies in the Field of Structural Control. In *European Meeting on Intelligent Structures*, Ischia, Italy.

Magonette, G., F. Marazzi, J. Molina, and V. Renda (2000). Structural Control: Experimental Activity at ELSA. In *Workshop on Mitigation of Seismic Risk Support to Recent Affected European Countries*, Belgirate, Verbania, Italy.

Magonette, G. and P. Negro (1998). Verification of the Pseudodynamic Test Method. *Journal of the European Association for Earthquake Engineering 1*.

Makris, N. (1997). Rigidity-Plasticity-Viscosity: Can Electrorheological Dampers Protect Base Isolated Structures from Near-Source Ground Motions? *Earthquake Engineering and Structural Dynamics 26*, 571–591.

Manavis, T., C. Yfoulis, A. Muir, and N. Pettit (1998). Computational Aspects of the Analysis of Piecewise Linear Systems. Technical Report 874, Control Systems Centre, University of Manchester.

Marazzi, F. (2003). Semi-active Control of Civil Structures: Implementation Aspects. PhD thesis, University of Pavia, Department of Structural Mechanics.

Marazzi, F. and G. Magonette (2001). Active and Semi-active Control of Structures: A Comparison. In *European Meeting on Intelligent Structures*, Ischia, Italy.

Marazzi, F., G. Magonette, and V. Renda (2002). From Active to Semi-active Control: Theoretical and Implementation Aspects. In F. Casciati

(Ed.), *Third World Conference on Structural Control (3WCSC)*, Volume 3, Como, Italy, pp. 627–634. ASC. Chichester: John Wiley & Sons, Ltd.

Meirovitch, L. (1990). *Dynamics and Control of Structures*. New York: John Wiley & Sons, Inc.

Mohler, R. (1973). *Bilinear Control Processes*. New York: Academic Press.

Molina, F. (2002). Pseudodynamic Tests on Rubber Base Isolators with Substructuring of the Superstructure and Strain Effect Compensation. *Earthquake Engineering and Structural Dynamics 31*, 1563–1582.

Mori, F., Y. Sugiyama, M. Suwa, H. Kurino, and I. Fukushima (2002). Application of Semi-Active Switching Oil Damper to an Actual 11-Storey Building. In F. Casciati (Ed.), *Third World Conference on Structural Control (3WCSC)*, Volume 2, Como, Italy, pp. 143–148. ASC. Chichester: John Wiley & Sons, Ltd.

Naeim, F. and J. Kelly (1999). *Design of Seismic Isolated Structures*. New York: John Wiley & Sons, Inc.

Nagarajaiah, S. and N. Varadarajan (2002). Response Control of Wind Excited Tall Building with Semiactive Variable Stiffness TMD Using Short Time Fourier Transform. In F. Casciati (Ed.), *Third World Conference on Structural Control (3WCSC)*, Volume 2, Como, Italy, pp. 315–320. ASC. Chichester: John Wiley & Sons, Ltd.

Nakashima, M. (1999). Real-Time On-Line Test for MDOF Systems. *Earthquake Engineering and Structural Dynamics 28*, 393–420.

Negro, P. and G. Magonette (1998). Experimental Methods in Structural Dynamics. *European Earthquake Engineering*, 29–39.

Niculescu, S., J. Dion, and L. Dugard (1996). Robust Stabilization for Uncertain Time-Delay Systems Containing Saturating Actuators. *IEEE Transactions on Automatic Control 41*(5), 742–747.

Nishitani, A., Y. Nitta, and Y. Ikeda (2003). Semiactive Structural-Control Based on Variable Slip-Force Level Dampers. *Journal of Engineering Mechanics 129*.

Nishitani, A., Y. Nitta, Y. Ikeda, S. Yamaguchi, and A. Kume (2002). Variable Slip-Force Level Damper Based-Control Utilizing Semiactive Oil Hydraulic Dampers. In F. Casciati (Ed.), *Third World Conference on Structural Control (3WCSC)*, Volume 2, Como, Italy, pp. 113–120. ASC. Chichester: John Wiley & Sons, Ltd.

Nitsche, R. (2001). Semi-Active Control of Friction Damped Systems. PhD thesis, University of Stuttgart, Institute of Mechanics.

Nitta, Y., A. Nishitani, A. Kume, and S. Yamaguchi (2002). Variable Slip-Force Level Damper Based Semiactive Structural Control Scheme Utilizing Absolute Acceleration Information. In F. Casciati

(Ed.), *Third World Conference on Structural Control (3WCSC)*, Volume 2, Como, Italy, pp. 337–342. ASC. Chichester: John Wiley & Sons, Ltd.

Niwa, N. (2002). Semi-Active Control Based on Maximization of Energy Transmission. In F. Casciati (Ed.), *Third World Conference on Structural Control (3WCSC)*, Volume 3, Como, Italy, pp. 635–640. ASC. Chichester: John Wiley & Sons, Ltd.

Noltingk, B. (1996). *Instrumentation - Reference Book*. Oxford: Butterworth–Heinemann.

Occhiuzzi, A. and F. Ricciardelli (2002). A Semi-Active TMD Control Law Applied to the Wind Benchmark Building. In F. Casciati (Ed.), *Third World Conference on Structural Control (3WCSC)*, Volume 3, Como, Italy, pp. 719–724. ASC. Chichester: John Wiley & Sons, Ltd.

Occhiuzzi, A. and G. Serino (1996). Energy Criteria for Application and Use of Active Switching Control Devices. In *First European Conference on Structural Control (1ECSC)*, Barcelona, Spain. EASC. Singapore: World Scientific.

Occhiuzzi, A. and G. Serino (2000). Earthquake Excitation Tests on a Prototype Semi-Actively Controlled Structure. In *Second European Conference on Structural Control (2ECSC)*, Champs-sur-Marne, France. ENPC.

Occhiuzzi, A. and G. Serino (2002). Control Strategies for Semi-Active Structural Control Devices. In F. Casciati (Ed.), *Third World Conference on Structural Control (3WCSC)*, Volume 3, Como, Italy, pp. 641–647. ASC. Chichester: John Wiley & Sons, Ltd.

Occhiuzzi, A., M. Spizzuoco, and G. Serino (2004). Semi-Active Control of Pedestrian-Induced Vibration in Footbridge Through MR Dampers in TMDs. In H. I. R. Flesch and M. Krommer (Eds), *Third European Conference on Structural Control (3ECSC)*, Volume 2, Vienna, Austria, pp. S6-24–S6-27. EASC: TU-Wien.

Palazzo, B. and L. Petti (1999). Response Spectra of Semiactively Controlled Systems by Using Algorithms Based on Energy Criteria. *European Earthquake Engineering 2*, 45–56.

Palazzo, B., L. Petti, and D. Mauriello (2001). Optimal Control Algorithms Based on Energy Criteria for Semi-Active Isolation. In *7th International Seminar on Seismic Isolation, Passive Energy Dissipation and Active Control of Vibrations of Structures*, Assisi, Italy.

Palazzo, B., L. Petti, and D. Mauriello (2002). Optimal Control Algorithms Based on Energy Criteria for Semiactive Isolation. In F. Casciati (Ed.), *Third World Conference on Structural Control (3WCSC)*, Volume 3, Como, Italy, pp. 649–657. ASC. Chichester: John Wiley & Sons, Ltd.

Patten, W., R. Sack, and Q. He (1994). Suppression of Vehicle-Induced Bridge Vibration via a Semiactive Structural Controller. In *First World Conference on Structural Control (1WCSC)*, Pasadena, California, USA. ACS.

Patten, W. N., C. Mo, J. Kuehn, J. Lee, and C. Khaw (1996). Hydraulic Semiactive Vibration Absorbers (SAVA); Separating Myth from Reality. In *IFAC 13th Triennial World Congress*, Volume L, Los Angeles, California, USA, pp. 157–162. International Federation of Automatic Control.

Pegon, P. and G. Magonette (1999). Continuous PsD Testing with Non-linear Substructuring: Recent Development for the VAB Project. Special Publication No. 99.142, Joint Research Centre, Ispra, Italy.

Pegon, P. and G. Magonette (2002). Continuous PsD Testing with Nonlinear Substructuring: Presentation of a Stable Parallel Inter-field Procedure. Special Publication No. I.02.167, Joint Research Centre, Ispra, Italy.

Pegon, P. and G. Magonette (2005). Continuous PsD Testing with Nonlinear Substructuring: Using the Operator Splitting Technique to Avoid Iterative Procedures. Special Publication No. I.05.30, Joint Research Centre, Ispra, Italy.

Petten, W. N., C. Mo, J. Kuehn, and J. Lee (1997). A Primer on Design of Semiactive Vibration Absorbers (SAVA). *Journal of Engineering Mechanics 124(1)*, 61–68.

Petten, W. N., J. Sun, G. Li, J. Kuehn, and G. Song (1999). Field Test on Intelligent Stiffener for Bridges at the I-35 Walnut Creek Bridge. *Earthquake Engineering and Structural Dynamics 28*, 109–126.

Petti, L. (2002). Optimal Control Algorithms for Semi-Active Isolated Bridges. In *Third World Conference on Structural Control (3WCSC)*, Como, Italy. ASC. Chichester: John Wiley & Sons, Ltd.

Pettit, N. (1995). *Analysis of Piecewise Linear Dynamical Systems*. Taunton, UK: Research Studies Press Ltd.

Pettit, N. and A. Miur (1997). Simple Control of Nonlinear Systems. In *ECC97*.

Pinkaew, T. and Y. Fujino (2001). Effectiveness of Semi-active Tuned Mass Dampers under Harmonic Excitation. *Engineering Structures 23*, 850–856.

Pinto, A., P. Negro, and F. Taucer (2004). Full-Scale Laboratory Testing: Strategies and Procedures to Meet the Needs of PBEE. In P. Fajfar and H. Krawinkler (Eds), *International Workshop - Performance Based Seismic Design: Concepts and Implementation*, Bled, Slovenia. Pacific Earthquake Engineering Research Center, Richmond, California, USA.

Pinto, V. (2002). Pseudodynamic Tests on a Large-scale Model of an Existing RC Bridge Using Non-linear Substructuring and Asynchronous Motion. Report EUR 20525 EN, Joint Research Centre, Ispra, Italy.

Preumont, A. (1997). *Vibration Control of Active Structures: An Introduction*. Dordrecht: Kluwer Academic.

Ramallo, J., H. Yoshioka, and B. J. Spencer (2004). A Two-Step Identification Technique for Semiactive Control Systems. *Journal of Structural Control & Health Monitoring 11*(4), 273–289.

Renda, V., G. Magonette, J. Molina, D. Tirelli, F. Marazzi, and T. Taucer (2002). The Joint Research Centre of the European Commission. In *IABSE Symposium: Towards a Better Built Environment - Innovation, Sustainability, Information Technology*, Melbourne, Australia.

Renda, V., G. Magonette, J. Molina, D. Tirelli, and F. Marazzi (2000) Activities of the European Laboratory for structural Assessment in the Field of Structural Control for Civil Building, Bridges and Architectural Heritage. In *Third International Workshop on Structural Control (3IWSC)*, Champs-sur-Marne, France. ENPC.

Renzi, E. (2001). Il Controllo Semi-attivo delle Vibrazioni Strutturali: Teoria e Applicazioni, PhD thesis, University of Rome "La Sapienza" (in Italian).

Renzi, E., M. D. Angelis, and V. Ciampi (2002). Passive and Semi-Active Seismic Control of a Three-Storey Steel Frame. In F. Casciati (Ed.), *Third World Conference on Structural Control (3WCSC)*, Volume 3, Como, Italy, pp. 501–506. ASC. Chichester: John Wiley & Sons, Ltd.

Repetto, M. P. and G. Solari (2001). Dynamic Alongwind Fatigue of Slender Structures. *Engineering Structures 23*, 1622–1633.

Rodellar, J. (2002). Complexity Issues of Structural Control. In *Third World Conference on Structural Control (3WCSC)*, Volume 1, Como, Italy, pp. 47–56. ASC. Chichester: John Wiley & Sons, Ltd.

Rodellar, J., N. Luo, R. Villamizar, U. Dorka, J. Garcia, G. Magonette, and A. Bossi (2004). Control Algorithms for Semiactive Control of Bridges. In H. I. R. Flesch and M. Krommer (Eds), *Third European Conference on Structural Control (3ECSC)*, Volume 2, Vienna, Austria, pp. S6-16–S6-19. EASC: TU-Wien.

Rodellar, J., N. Luo, R. Villamizar, and J. Vehi (2003). Robust Control Law for a Friction-Based Semiactive Controller of a Two-Span Bridge. In *Smart Structures and Materials for NDE Systems and NDE for Health Monitoring and Diagnostics, Proceedings of SPIE The International Society for Optical Engineering*, Volume 5057 of *Smart Systems and NDE for Civil Infrastructures [28]*.

Ryan, E. and N. Buckingham (1983). On Asymptotically Stabilizing Feedback Control of Bilinear Systems. *IEEE Transactions on Automatic Control 28*(8), 863–864.

Sadek, F. and B. Mohraz (1998a). Semi-Active Control Algorithms for Structures with Variable Dampers. *Journal of Engineering Mechanics, ASCE 124*(9), 981–990.

Sadek, F. and B. Mohraz (1998b). Semiactive Control Algorithms for Structures with Variable Dampers. *Journal of Engineering Mechanics 124*.

Schmidt, K. and U. Dorka (2002). Seismic Retrofitting of Residential Building with HYDE Systems. In *Third World Conference on Structural Control (3WCSC)*, Como, Italy. ASC. Chichester: John Wiley & Sons, Ltd.

Serino, G. and A. Occhiuzzi (1994). The Energy Approach in Active/Hybrid Vibration Control. In *First World Conference on Structural Control (1WCSC)*, Pasadena, California, USA. ACS.

Serino, G. and A. Occhiuzzi (2000). Experimental Characterisation of an Oleodynamic Semi-Active Damper and Evaluation of Operating Delays. In *Second European Conference on Structural Control (2ECSC)*, Champssur-Marne, France. ENPC.

Serino, G., A. Occhiuzzi, M. Spizzuoco, C. Seiler, and Fischer (2002). Semi-Active Control via MR Dampers: Algorithms, Numerical Modeling and Prediction of the Resulting Response of Structures. In F. Casciati (Ed.), *Third World Conference on Structural Control (3WCSC)*, Volume 2, Como, Italy, pp. 1113–1118. ASC. Chichester: John Wiley & Sons, Ltd.

Shampine, L. and S. Thompson (2000). Solving Delay Differential Equations with dde23. *Journal of Engineering Mechanics*. Available from http://www.runet.edu/thompson/webddes.

Shing, P. and S. Mahin (1984). Pseudodynamic Test Method for Seismic Performance Evaluation: Theory and Implementation. Report UCB/EERC-84/01, Earthquake Engineering Research Center, University of California, Berkeley, USA.

Shiozaki, Y., T. Hiwatashi, H. Fujitani, M. Iiba, K. Hata, K. Sunakoda, and S. Soda (2002). Study of Response Control by MR Damper for Base-Isolated Building. In F. Casciati (Ed.), *Third World Conference on Structural Control (3WCSC)*, Volume 2, Como, Italy, pp. 137–142. ASC. Chichester: John Wiley & Sons, Ltd.

Shrestha, S. M. and J. Ghaboussi (1998). Evolution of Optimum Shapes Using Genetic Algorithm. *Journal of Structural Engineering 124*(11), 1331–1338.

Smith, S. W. (1999). *The Scientist and Engineer's Guide to Digital Signal Processing*. San Diego, California: California Technical Publishing.

Sontag, E. (1981). Nonlinear Regulation: The Piecewise Linear Approach. *IEEE Transactions on Automatic Control 26*(2), 346–358.

Soong, T. (2002). Structural Control: Theory versus Practice. In *Third World Conference on Structural Control (3WCSC)*, Volume 1, Como, Italy, pp. 15–32. ASC. Chichester: John Wiley & Sons, Ltd.

Soong, T. T. (1989). *Active Structural Control: Theory and Practice*. Harlow: Longman Scientific and Technical.

Soong, T. T. and G. F. Dargush (1997). *Passive Energy Dissipation Systems in Structural Engineering*. Chichester: John Wiley & Sons, Ltd.

Soong, T. T. and B. F. Spencer (2000). Active, Semi-Active and Hybrid Control of Structures. In *12 World Conference on Earthquake Engineering (12WCEE)*, paper no. 2834, Auckland, New Zealand.

Sorace, S. and G. Terenzi (2001). Non-linear Dynamic Modeling and Design Procedure of FV Spring-Dampers for Base Isolation. *Engineering Structures 23*, 1556–1567.

Spencer, B., E. Johnson, and J. Ramallo (2000). Smart Isolation for Seismic Control. *JSME International Journal, Series C 43*(3), 704–711.

Spencer, B. F. and T. T. Soong (1999). New Applications and Development of Active, Semi-Active and Hybrid Control Techniques for Seismic and Non-Seismic Vibration in the USA. In *International Post-SMiRT Conference Seminar on Seismic Isolations, Passive Energy Dissipation and Active Control of Vibration of Structures*, Cheju, Korea.

Spencer, B. F. J. (2004). Benchmark Structural Control Problems for Seismic-and Wind-Excited Structures. *Journal of Engineering Mechanics 130*.

Spencer, B. J. and M. Sain (1997). Controlling Buildings: A New Frontier in Feedback. *Control Systems, IEEE 17*(8), 18–35.

Spizzuoco, M., A. Occhiuzzi, and G. Serino (2004). A Semi-Active MR Damper-Brace System's Control Law Applied to the Earthquake Bench-mark Building. In H. I. R. Flesch and M. Krommer (Eds), *Third European Conference on Structural Control (3ECSC)*, Volume 2, Vienna, Austria, pp. S1-227–S1-230. EASC: TU-Wien.

Spizzuoco, M. and C. Seiler (2002). Numerical Evaluation of the Earthquake Response of Semi-Actively Controlled Building and Bridge Structures. In F. Casciati (Ed.), *Third World Conference on Structural Control (3WCSC)*, Volume 3, Como, Italy, pp. 483–488. ASC. Chichester: John Wiley & Sons, Ltd.

Stoten, D. (2002). Adaptive Control of Shaking Tables Using the Minimal Control Synthesis Algorithm. *Philosophical Transactions of the Royal Society 359*(1786), 1697–1723.

Sun, L., Y. Fujino, P. Chaiseri, and B. M. Pacheco (1995). The properties of Tuned Liquid Dampers Using a TMD Analogy. *Earthquake Engineering and Structural Dynamics 24*, 967–976.

Symans, M. and M. Constantinou (1998). Semi-Active Control Systems for Seismic Protection of Structures: A State-of-the-Art Review. *Engineering Structures, The Journal of Earthquake, Wind and Ocean Engineering 21*(6), 469–487.

Tagami, J., H. Koshida, H. Kurino, T. Sugiyama, M. Suwa, and F. Mori (2002). Forced Vibration Test of an 11-Storey Building with Semi-Active Switching Oil Damper. In F. Casciati (Ed.), *Third World Conference on Structural Control (3WCSC)*, Volume 2, Como, Italy, pp. 75–80. ASC. Chichester: John Wiley & Sons, Ltd.

Taucer, F. (2005). Recent Advances and Future Needs in Experimental Earthquake Engineering. CASCADE Project Report, LNEC, Lisbon, Portugal.

Temini, H., S. El-Borgi, S. Choura, and F. Sadek (2004). Time Delay Effects on Semi-Active Control of Seismically Excited Nonlinear Structures. In H. I. R. Flesch and M. Krommer (Eds), *Third European Conference on Structural Control (3ECSC)*, Volume 2, Vienna, Austria, pp. S1-211–S1-218. EASC: TU-Wien.

Vestroni, F. and D. Capecchi (2000). Damage Detection in Beam Structures Based on Measurements of Natural Frequencies. *Journal of Engineering Mechanics 126(7)*, 761–768.

Vestroni, F. and W. Lacarbonara (2002). Feasibility of a Vibration Adsorber Based on Hysteresis. In *Third World Conference on Structural Control (3WCSC)*, Como, Italy. ASC. Chichester: John Wiley & Sons, Ltd.

Vulcano, A. and F. Mazza (1999). The Seismic Response of Damped Frames Using Different Dissipative Braces: A Parametric Study. In *Second International Symposium on Earthquake Resistant Engineering Structures*, Catania, Italy, pp. 267–278.

Weber, F., G. Feltrin, and M. Motavalli (2004). Damping Potential of Controlled MR Dampers. In H. I. R. Flesch and M. Krommer (Eds), *Third European Conference on Structural Control (3ECSC)*, Volume 2, Vienna, Austria, pp. S2-34–S2-37. EASC: TU-Wien.

Williams, M. (2001). Dynamic Testing of Structures. *Philosophical Transactions of the Royal Society 359*(1786), 1647–1929.

Wongprasert, N. and M. D. Symans (2002). Experimental Evaluation of a Smart Base-Isolation System Consisting of Spherical Sliding Bearings and Variable Fluid Dampers. In F. Casciati (Ed.), *Third World Conference on Structural Control (3WCSC)*, Volume 2, Como, Italy, pp. 331–336. ASC. Chichester: John Wiley & Sons, Ltd.

Yamamoto, M., M. Higashino, and S. Aizawa (2002). Development of Semi-Active Mass Damper System Using Oil Damper with Solenoid Valves. In F. Casciati (Ed.), *Third World Conference on Structural Control (3WCSC)*, Volume 2, Como, Italy, pp. 343–349. ASC. Chichester: John Wiley & Sons, Ltd.

Yang, J. N., J.-H. Kim, and A. K. Agrawal (2000). Resetting Semiactive Stiffiness Damper for Seismic Response Control. *Journal of Engineering Mechanics 126*.

Yfoulis, C., A. Muir, P. Wellstead, and N. Pettit (1998). Stabilization of Orthogonal Piecewise Linear Systems Using Piecewise Linear Lyapunov-Like Functions. Technical Report 875, Control Systems Centre, University of Manchester, UK.

Yoshida, J., M. Abe, Y. Fujino, and H. Watanabe (2004). Three-Dimensional Finite-Element Analysis of High Damping Rubber Bearings. *Journal of Engineering Mechanics 130*.

Yoshida, O. and S. J. Dyke (2004). Seismic Control of a Nonlinear Benchmark Building Using Smart Dampers. *Journal of Engineering Mechanics 130*.

Index

Technology of Semiactive Devices and Applications in Vibration Mitigation Fabio Casciati, Georges Magonette and Francesco Marazzi